Ville Mustonen

Master's Thesis

Development of a health chair for non-invasive patient monitoring

School of Electrical Engineering

Thesis submitted for examination for the degree of Master of Science in Technology.
Espoo 26.09.2013

Thesis supervisor:
Prof. Raimo Sepponen

Thesis instructor:
Lic.Sc. (Tech.) Matti Linnavuo

Aalto University
School of Electrical
Engineering

AALTO UNIVERSITY
SCHOOL OF ELECTRICAL ENGINEERING

ABSTARCT OF THE MASTER´S THESIS

Author: Ville Mustonen

Title: Development of a health chair for non-invasive patient monitoring

Date: 26.09.2013 Language: English Number of pages: 69 + 33

School: School of Electrical Engineering

Department: Department of Electronics

Professorship: Applied Electronics Code: S-66

Supervisor: Prof. Raimo Sepponen

Instructor: Lic.Sc. (Tech.) Matti Linnavuo

Aalto University's Health Factory executed development process to realize a health chair for monitoring patient state of health. Aim of this master's thesis was to participate into the technical development of the health chair. This included designing wanted measurements to pilot designs from selected OEM modules. Including all the necessary coupling and programming to implement modules to monitoring state. The thesis introduces LabVIEW programs and couplings done to these modules on each pilot design. Aim was also to design, execute and test estimating of patient's systolic blood pressure with pulse transit time method. A design of dry-electrode contact electrocardiography measurement from chosen ECG module was supposed to be realized. Automated calculations of RR and QT intervals were done. The thesis also collects information related to realize pilot design measurements.

The thesis introduces health chair's first pilot design, which worked as test platform to test the chosen measurement modules and verify their compatibility to use. Necessary programs and couplings were made to monitor the measurements. Secondly the master's thesis introduces second health chair pilot design. The design was more developed. It included blood pressure, weight, photoplethysmography, electrical bioimpedance, blood oxygen saturation and heart rate measurements. All these measurement were executed on this health chair. The third pilot design was not finished during this master's thesis. The third pilot design was designed to include electrocardiography, weight, bioelectrical impedance, blood oxygen saturation, heart rate and photoplethysmography measurement and estimation of systolic blood pressure from pulse transit time. The thesis introduces designed dry-electrode ECG measurement. It introduces two systolic blood pressure estimation methods and RR and QT interval calculations. The calculations and systolic blood pressure estimation methods were made with LabVIEW. The designs of these programs are presented.

Every measurement was completed on each module. Tests were made to five persons from different age categories. Firstly, functioning of second pilot design measurements were tested. Aim of the test was to verify that measurements could be executed with second pilot design. Results are presented in the thesis and refer that all the tests were completed. Secondly, usability of RR and QT interval calculations were tested. Aim of the test was to compare the results made with automated LabVIEW measurements and manually calculated result with Matlab. RR interval calculations had smaller standard deviation and median error than QT interval calculations. RR calculations were considered precise. Lastly, systolic blood pressure was estimated with measured pulse transit times from these five test persons. Two different estimation methods were used. Considering the results the method is neither compatible to determine absolute blood pressure or detecting small changes of systolic blood pressure but could be compatible for monitoring systolic blood pressure in long periods.

Keywords: patient monitoring, electrocardiogram, oxygen saturation, LabVIEW, photoplethysmogram, pulse arrival time, pulse transit time, RR interval, QT interval

AALTO-YLIOPISTO
SÄHKÖTEKNIIKAN KORKEAKOULU

DIPLOMITYÖN TIIVISTELMÄ (FINNISH)

Tekijä: Ville Mustonen

Työn nimi: Terveystuolin kehitys potilaan kajoamattomaan mittaukseen

Päivämäärä: 26.9.2013 Kieli: Englanti Sivumäärä: 69 + 33

Korkeakoulu: Sähkötekniikan korkeakoulu

Laitos: Elektroniikan laitos

Professuuri: Sovellettu Elektroniikka Koodi: S-66

Työn valvoja: Prof. Raimo Sepponen

Työn ohjaaja: TkL Matti Linnavuo

Tämän diplomityön tarkoituksena oli osallistua Aalto-yliopiston Health Factoryn kehittämän terveystuolin tekniseen kehitykseen. Terveystuolia kehitettiin potilaan terveydentilan seurantaan. Terveystuolin kehitys tapahtui toteuttamalla tarvittavat mittausmoduulit monitorointiasteelle. Diplomityössä esitellään pilottituoleihin valituille moduulille tehdyt LabVIEW-ohjelmat ja tarvittavat kytkennät. Nämä mahdollistivat mittausmoduuleilla monitoroinnin. Tarkoituksena oli myös suunnitella, toteuttaa ja testata pulssiaikaviiveellä toteutettu potilaan systolisen verenpaineen arviointi. Potilaan EKG oli tarkoitus mitata kuivaelektrodeilla, joiden toteutus esitellään. Tarkoituksena oli myös toteuttaa automatisoitu RR- ja QT-intervallien mittaus valitulle EKG-moduulille. Myös tiedon keruu pilottien kehitysvaiheista oli osatavoitteena diplomityössä.

Diplomityö esittelee terveystuolin ensimmäisen pilotin, joka toimi koealustana valituille moduuleilla. Sen tarkoituksena oli kokeilla moduulien toimivuus käyttötarkoitukseen. Käyttöönottoon tehdyt tarvittavat LabVIEW-ohjelmat ja kytkennät tehtiin ja ne esitellään. Terveystuolin toinen pilotti toimi koekäyttötuolina ja muistutti enemmän lopullista terveystuolia. Se sisälsi verenpaine-, paino-, plethysmografia-, kudosimpedanssi-, happisaturaatio- ja sykemittaukset. Näihin toteutetut ohjelmat ja kytkennät esitellään. Kolmas pilotti ei valmistunut tämän diplomityön aikana. Sen kehitys oli tarkoituskin jatkua. Tuolin oli tarkoitus sisältää EKG-, paino-, kudosimpedanssi-, happisaturaatio-, syke- ja plethymografiamittaukset sekä systolisen verenpaineen arvioinnin pulssiaikaviiveen avulla. Diplomityö esittelee siihen kuivaelektrodi kytkennän, joka suunniteltiin EKG-mittaukseen. Tehdyt RR-ja QT-intervallien automaattiset mittausmenetelmät esitellään. Suunnitellut menetelmät systolisen verenpaineen arviointiin pulssiaikaviiveellä esitellään.

Diplomityössä toteutettiin mittaukset onnistuneesti jokaiseen siinä käytettyyn mittausmoduuliin. Työssä suoritettiin kokeita viidelle henkilölle. Ensinnäkin terveystuolin toisen pilotin mittaukset suoritettiin. Tulokset esitellään ja todettiin että kaikki mittaukset on toteutettavissa. Toiseksi RR- ja QT-intervallien automaattinen laskenta testattiin. LabVIEW-ohjelman laskemia tuloksia verrattiin MatLabilla manuaalisesti mitattuihin tuloksiin. RR-intervalleilla oli pienempi standardi deviaatio ja pienempi mediaani virhe kuin QT-intervalleilla. Ne saavuttivat tyydyttävän tarkkuuden. Viimeiseksi systolisen verenpaineen arviointi pulssiaikaviiveellä kokeiltiin kahdella eri tavalla. Tuloksissa todetaan että pulssiaikaviive ei ole sopiva absoluuttisen verenpaineen arviointiin, eikä sen tarkkuus riitä huomioimaan pieniä verenpaineen muutoksia, mutta se voisi olla sopiva menetelmä pitkä aikaiseen verenpaineen seurantaan.

Avainsanat: terveystuoli, monitorointi, elektrokardiogrammi, pulssioksimetri, happisaturaatio , LabVIEW, plethysmogrammi, pulssiaikaviive, RR-intervalli, QT-intervalli

Preface

This master's thesis was made in Aalto University School of Electrical Engineering in laboratory of Applied Electronics. The writer did not do all of the electronics, programs, done physical work or designs. Health chair pilots were results of teamwork.

I want to thank my thesis supervisor professor Raimo Sepponen from the possibility to do the thesis. Also, I want to thank Mikko Paukkunen and Heikki Ruotoistenmäki for all the help. Above all I want to thank Matti Linnavuo for crucial advises and help, even during his holidays.

"It is clear that bioengineers of the future will have a tremendous impact on the quality of human life." - Joseph D. Bronzino, The Biomedical Engineering Handbook.

Helsinki 26th of September, 2013

Ville Mustonen

Contents

Presented figures

Presented tables

Symbols and abbreviations

Symbols

A_T	total absorbance at wavelength λ
I	transmitted light
I_0	incident intensity
P_b	base blood pressure
P_e	estimated blood pressure
T_b	PAT value corresponding base blood pressure
V	volume
V_{ep}	electrode polarization voltage
V_{TUS}	measured voltage in tissue under study
Z_{TUS}	impedance in tissue under study
ε_λ	absorptivity of the absorbent at wavelength λ
c	concentration of the absorbent
d	optical path length
l	optical path-length of the sample
γ	an elastic modulus coefficient of the vessels
ρ	resistivity of conductive material.

Abbreviations

AC	Alternating current
Ag/Ag-Cl	Silver/silver-chloride
ASCII	American standard code for information interchange
AV	Atria ventricular
BELA	Body electrical loss analysis
BIA	Bioelectrical impedance analysis
BP	Blood pressure
BPV	Blood pressure variability
BW	Body water
CRC	Cyclic redundancy check
DBP	Diastolic blood pressure
DC	Direct current
EBI	Electrical bioimpedance
ECG	Electrocardiography
ECW	Extra cellular water
FFM	Fat free mass
GUI	Graphical user interface
Hb	Reduced haemoglobin
HbO_2	Oxygenated haemoglobin
HEMA	Institute of Healthcare Engineering, Management and Architecture
HR	Heart rate
HRV	Heart rate variability
LabVIEW	Laboratory Virtual Instrumentation Engineering Workbench
LSB	Least significant bit
MF-BIA	Multi frequency bioimpedance analysis
MV	Minute volume
NIBP	Non-invasive blood pressure
OEM	Original equipment manufacturer
PAT	Pulse arrival time
PEP	Pulse-ejection time
POX	Partial oxidation
PPG	Photoplethysmography
PPP	Point-to-Point Protocol
PTT	Pulse transit time
PWV	Pulse wave velocity
SA	Sinoatrial
SBP	Systolic blood pressure
SF-BIA	Single frequency bioimpedance analysis
SpO_2	Peripheral blood oxygen saturation
TBW	Total body water
VI	Virtual instrument
VISA	The Virtual Instrument Software Architecture
bpm	beats per minute
dia	diastolic
mmHg	millimeters of mercury
subVI	sub virtual instrument
sys	Systolic

1 Introduction

1.1 Background

In developing countries and in majority of developed countries cardiovascular diseases are the major death cause in adults and in the elderly people. The diseases result in substantial disability and loss of productivity. They escalate the costs of health care, especially in presence of elderly people. (*Sans et la. 1997*) Cardiovascular diseases are the main cause of death within the range of 44-64 years, and the second most frequent cause of death of people between 24 and 44 years. An early recognition of symptoms, and warning of the patient or doctor, would enable preventive actions to avoid the attack and thus the risk of irreparable damage to organs or even death. Rapid advancement of medical technology has contributed to significant improvement in patient care. Partly because of technologies advanced, within the last 20 years the life expectancy has shifted from about 72 years to 80 years. At the same time, the costs of health care have increased due to treatments. The challenge for today's engineers is to develop new or improved methods of preventive care and to decrease the costs of instrumentation as well as its use. (*Gruetzmann 2007*)

Monitoring is repeated testing aimed to guide and manages chronic or recurrent condition. Monitoring is a central activity in the management of patients and a major part of the ritual of routine visits for most chronic diseases. Measuring patient's current state and responses to treatment is essential to managing many diseases. At the moment, many acute diseases diagnosis begins with clinical diagnosis testing. This focus should soon shift to monitoring to effectiveness the treatment. *(Glasziou et al. 2008)* Aim of patient monitoring is to help to evaluate important physiological variables during wanted moments. These values or changing trends are important to know for their clinical or research evaluation. At the end, patient monitoring aims to prevent patient losses by:

- Organizing information
- Displaying the information in form that eases the care of patient
- Comparing multiple factors that it would be possible to show clear presentation of clinical problems
- Processing information that alarms can be set
- Producing information leaning on automatically collected information
- Making better care with less healthcare personnel possible *(Reijula 2007, p. 11-12)*

This master's thesis and research related are focused to develop an innovative health chair for monitoring patient's cardiovascular state.

1.2 Related researches

This thesis is part of larger investigation conducted by Aalto Health Factory. It is a part of Aalto University concentrated to advance health and welfare technology. The aim of this project is to design and implement a chair for monitoring patient's cardiovascular

state of health. The whole project aims to result in a product to do fast and easy cardiovascular measurements, all collected in health chair. Aim of the project is to provide an inexperienced easiness for wanted patient measurements and to integrate the existing measurements to one health chair concept.

Participants in the project of the health chair were the Institute of Healthcare Engineering, Management and Architecture (HEMA). It is a research group concentrated on the production and development of health services. HEMA is part of Aalto University *(HEMA 2013).* To technical development of the chair were mainly participated staffs of Aalto University's laboratory of Applied Electronics. On the first state, the technical main focus of this research project is to actualize a working pilot designs from patient monitoring health chair, which would be further developed afterwards. This master's thesis has been written during that time.

1.3 Aim of this thesis

Aim of this master's thesis is to participate in to technical development of the health chair by realizing wanted measurements to health chair pilot designs from selected OEM (Original Equipment Manufacturer) modules. This includes doing all the necessary coupling and programming to implement the measurements. The measurements realized to second pilot design were tested. Tests were conducted to confirm the measurements could be done. In addition, aim was to design automated calculations of RR and QT intervals from ECG module and test their compatibility to use. Aim was also to design, execute and test estimating of patient blood pressure from pulse transit time (PTT). Two different estimating methods was implemented and tested. The thesis introduces a design of dry-electrode contact electrocardiography (ECG) measurement from chosen OEM module. It also collects information related from realized pilot designs measurements.

1.4 Introduction to the thesis

The aim of the thesis was not to make a product, but to realize pilot design for development of a product. The electronics were mostly made using OEM modules to speed up development process; exceptions are explained in subsequent chapters. The programs were mostly implemented with LabVIEW (Laboratory Virtual Instrument Engineering Workbench) program. The information in this master's thesis is limited to only measurements realized in the pilot designs. The aim of the thesis is not to decide the factors measured to monitor patient's health state or methods used to estimate patient's state of health. The thesis is a part of the larger project, which aims to commercialize the health chair product and have been done by instructions and directions given.

This master's thesis explains and clarifies work done related to bioelectrical instrumentation and programs designed during the research. Firstly the thesis introduces theoretical physiological background of realized measurements. It introduces the fundamentals of physiology to help to understand the fundamentals of measurements. Only necessary information to reader is introduced. It explains the fundamentals of human cardiovascular system to help to understand the fundamentals of electrocardiography. The

thesis explains related issues from physiology of blood pressure. Secondly, the master's thesis introduces shortly theory how measurement devices functions. Also, the basics of health information, which measurements provide, are introduced. After, it introduces pilot designs and realized programs, electronics and ensembles done during the thesis process. The part tells the measurement devices chosen and pilot design made. It explains the design and implementation process of the devices. In this part, the design and programming of communication and the graphical user interface (GUI) is also explained. The health chair's pilot designs and their parts made will be introduced in chronological order. Lastly, the thesis introduces test and results done and discusses about result and possible improvements to the health chair.

2 Physiology related to the measurements

2.1 Physiology of heart

The heart is the pump that circulates blood in cardiovascular system. The heart rests near midline of thorax. About two thirds of its mass is on left of the bodyline. Its average mass is 250 grams in adult females and 300 g in adult males. It is surrounded by pericardium, which surrounds and protects the heart. It confines the heart to its position and gives it sufficient freedom to move in rapid contradictions. The walls of the heart consist from three layers: the epicardium, the myocardium and the endocardium. The epicardium is the external layer and it gives the slippery texture to the outermost surface of the heart. The myocardium is the cardiac muscle tissue and it is responsible of pumping action. The endocardium provides a smooth lining for the chamber and covers the heart valves. The heart has four chambers. It has two superior chambers, which are called atria's. The two inferior chambers are ventricles. Figure 1 presents the anatomy of the heart: its atriums, ventricles, associated major vessels and cardiac conduction system. (*Tortora & Derrickson 2007, p. 696-699)*

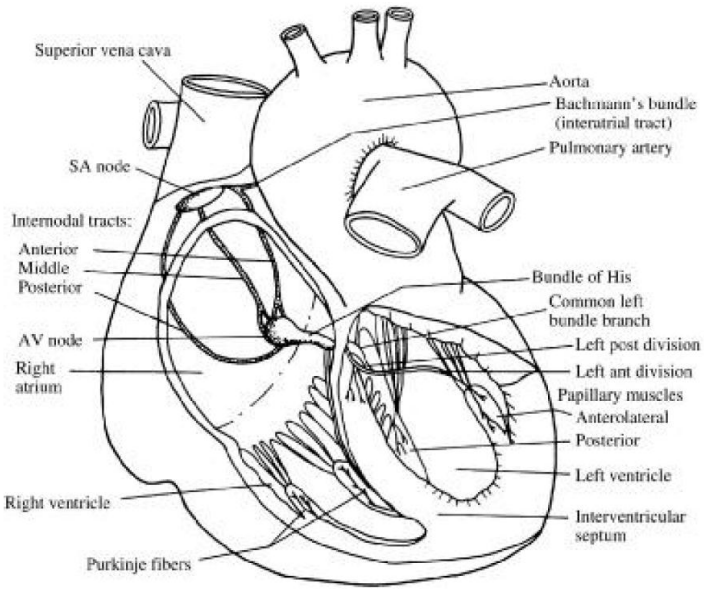

Figure 1 presents the anatomy of the heart: its atriums, ventricles, associated major vessels and cardiac conduction system. *(Webster 2010, p. 148)*

2.1 Cardiac conduction system

Contraction of heart muscle cells requires depolarization, plateau and repolarization phase of their cell membranes caused by movement of ions. *(Malmivuo & Plonsey 1995, Tortora & Derrickson 2007, p. 712)* Heart's specialized muscle fibres are called autorhytmic fibres because they are self-excitable. About 1% of heart's cardiac muscle fibres are autorhytmic fibres. They work as a source of heart's electrical activity. Autorhytmic fibres act as a specialized network repeatedly generating action potential and making heart to contract. The most importantly they work as pacemaker cell making heart to contract. They form the conduction system which is able the cardiac excitation to conduct through heart. This ensures that the chambers of heart contract in needed manner. *(Tortora & Derrickson 2007, p. 710)*

The cardiac action potential propagates through the conduction system in the following way. The wave is generated in sinoatrial (SA) node. It is located in right atrial wall. SA node cells depolarize repeatedly and spontaneously. SA node cells do not have stable resting potential. This depolarization is called pacemaker potential. When it reaches its threshold it triggers the action potential. Action potentials propagate from SA node to via gab junction to atrial muscle fibres, what is followed by atrial contraction. After the atrial depolarization it reaches atrioventricular (AV) node, which is located in septum between the atria's. From AV node wave propagate AV bundle. It is the only site where wave can conduct from atria to the ventricles. Wave's propagation is slowed down in AV node, because fibres here have fewer gab junctions and smaller diameter. This pause enables ventricular filling and is desired. After AV bundle propagation reaches the ventricles and then proceeds along right and left bundle branches to Purkinje fibres to inner walls of ventricles. (*Malmivuo & Plonsey 1995; Tortora & Derrickson 2007, p. 710-714)* The cells constituting from ventricular myocardium are coupled together by gap junctions. Healthy ventricular myocardium has very low resistance. In heart propagating wave can propagate to areas, which are still at rest potential. Studies show that activation wave front proceeds uniformly from endocardium to epicardium and from upper section to lower section. *(Malmivuo & Plonsey 1995)*

2.2 Cardiac cycle

Cardiac cycle includes all events in one heartbeat. It consists from atrial systole and diastole and also ventricular systole and diastole. In cardiac cycle the atria's and ventricles contract and relax forcing blood from higher-pressure areas to lower pressure areas. Cardiac cycle starts from atrial systole where atria's are contracting and ventricles are relaxed. Depolarization of the SA node causes the atrial depolarization, when atrial systole starts. Atrial contraction force blood from atria's to ventricles. It is followed by atrial diastole and ventricular systole. In ventricular systole the ventricles are contracting. It is caused by ventricular depolarization. Ventricular systole forces blood from ventricles to aorta and pulmonary trunk. Ventricular systole is followed by ventricular diastole caused by repolarization. Last period during cardiac cycle is relaxation period then both atria's and ventricles are both relaxed. When ventricular pressure drops lower than atrial pressure ventricular filling starts. *(Tortora & Derrickson 2007, p. 716)*

2.3 Pulse and heart rate

Pulse is pressure wave resulting from heart's pumping. It is born when blood is rushing out from left ventricles during systole and expanding walls of aorta. During diastole pulse is born when blood pressure decreases and walls of arteries squeeze the blood forward. Pulse is raised from the bottom of the aorta. Pulse advances wave like in the arteries. It advances faster than blood circulating in arteries. Pulse can be detected from multiple of the largest arteries. (*Haarnoja 2012, p. 8-9*) Heart rate is amount of heartbeats per amount of time. It is normally measured in beats per minute (bpm). Without hormonal or neural effect, human heart would beat 100 times per minutes. This is the rhythm of SA node impulses. With hormonal and neural effect heart beat rate can be more or less. Pulse rate is normally same as heart rate. *(Tortora & Derrickson 2007, p. 753)* The beat-to-beat heart rate variability (HRV) is well known to carry a great deal of

information about the dynamic features of cardiovascular control mechanisms. *(Ma & Zhang 2005)*

2.4 Blood pressure

Blood pressure maintains the circulation in our bodies so that oxygen and nutrition transportation to cells are working. It transports necessary nutrition and oxygen to cells and removes their waste products. When blood pressure is too high it can damage tissues and cells in our body. The circulatory system consists from two circulatory systems: pulmonary circulation and systemic circulation. Pulmonary circulation circulates the blood through lungs and pulmonary system. Systemic circulation circulates through rest of our body. Blood is moved through these systems by two pumps, the right and left ventricles of the heart. The left side of the heart carries heavier workload, because pushing blood through muscles is heavier. Blood is under pressure at all points through out both systems in arteries, capillaries and veins otherwise it would not circulate. *(Fahey et al. 2004, p.7-8; Larkin 2005, p.10)*

Blood pressure is determined by the amount of blood ejected into circulation (cardiac output) and the forces of the circulatory system that impede blood flow (total peripheral resistance). Cardiac output is determined by heart rate and stroke volume, increase in one increases blood pressure at the end. Total peripheral resistance is compromised of the degree of vasodilation and vasoconstriction. All physiologic and physiological states that affect blood pressure will do so by altering cardiac output, total peripheral resistance or combination of two. *(Larkin 2005, p.9)* Several systems of the body directly influence blood flow through the body and the magnitude of the blood pressure, including:

- The metabolic demands of the local tissue and associated blood vessels
- The autonomic nervous system
- The neuroendocrine system the excretion of fluid by the kidney
- Extensive feedback system that involves central nervous activity *(Larkin 2005, p. 9-10)*

Systolic blood pressure (SBP) is the force of blood pressure on arterial walls just after ventricular contraction. Diastolic blood pressure (DBP) represents the force remaining in the arteries during ventricular relaxation. *(Tortora & Derrickson 2007, p. 754)* Blood pressure is typically described first systolic and then diastolic and it is described with millimeters of mercury (mmHg) because of mercury used in historical measuring devices. An average healthy blood pressure of a person is 125/70 mmHg. *(Fahey et al. 2004 p.11; Larkin 2005 p. 32).* According to Ma & Chang *(2005),* especially in recent years, blood pressure variability (BPV) receives increasing attention because it provides independent information about autonomic cardiovascular regulation and prognostic indications for cardiovascular mortality. Many studies have been carried out in order to correlate BPV with various pathologies in autonomic nervous system.

3 Theory of the measurements

3.1 Electrocardiography

Electrocardiography (ECG) is registering heart's electrical action potentials. These action potentials are rather strong. They are conducted through whole body because of body's own fluids thus they can be detected almost anywhere from the surface of human body. To make ECG measurement results comparable with each other, there have been developed standard measurement methods. With continuous ECG recording the exceptional electrical or muscular behaviour can be detected. (*Haarnoja 2012, p.11*)

The 12-lead ECG system is most commonly used clinical ECG system. There six of electrodes are attached to the limbs, so called precordial leads, and three to the limbs, so called limb leads. Last three of leads are called Einthoven leads. Einthoven leads, presented in figure 2 R,L and F, describes potential differences of certain points. Over 90% of heart's electrical activity could be sufficiently explained with these three leads. Two of the limb leads and one precordial limb lead would be needed. *(Malmivuo & Plonsey 1995)*

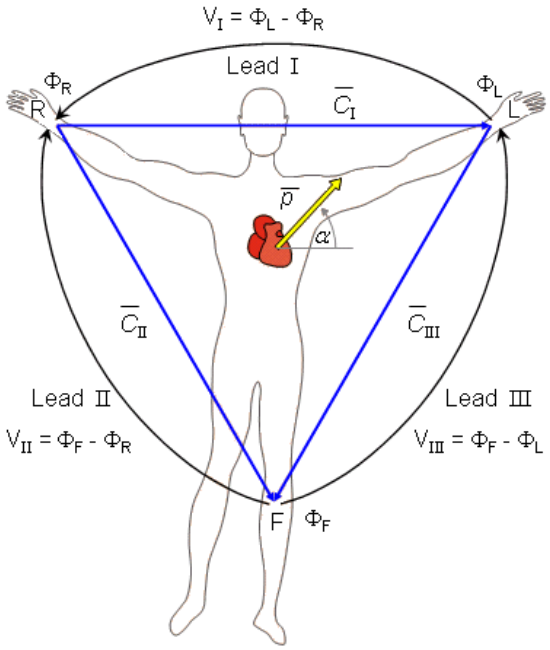

Figure 2 presents Einthoven limb leads (R, L, F) and Einthoven triangle is marked with blue. *(Malmivuo & Plonsey 1995, figure modified)*

Einthoven triangle, marked with blue in figure 2, is an approximate description of the lead vectors associated with the leads. Einthoven limb lead placements are used in ECG signal recordings to detect ECG signal. The voltages measured by the three limb leads are proportional to the projections of the electric heart vector on the sides of the lead vector triangle, Einthoven limb leads are defined in the following way.

Lead I: $V_I = \Phi_L - \Phi_R$
Lead II: $V_{II} = \Phi_F - \Phi_R$
Lead III: $V_{III} = \Phi_F - \Phi_L$

, where V_I = the voltage of Lead I
V_{II} = the voltage of Lead II
V_{III} = the voltage of Lead III
Φ_L = potential at the left arm
Φ_R = potential at the right arm
Φ_F = potential at the left foot

In figure 3 we can see PQRST-complex of the normal healthy heart. From the complex we can differentiate that the P wave, which shows the amplitude and time of atrial depolarization. Q valley can be detected after P wave. QRS-wave has the biggest amplitude and it is result from ventricular depolarization. T wave is the result of ventricular repolarization. Figure 3 also presents QT interval, which is calculated from beginning of Q wave to the end of T wave. RR interval is interval between R peaks of two separate PQRST complexes. According to Baura *(2002, p. 166)* ECG signals are typically in the range of ± 2mV and require bandwidth of 0,005 to 150 Hz to be recorded.

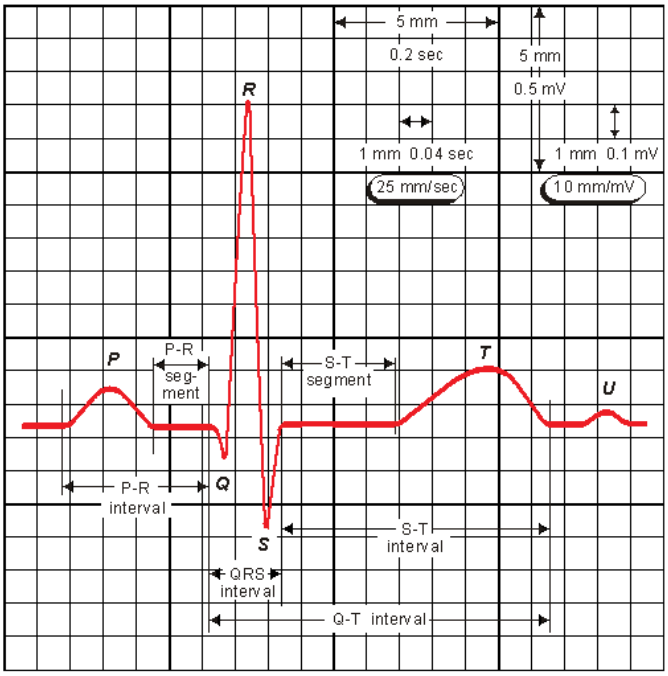

Figure 3 describes the normal electrocardiogram where QRS-complex and P-,T-,U-waves can be noted. *(Malmivuo & Plonsey 1995, figure modified)*

The generation of actual ECG wave can be described by supposing that one side of the cells are completely at rest phase, their potential is zero. Through cardiac conduction system explained, a propagating wave once initiated continues to propagate to the parts still at rest, because of very low resistance of the heart. In figure 4 formation of ECG signal in the Einthoven leads is presented. *(Malmivuo & Plonsey 1995)*

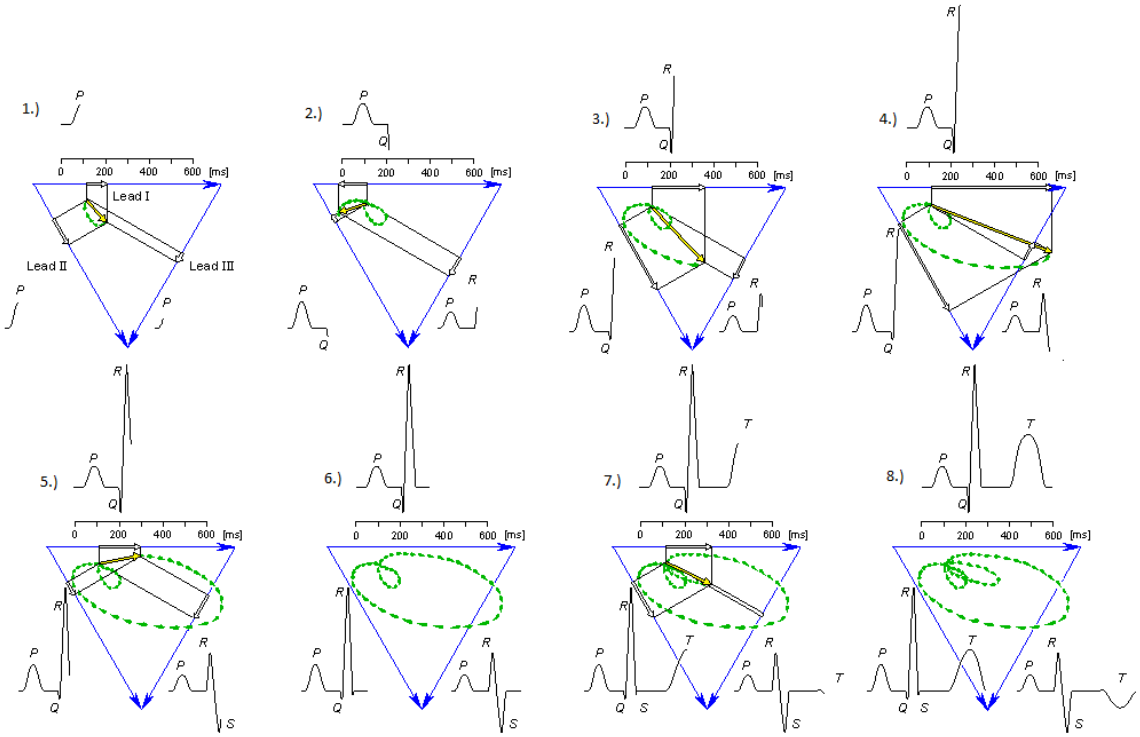

Figure 4 clarifies formation of ECG signal in the Einthoven leads. Einthoven triangle marked with blue. Resultant vector of electrical activity wave front (green) is illustrated with thick yellow arrow. *(Malmivuo & Plonsey 1995, figure modified)*

In figure 4, formation of ECG signal in the Einthoven leads is presented. Next presentation assumes that heart has electrophysiological behaviour of uniform fibres and the sequence of activation wave front has been plotted from which spatial gradient is taken. The formation of ECG signal in the Einthoven leads can be described by following way:

1. Electrical activation begins at sinus node and the wave front spreads along atrial walls. The resultant vector compared on each measuring leads is positive.
2. Next propagation reaches the AV node where the propagation wave is slowed down, when P wave is formed. Once the wave has reached the ventricles the propagation proceeds along the Purkinje fibres to inner wall. This ventricular depolarization starts from the left side of the walls separating ventricles, called ventricular septum, and therefore resultant dipole point to right. This causes a negative signal in leads I and II which forms Q valley.
3. Then propagating wave occurs in both sides of the septum and their electric forces cancel. At the same time activation in apex is occurring when the resultant vector points to apex.
4. Then the propagating wave reaches the wall of right ventricle and last the wall of left ventricles, because on the ventricular wall is thicker. This is how the activation on left ventricle can continue even after right ventricle's depolarization. n. Because there are no compensating forces on right, the resultant vector pointing left reaches it maximum, R peak is formed.
5. After the depolarization wave continues to propagate. Because its area is continuously decreasing, the magnitude is continuously decreasing.
6. Until the whole ventricular muscle is depolarized.

7. The last to depolarize are basal regions of the ventricles, T wave is formed. *(Malmivuo & Plonsey 1995)*

In clinical practice it is possible to make accurate ECG diagnoses in some diseases and to estimate other diseases with acceptable probability from it. According to Malmivuo & Plonsey *(1995)*, cardiac diagnosis often needs to be verified or completely made with other diagnostic methods. There are many main application areas of ECG diagnosis, but relevant, when considering health chair, are arrhythmias and disorders in the activation sequence. Basics of cardiac rhythm diagnosis are differentiation in PQRST-wave. Because anatomical differentiations depolarization and repolarization produce clearly differentiable reflections identification of normal QRS-complex from the P and T wave does not create difficulties. One of possible diagnoses made with health chair could be atrial flutter when the heart is sufficiently elevated so that isoelectric interval between the end of T and beginning of P disappears. In atrial flutter impulses, travel in circular course in atria. When atrial activation is fully irregular and produces irregular fluctuations in baseline it is called atrial fibrillation. In ventricular arrhythmias ventricular depolarization is distorted and is clearly detectable because of its high amplitude. *(Malmivuo & Plonsey 1995)* Disorders in activation sequence can be detected by analysing QT and RR intervals. QT interval means the time interval between the Q wave and the end of T wave. RR interval means the time interval between R peaks of the two consecutive waves. These intervals give essential information about risk of sudden death or dangerous arrhythmias. *(NIH 2013)*

3.1 Pulse oximetry

Pulse oximetery is a monitoring technique for monitoring patient's partial blood oxygen saturation (SpO2), plehtymography signal and pulse rate. Plethysmography signal tells the changes of volume of blood in the part measured, for instance earflap of fingertip. In figure 5 is a typical photoplethysmograpic signal and SpO_2 value measured with pulse oximeter. *(Moyle 2012, p. 5, 17)*

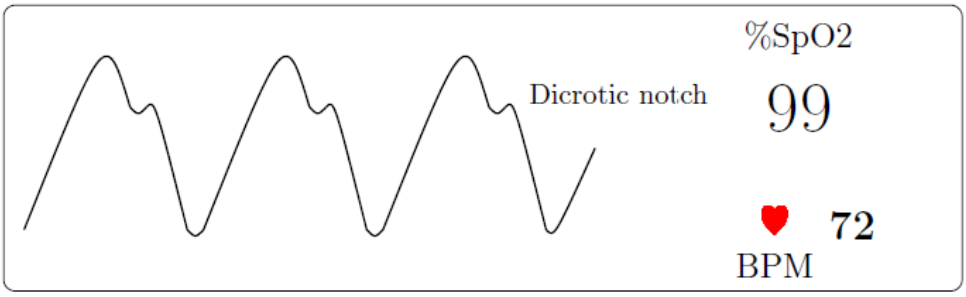

Figure 5 is a typical view of pulse oximetry where plethysmogram wave, SpO2 and pulse rate is shown. *(Urpalainen 2011, p. 9)*

The early generations of pulse oximeters all used same wavelengths, 660 nm (red) and 940 nm (infrared) generated in a probe by combining light-emitting diode with a photo detector, thus providing a compact probe for attachment to the fingertip of ear. Modern pulse oximeters, for instance transmission, reflection and intrauterine, make use of other wavelengths. Nowadays, much greater range of wavelengths is available. *(Moyle 2012, p. 5, 17)*

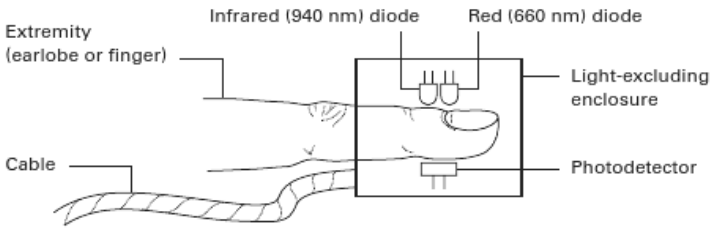

Figure 6 includes components of pulse oximeter finger probe. *(Moyle 2002, p. 18)*

Two-wavelength pulse oximetry is based on two principles: distinction of aerterial blood pulsation from other tissue and different absorption spectra of oxyhemoglobin (HbO_2) and reduced hemoglobin (Hb). Pulse oximetry can differentiate between pulsatile arterial blood and venous capillary blood, which is smooth and flowing. It is essential tool in current practice of medicine. Current two wavelengths pulse oximeters function by comparing the absorption of energy at two-wavelengths, usually 660 nm and 940 nm. A value of partial blood oxygen saturation (SpO_2) is determined from the ratio of the absorption of the energy at these wavelengths. Oximetry by any spectrophotometric method relies on the changes of absorption of electromagnetic energy with change in the percentage of oxygen bound to the haemoglobin molecule. Oxyhaemoglobin and reduced haemoglobin have their own characteristic colours described with their excitation coefficient. Wavelengths most commonly used in pulse oximeters 660 nm (red) and 940 nm (infrared) are marked to figure 7. These wavelengths have been chosen because of large difference between absorptions of haemoglobin (HbO_2) and reduced haemoglobin (Hb). (*Moyle 2002, p. 15-19)*

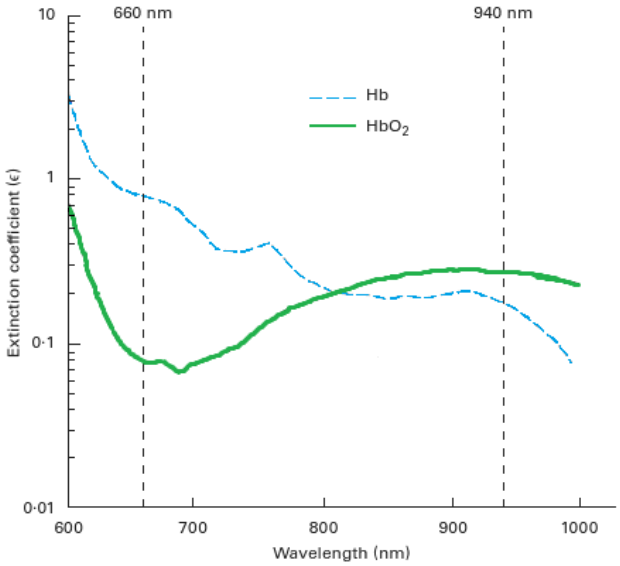

Figure 7 presents the absorption spectra of oxygenated and deoxygenated haemoglobin on the most used wavelengths. *(Moyle 2002, p.16, figure modified)*

The measuring principle of pulse oximetry is based on Beer-Lambert law. It describes relation of the absorption of light to the properties of material through it is travelling.

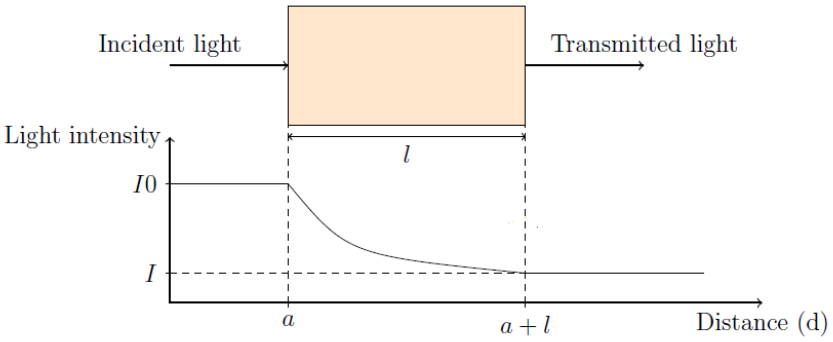

Figure 8 present a basic demonstration of oximeter. *(Modified from Upralainen 2011 p. 10; Baura 2002 p.73)*

Mathematically law can be expressed as in equation 1:

$$I = I_0 e^{-\varepsilon_\lambda c l} \qquad (1)$$

, where I is transmitted light
I_0 is the incident intensity
ε_λ is the absorptivity of the absorbent at wavelength λ
c is the concentration of the absorbent
l is the optical path-length of the sample

Beer-Lambert law holds only for monochromatic radiation through a homogenous and isotropic medium, it is valid when there is one unknown substance solution, which is clear and non-turbid, and constant path-length. There should not be chemical reaction between the absorbent and solvent and no possibility of photochemical reaction. Although principle of pulse oximeter relies on Lamber-Beer law, conditions make it clear that calibration of pulse oximeter is empirical. This is because of variable path length, different substances in the tissue apart from haemoglobin and the diffusion, refraction and reflection of the tissues. The unscattered absorbance of this process is the natural logarithm of the ratio of transmitted light to incident intensity

$$A_\lambda = -ln\frac{I}{I_0} = \varepsilon_\lambda c l \qquad (2)$$

, where A is absorbance at wavelength λ

When more than one substance absorbs light, each absorber contributes its part in total absorbance, presented in equation 3:

$$A_{T\lambda} = \sum_{i=1}^{n} \varepsilon_{\lambda_i} c_i l_i \qquad (3)$$

, where A_T is total absorbance at wavelength λ
n presents number of absorbers

If two wavelengths of light are transmitted through a sample containing only HbO_2 and Hb, the functional arterial oxygen saturation can be determined as (*Baura 2008 p. 5; Baura 2002 p.69):*

$$S_pO_2 = \frac{[HbO_2]}{[Hb]+[HbO_2]} \quad (4)$$

Because the extinction coefficient of haemoglobin and deoxygenated haemoglobin differ at each wavelength their respective concentrations can be determined from equation 3 by solving for two unknown concentration using two wavelengths equations. These concentrations are substituted in equation 4 to determine oxygen saturation using two wavelengths the total absorbance can be written by using equation 3.

$$A_{red} = \varepsilon_{0_{red}} c_0 l_0 + \varepsilon_{d_{red}} c_d l_d + \varepsilon_{x_{red}} c_x l_x + A_{y_{red}} \quad (5)$$

$$A_{ired} = \varepsilon_{0_{ired}} c_0 l_0 + \varepsilon_{d_{ired}} c_d l_d + \varepsilon_{x_{ired}} c_x l_x + A_{y_{ired}} \quad (6)$$

, where subscript *0* refers arterial oxyhaemoglobin
subscript *d* to arterial deoxyhaemglobin
subscript *x* refers to variable absorbance not from arterial absorbance
subscript *y* refers to nonspecific sources of optical attenuation

To isolate the contributions of arterial blood, only the pulsating absorbances are analysed. By taking the time derivative from the absorbances. The last two terms in equations 5 and 6 go to zero.

$$R = \frac{\frac{dA_{red}}{dt}}{\frac{dA_{ired}}{dt}} = \frac{\varepsilon_{0_{red}} c_0 \frac{l_0}{dt} + \varepsilon_{d_{red}} c_d \frac{l_d}{dt}}{\varepsilon_{0_{ired}} c_0 \frac{l_0}{dt} + \varepsilon_{d_{ired}} c_d \frac{l_d}{dt}} \quad (7)$$

In addition, an assumption that blood bath length changes dl_0/dt *and* dl_d/dt are equivalent. The ratio *R* of two absorbance derivatives remains constant:

$$R = \frac{\varepsilon_{0_{red}} c_0 + \varepsilon_{d_{red}} c_d}{\varepsilon_{0_{ired}} c_0 + \varepsilon_{d_{ired}} c_d} \quad (8)$$

Recalling the equation 4 that functional arterial oxygen saturation is calculated from $c_0 = [HbO_2]$ and $c_d = [Hb]$. By solving the relationship of c_0 and c_d from equation 8, we get relationship of $[HbO_2]$ and $[Hb]$. Then by placing these to equation 4, we can calculate the SpO_2 value what leads to: *(Baura 2002 p.69-74; Baura 2008 p. 54-55; Urpalainen 2011, p. 10-13)*

$$SpO_2 = \frac{\varepsilon_{d_{ired}} \cdot R - \varepsilon_{d_{red}}}{\left(\varepsilon_{0_{red}} - \varepsilon_{d_{red}}\right) - \left(\varepsilon_{0_{ired}} - \varepsilon_{d_{ired}}\right) \cdot R} \quad (9)$$

Photoplethysmogram is optically obtained plethysmogram, which is a volumetric measurement of an organ. Photoplethysmographic (PPG) signal is a transmission signal of altering arterial blood component. It is normalized with constant component reflecting the absorption of static arterial blood component, venous blood and other tissues *(Moyle 2002, p. 5- 11*). The most important function of PPG is to ensure the functionality of the pulse oximeter. If PPG signal indicates strong dissimilarity during dicrotic notch the SpO_2 value could be unreliable. In addition, to recognizing unreliable SpO_2 measurement, it can also be used in diagnosing cardiac functions, vascular compliance and perhipheral blood flow. (*Moyle 2002, p.52- 53*) Researches have suggested it could be used to determine systolic blood pressure with pulse transit time method. *(Hey et al. 200; Espina 2006)*

Photoplethysmography is composed from pulsatile component (AC) and non-pulsatile component (DC). Ac is synchronized with the heart and to arterial pulsation, while DC is related to light absorption in the tissue, vein and diastolic arterial blood volume. According to Lambert-Beer law presented in equation 1, the photo detector detects photons not absorbed in blood so AC is generated by the optical path length, that changes due to increase of blood volume. The waveform of general PPG can be gained by inversing or subtracting the amount of light not absorbed at a constant. *(Lee et al. 2011)* Figure 9 present a typical photoplethymographic signal.

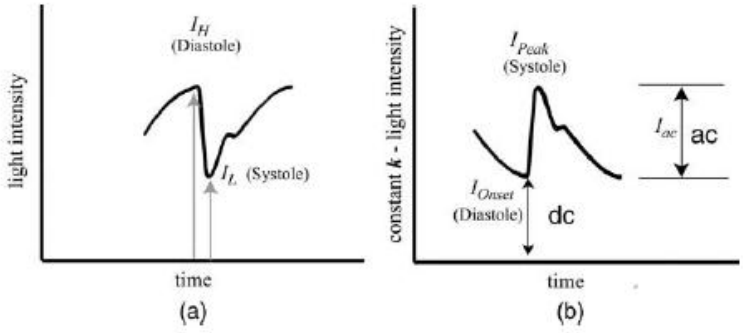

Figure 9 presents a typical photoplethysmographic signal. (a) A raw signal measured from a photo detector. (b) Final signal, constant *k*-reflect light intensity. *(Lee et al. 2011)*

The onset and peak of PPG and constant *(k)* can be represented with equations 10 and 11.

$$I_H = I_0 e^{-b_{dc} d_{dc}} e^{-b_{Hb+HbO2} d_{min}} = k - I_{onset} \qquad (10)$$

, where I_H is the large value of the reflected amount of light and the onset point of PPG
$b_{dc} = \varepsilon_{dc}(\lambda) c_{dc}(\lambda)$ is a function of absorption and attenuation constant
$\varepsilon_{dc}(\lambda)$ is an extinction coefficient
$c_{dc}(\lambda)$ is a concentration of absorbing substance
d_{dc} is optical path length
Hb stands for haemoglobin
HbO_2 stands for oxyhaemoglobin
d_{min} is basal diameter of arterial vessel before pulsation
I_{onset} is a DC component and a non-pulsatile component of PPG signal

$$I_L = I_0 e^{-\varepsilon_{dc} c_{dc} d} e^{-b_{Hb+HbO2} d_{max}} = k - I_{peak} \qquad (11)$$

, where I_L is the small value of the reflected amount of light and peak of PPG point
I_{peak} is the peak value of pulsatile PPG component
d_{max} is the maximum variation of arterial diameter during pulsation

PPGs AC component can be presented by subtracting (I_H) from peak (I_L), in equation 12.

$$I_{ac} = I_L - I_H \qquad (12)$$

3.2 Blood pressure measurements

There are variety of blood pressure measuring methods such as intra-arterial method, auscultatory method and oscillometric method. The first method established was direct intra-arterial recording method. In intra-arterial method, the catheters are positioned directly into circulatory system. It permits continuous measurement of blood pressure on a beat-to-beat basis. Thus momentary fluctuations of blood can be detected. These measures are still considered to be golden standards of blood pressure measurement, but its impracticality for clinic use is widely recognized. A value of blood pressure is usually presented in millimetre of mercury (mmHg), for historical reasons. The primary method to determine blood pressure these days is auscultatory method, invented by Riva-Rocci in 1896. It is non-invasive and determines the blood pressure with the help of cuff wrapped around arm or length. The cuff is filled until the blood flow is entirely blocked. When air pressure is slowly released from the cuff audible sound can be detected with stethoscope, by now variety of device has invented to detect sounds automatically. Systolic blood pressure (SBP) is detected first when blood begins to resume and sounds can be heard. When air pressure is lowered more, then disappearances of these sounds coincide with diastolic blood pressure (DBP). In ausclutatory method the examiner must attend to several factors: an occluding cuff of appropriate size, standard arm placement, positioning of cuff at heart level having the patient adapt to stands body posture. A second type of non-invasive blood pressure measurement is oscillometric method. It operates by sensing the magnitude of oscillations caused by the blood as it begins to flow again into the limb. This marked increase in amplitude of oscillation is SBP value. DBP value is marked when oscillations levels off. Although the oscillation with the greatest amplitude has been proven to reliably correspond with mean arterial pressure determination, SBP and DBP values are often less accurate than in auscultatory measures. It tends to overestimate SBP and underestimate DBP. Both auscultatory and oscillometric methods of blood pressure are intermittent methods. A single determination of blood pressure can take entire minute to obtain. Additionally, a brief rest period is recommended between the measures that allow circulation under cuff to return normal. *(Larkin 2005, p. 31-35)*

In addition, two non-invasive blood pressure methods have been developed: the vascular unloading method and pulse transit time method. Vascular unloading method obtains estimates of blood pressure from small-pressurized cuff positioned over a finger in con-

junction with photoplethysmograph. Blood flow oscillations are sensed by the encircling finger cuff and translated into beat-to-beat estimates of blood pressure. The cuff stays pressurized during the measurement and can become uncomfortable for during extended measurement periods. The method is under criticisms. Larkin *(200,5 p. 35)* tells that various studies report that it underestimates blood pressure or it over estimates it. Despite of its inaccuracy in the continuous finger arterial recordings, Parati *(et al. 1989)* suggested that in could provide a reliable index of change in blood pressure in response to acute environmental stimuli. *(Larkin 2005, p. 35)*

Another non-invasive blood pressure method is pulse transit time (PTT) method. It reflects the time the pulse wave takes to travel from heart to the site in peripheral circulation, typically finger of earlobe. It measures the time between initiation of cardiac contraction from the electrocardiogram (ECG) to arrival of pulse wave at peripheral site measured with photoplethysmography, usually finger or earlobe. When arterial pressure increases the pulse wave travels more quickly and lowers pulse transit time and conversely when blood pressure decreases PTT lengthens *(Zakaria et al. 2010; Larkin 2005 p. 35).* Although studies are comparing PTT with blood pressure, they have yielded significant inverse correlation between PTT and systolic blood pressure, not diastolic blood pressure *(Chen 2000; Zakaria 2010).* According to Larkin *(2005, p.35),* Newlin *(1981)* disagreed that PTT presents the index of blood pressure. He had considerable evidence suggesting that it was more strongly linked to beta-adreneric cardiac activity than to blood pressure. Hey *(et al. 2009)* tells in his paper that with PTT one can get comprehensive information about cardiovascular state. It was noted that longer the length between heart and the PPG measurement point, for instance fingertip, the smaller are the error in time domain. This is one reason why the fingertip is most used PPG measurement point, although fingertip as a measurement point is more prone to error caused by movement. *(Hey et al. 2009*)

According to various researches calculating PTT measurement has been started from the peak of ECG's R wave *(Chen et al. 2000; Hey et al. 2009; Ma & Zhang 2005; McCarthy et al. 2011; Zakaria et al. 2010).* Some papers introduce that PTT can be calculated from the peak of ECG R-wave and to the peak of the PPG signal *(McCarthy et al. 2011; Zakaria et al. 2010).* According to McCarthy's *(et al. 2011)* investigation PTT measured from peak-to-peak shows good correlation with measured SPB with clinically validate blood pressure measurement device. The mean difference between all the results for each of the volunteer was less than 3 mmHg. However, there was quite large standard deviation. It must be noted that blood pressure tracking was done using constant recalibration at 5 minutes intervals. Zakaria *(et al. 2010)* also measured SBP with PTT from peak of the ECG's R wave to peak of the PPG wave. He claims that measuring PTT from peak of the R wave to the peak of the PPG-wave is widely accepted. Zakaria accomplished different experiments in only relax condition and in relax, exercise and recovery condition. The most accurate results were collected from an individual in three different conditions. The result of investigation was that using the method to estimate SBP with help of PTT is achievable. *(Zakaria et al. 2010)*

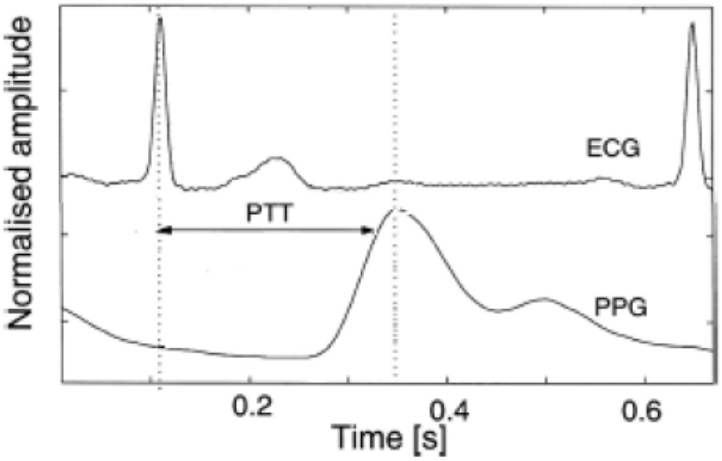

Figure 10 shows the definition of pulse transit time in various studies. *(McCarthy et al. 2011)*

Chen *(et al. 2000)* measured PTT from peak of R wave to the onset of PPG wave. He found reliable information that SBP changes can be extracted from the variation in pulse arrival time although it is not enough accurate to estimate absolute blood pressure. Chen speaks in his paper about pulse arrival time (PAT) instead of PTT. Many speak about PTT meaning same as Chen's PAT. He divides pulse arrival time (PAT) consisting from two components: the isovolumetric contraction time or pre-ejection period (PEP) and pulse transit time (PTT). The contraction time is the interval during contraction of myocardium when intraventricular pressure rises sufficiently to open the aortic valve and push blood out of the ventricles. Chen explains that isovolumetric contraction time has been found to be sensitive to the sympathetic nerve system rather than blood pressure. For instance some beta-adrenergic blocking agents have been found to reduce isovolumetric contraction time. He speaks that pulse transit time indicates the time delay from aortic opening to the arrival of the blood pulse wave at peripheral vessels, which is inversely proportional to the pulse wave velocity. As well, Chen determines that method is neither compatible to determine absolute blood pressure or detecting small changes of blood pressure but is compatible for monitoring blood pressure in long periods. Chen proposes that to determine slow changes in blood pressure intermittent calibration measurement could be used when measuring SBP continuously. Chen proposes that by integrating the estimation algorithm into an automatic system of cuff control a convenient non-invasive blood pressure monitoring system can be realized. In his research he examined 20 patients during cardiovascular surgery. The estimated values of SBP were compared with values measured invasively. The result showed the correlation coefficient 0.97 ± 0.002 (mean ± standard deviation) and error remained with in ±10% in 97.8 %. *(Chen et al. 2000)*

Hey *(et al. 2009)* introduces that PTT can be determined by calculating the time difference between R-wave of the ECG signal and P-base point of the PPG signal. P-base point corresponds to the intersection point between the maximal slope during systolic rise phase and the horizontal line going through the point having the absolute minimum, introduced in figure 11. He explains that the main advantage of using the P-base point is that it guarantees a better noise and artefact robustness, because it is determined out of two characteristic points in the pulse wave. *(Hey et al. 2009)*

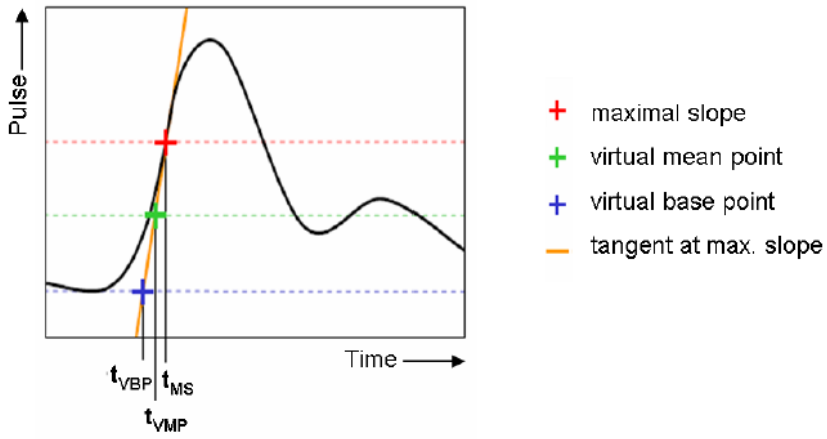

Figure 11 describe determination of the virtual base point or P-base point. *(Hey et al. 2009)*

Hey *(et al. 2009)* suggests that due to physiological and anatomical limitations limitation such as pulse wave velocity and length of blood vessel segment, the PTT is constrained to be in a defined interval, which he suggests to be 0,11- 0,475 seconds. In this calculation, he considers a minimal pulse wave velocity to be 4 m/s and maximal 20 m/s a minimal length of the measurement segment to be 0,2 m to 1,5 m. In addition he estimates the maximal pre-ejection period (PEP) to be 0,1 s, which is compromised. *(Hey et al. 2009)* This is harsh approximation but gives an idea of the length of the PTT.

PTT is influenced by multiple physiological and anatomical factors, such as cardiac output, the elastic properties of arteries (arterial stiffness, arterial diameter), blood viscosity venous return and other cardiovascular variability's *(Ma & Zhang 2005; Zakaria et al. 2010).* The main difficulty of the method is that the elasticity of the vessel wall is not constant. It has been found to differ individually and is affected by neuro-humoral factors. It has been suggested that PTT might not be sufficient to estimate absolute blood pressure. *(Chen et al. 2000)* Commonly PTT has been inversely related to systolic blood pressure. In papers of Zakaria *(et al. 2010)*, Ma and Zhang (*2005)*, they propose that it could be a good parameter to indicate blood pressure changes. They present that PTT has been suggested as a non-invasive and cuff less means for continuous blood pressure measurement in many researches. Ma and Chang *(2005)* present, same as Chen *(et al. 2000)*, Zakaria *(et al. 2010)* and McCarthy *(et al. 2011)*, that short-term variability in PTT and blood pressures is expected to be highly correlated with each other in certain circumstances. Ma and Chang also explain that both blood pressure and PTT are important signs of cardiovascular circulation the association between the short-term fluctuations in them could also convey important information of regulatory mechanism within cardiovascular system. In paper, they conclude that PTT is highly associated with blood pressure and can be potentially used for blood pressure variability estimation for subject at static body state. Ma and Zhang *(2005),* Zakaria *(et al. 2010)*, Chen *(et al. 2000)* and McCarthy *(et al. 2011)* states PTT is ideal for continuous 24-hour blood pressure measurement since it is both cuff less and non-

invasive therefore comfortable and unobtrusive for the patient.

Blood pressure is normally presented in millimetres of mercury (mmHg). Pulse arrival time in units of milliseconds tells a little for health care personnel who have not been engrossed with the matter. If blood pressure is presented using pulse arrival time it must be converted millimetre of mercury, which is more informative to health care personnel. Chen *(et al. 2000)* estimated blood pressure using pulse arrival time by using a system with automatic cuff inflation and deflection to acquire intermittent SBP values. Chen (*et al. 2000*) concluded equation 13 by using pulse wave velocity, gravitational properties and properties of vessel, blood and blood pressure.

$$P_e = P_b - \frac{2}{\gamma T_b}\Delta T \qquad (13)$$

, where P_e is estimated blood pressure
P_b is base blood pressure
γ is an elastic modulus coefficient of the vessels
T_b is PTT value corresponding P_b
ΔT is changes in pulse arrival time

According to Chen (*et al. 2000*) in equation 13 elastic modulus coefficient *(γ)* of the vessels ranges from 0.016 to 0.018 $mmHg^{-1}$ what depends on the particular vessel. He claims that blood pressure estimation can be given during short period of time if the change in vessel elasticity is negligible. He adds that the coefficients should be determined by repeating the calibration and that coefficient are only valid if elasticity of the arterial walls stays constant. McCarthy *(et al. 2011)* used almost same formula as Chen *(et al. 2000).*

3.3 Bioelectrical impedance

The electrical bioimpedance (EBI) has many practical applications related to monitor physiological events. For instance, impedance plethysmography measures small changes in electrical resistance in some regions of the body to asses changes in blood volume. Bioelectrical impedance analysis (BIA) makes use of EBI in the assessment of the amount of body water and body composition. *(Blomqvist 2012)* BIA is a simple inexpensive, quick and non-invasive technique for measuring body composition. *(Muobarak 2012)* Impedance (Z) describes circuit's property to resist electrical current (I) when a voltage (U) is over the circuit. Impedance describes relation of voltage and current with following equation:

$$Z = \frac{U}{I} = R + jX \qquad (14)$$

, where Z is impedance
U is voltage
I is current

R is resistance
X is reactance

When considering alternating current (AC), the phase of voltage and current can be can be different. This is why complex values are used to present impedance. Electrical bioimpedance (EBI) or bioelectrical impedance describes tissue's property to resist electrical currents. Biological tissue consists from cells surrounded by extracellular medium. Cells are composed of several organelles and intra cellular medium enclosed by cell membrane. (*Ruiz 2011, p.6*) Bioelectrical impedance analysis (BIA) allows the determination of fat-free mass (FFM) and total body water (TBW) in subjects without fluid and electrode abnormalities *(Kyle et al. 2004).* The electrical impedance of the material is given by impedance times its shape factor. The shape factor depends on the length of the volume conductor and the available surface for the electrical current to flow. *(Martinez 2007, p.22)* The principle of bioelectrical impedance analysis (BIA) from human body can be described with help of a cylinder, in figure 12.*(Kyle et al. 2004)*

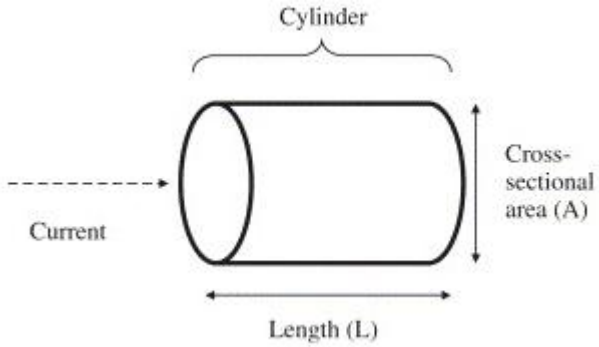

Figure 12 shows the cylinder model from the relationship between impedance and geometry. *(Kyle et al. 2004)*

Kyle *(et al. 2004)* explains in his paper about the electrical properties of body that although body is not a uniform cylinder and its conductivity is not constant, an empirical relationship can be established between impedance quotient and volume of water. Water contains electrolytes that conduct the electrical current through body. The resistance *(R)* of a length of homogenous conductive material of uniform cross-sectional area is proportional to its length *(L)* and it is inversely proportional to its cross sectional area *(A)* described in equation 13. *(Kyle et al. 2004)*

$$R = \frac{\rho L}{A} = \frac{\rho L^2}{V} \tag{15}$$

, where ρ is the resistivity of conductive material.
L is length
A is cross-sectional area
V is volume

Due to body's field inhomogeneity the equivalent cylinder model must be matched with an appropriate coefficient to real geometry. This coefficient depends on various factors and the anatomy of the segment under investigation. Other challenges are that in practice it is easier to measure height than conductive length and body has two types of re-

sistivity to an electrical current: resistance and reactance. The capacitive resistance (reactance) arises from cell membranes and resistance from cellular fluids. There have been presented variety of cellular circuit models. Figure 13 demonstrates one of the most used simple equivalent cell circuit model, as well known as Fricke's electrical model. The capacitive component *(C)* is related to bilayer of cell membrane *(Ruiz 2011, p.6)*, sometimes presented as capacitive reactance (X_C) (*Kyle et al. 2004)*, R_e *is* extra cellular water *(mostly* H_2O*-Na*) and R_i intra cellular water *(mostly* H_2O*-K). (Ruiz 2011; Kyle et al. 2004)*

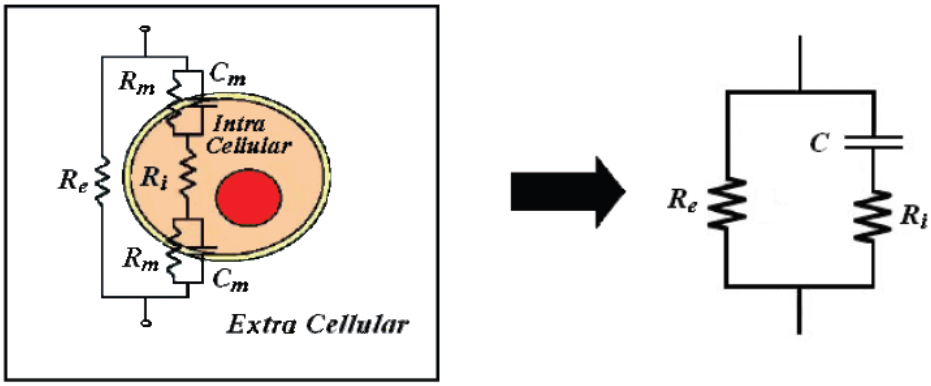

Figure 13 describe Fricke's electrical model and circuit presentation on the right after simplification. Membrane resistance R_m is very small and thus disregarded. *(Ruiz 2011 p.6; figure modified)*

From figure 13 can be seen that at zero or low frequency current does not penetrate cell membranes acting as insulator. Therefore the current passes through extra cellular fluid, which is responsible from measured *R* of total body resistance. Theoretically at infinite the capacitor behaves as perfect capacitor. Therefore the total body resistance represents both the extracellular and intracellular fluid (total body water, TBW). Since practical constrains prevent the use of direct current (DC) and infinite high frequency alternating current (AC), the R values for these frequencies are predicted using Cole-Cole plot presented in figure 14. *(Kyle et al. 2004)*

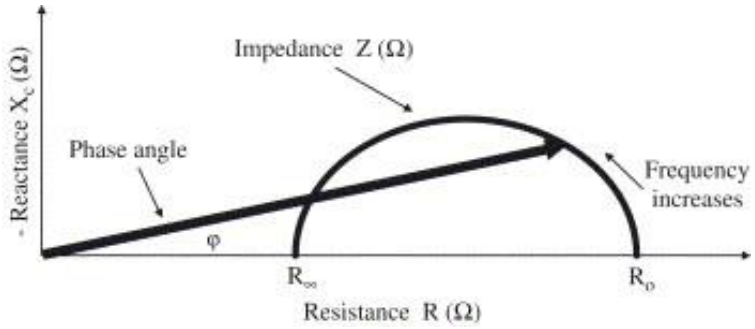

Figure 14 presents Cole-Cole plot where phase angel's *(φ)* relationship with resistance *(R)*, reactance *(X_C)* and impedance *(Z)* are presented. *(Kyle et al. 2004)*

There are several methods for bioelectrical impedance analysis (BIA). Considering this thesis it is necessary for reader to introduce single frequency BIA (SF-BIA) and multi-frequency BIA (MF-BIA). SF-BIA is measured with single frequency, generally 50 kHz. Electrodes are typically placed on the right hand and the right ankle. With single frequency it is not possible to measure total body water (TBW). With SF-BIA one can

have estimates from fat free mass (FFM) and TBW based on mixture of empirical theories. MF-BIA includes impedance in multiple frequencies. It uses empirical linear regression models. It can be used to evaluate FFM, TBW, intra cellular water (ICW) and extra cellular water (ECW). At frequencies under 5 kHz and above 200 kHz poor reproducibility of the measurements has been noted *(Kyle et al. 2004)*. MF-BIA has proven to be less biased and more precise than the SF-BIA for extracellular fluid estimation but more biased and less precise for TBW estimation *(Ruiz 2011, p.7-8).* According to Webster *(2010, p. 372)* the advantages of electrical-impedance plethysmography, meaning in this case measuring volume changes, are that it is non-invasive and it is relatively simple to use. The disadvantages are that it is not sufficiently accurate for many of the attempted applications and that even the cause of the change in impedance is not clear in some cases. Muobarak *(2012)* explains that BIA can be used for estimating overall survival of cancer patients. It also gives relevant information about FFM, body fat and body cellular mass.

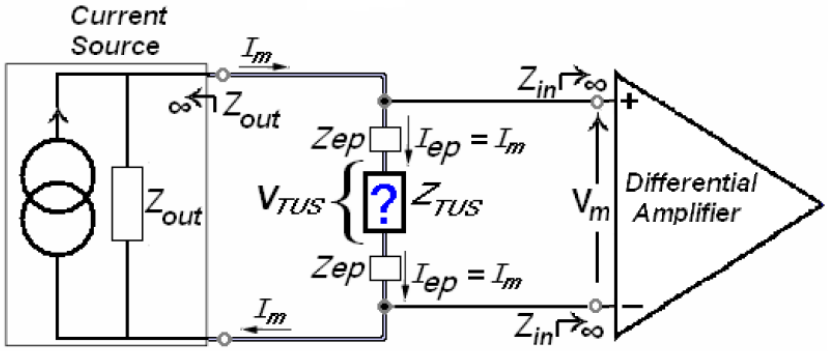

Figure 15 a two-electrode bioelectric impedance instrumentation setup. In figure Z_{ep} is sensing electrode polarization impedance, V_{TUS} is measured voltage in tissue under study and Z_{TUS} its impedance and V_m measured voltage. *(Martinez 200,7 p.32, figure modified)*

EBI measurement is performed measuring the current generated by a known voltage applied on the tissue. The voltage is measured with differential amplifier. In the two-electrode configuration the same two electrodes are used to current injection and for sensing of resulting voltage signal. The main drawback of two-electrode instrumentation setup is that the same two electrodes are used for electrical current injection and sensing resulting voltage. The voltage generated by the electrode polarization impedance *(Z_{ep})*, in figure 15, is included into the voltage measurement. It cannot be distinguished. The voltage has been generated by current flowing through tissue or by the current flowing across the skin-electrode interface. Equations from 16 to 19 show the influence of the electrode polarization impedance *(Z_{ep})* on the calculations of the measured impedance (Z_m) from the measured voltage *(V_m)*. *(Martinez 2007 p.32; Ruiz 2011 p. 9)*

$$Z_m = \frac{V_m}{I_m} \qquad (16)$$

, where Z_m is measured impedance
V_m is measured voltage
I_m is measured current

$$V_m = V_{ep} + V_{TUS} + V_{ep} = V_{TUS} + 2V_{ep} \quad (17)$$

, where V_{TUS} is measured voltage
V_{ep} is electrode polarization voltage

$$V_{ep} = I_m Z_{ep} \quad (18)$$

, where Z_{ep} is electrode polarization impedance

$$Z_m = \frac{V_{TUS}+2V_{ep}}{I_m} = Z_{TUS} + 2Z_{ep} \quad (19)$$

, where Z_{TUS} is impedance in tissue under study

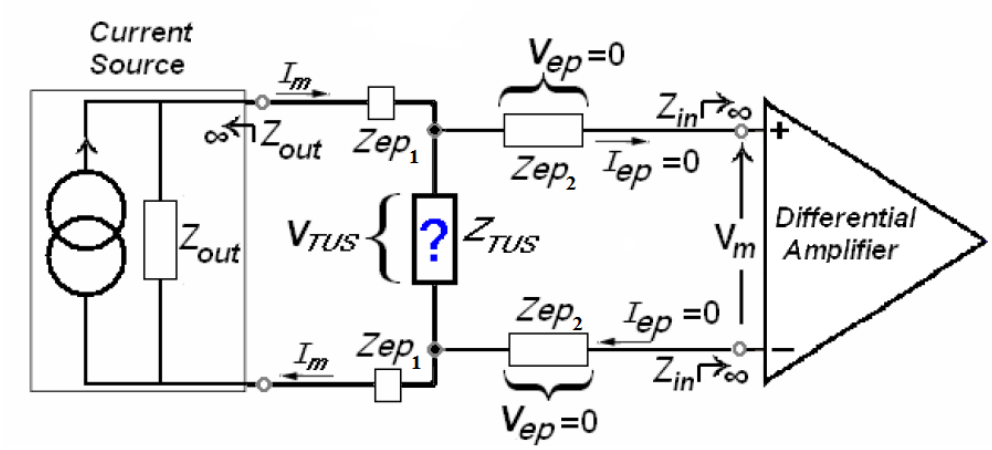

Figure 16 presents a four-electrode bioelectric impedance instrumentation setup. In figure Z_{ep} is sensing electrode polarization impedance, V_{TUS} is measured voltage in tissue under study and Z_{TUS} its impedance and V_m measured voltage. *(Martinez 2007, p. 32, figure modified)*

In the four-electrode model, presented in figure 16, the current injected and response measured is done with two different electrode pairs. One electrode pair *(Z_{ep1})* is used to lead the current to the tissue under study, while second pair of electrodes (Z_{ep2}) is used to measure the voltage over tissue under study *(V_{TUS})*. With this configuration the voltage generated of the injecting leads *(Zep_1)* does not affect the voltage measurement. Considering equations 18 and 19 and that the current *(I_{ep})* flowing through the measuring electrodes is zero, when V_{ep} comes to zero, then the impedance measured *(Z_m)* is the impedance under study, presented in equation 20. *(Martinez 2007 p. 32; Ruiz 2011 p. 9-10)*

$$Z_m = \frac{V_{TUS}+2V_{ep}}{I_m} = Z_{TUS} \quad (20)$$

, where Z_m is measured impedance
V_{TUS} is measured voltage
V_{ep} is electrode polarization voltage
I_m is measured current
Z_{TUS} is impedance in tissue under study

According to Ruiz *(2011, p.11-12)* bioelectrical impedance can be affected by several other errors. There might occur unwanted capacitance in the measurement system, which will increase sensing electrode polarization impedance between sensing electrodes. These capacitances may come from capacitance between electrode leads, between body limbs and earth or between leads and ground. Effects of these capacitive leakages are small at low frequencies but can cause a tail or hook at high frequencies to Cole-Cole plot.

4 First pilot

4.1 Aim of the first pilot

The first pilot design was implemented to test the measurement devices compatibility to intended use. First pilot design worked as test platform during the whole process to test the measurement on by one in a health chair concept. The aim was to evaluate functionality of the chosen measurement modules and to assure that called measurements could be done. At this stage, it was important to evaluate the reproducibility and repeatability of the constructed pilot as a product. Following measurements were implemented:

- Electrocardiography (ECG)
- Heart rate (HR)
- Photoplethysmography (PPG)
- Partial oxygen saturation (POX)
- Electrical bioimpedance (EBI)
- Weight

4.2 Outlines of the first pilot

To better the patience comfort and to fasten ECG measurement, it was implemented with dry electrodes. Measurement points were at the hands and wrist of the patient. Then there was not need to fix electrodes on body and only pre-measurement needed would be rising of sleeve. Like Lim (et al. 2006) explained that although fixed-on-skin electrodes are reliable and give good signal quality they are inadequate and incompatible for long-term everyday measurements. Skin electrodes were incompatible solution because of necessary fixation on the body surface and their usage would also extend the pre-measurement time. To evaluate the measurements compatibility fixed-on-environment electrodes were chosen. In this case electrodes were integrated to chair armrests. Dry-electrode measurement was tested on first pilot design, but implemented only to third pilot design. Other limit to pilot design was not seen necessary.

4.3 Realization of the first pilot

Realization of first pilot design was made on wooden chair. Each module was attached on chair and tested one by one. On each commercial module LabVIEW program was made. Bioelectrical impedance module was tested with its own available program. All the testing of modules and implemented programs is explained in following chapters.

Instrumentation of electrocardiography measurement was made on EMB1 board and its available starter kit. Both are products of Corscience *(Corscience EMB1 2010)*. Module was compatible to patient monitoring with only necessary of 1-channel and four lead lead electrodes from which two were measurement electrodes. It also included real-time R wave trigger via hardware or communication protocol. There it could be synchronized to cardiac cycle from where pulse transit time could be measured. Testing of ECG module was made first with Ag/Ag-Cl skin electrodes. After receiving satisfying signal dry-electrodes made from stainless steel were used.

A pulse oximeter board ChipOx made by Corscience was chosen because of its low current consumption, which would make it compatible for battery operation. It also included output of raw plethysmograph signal in real-time, which would make compatible for pulse transit time analyses. *(Corscience ChipOx 2010)* Options for PPG and partial oxygen saturation measurements were fingertip or earflap. Those are two most traditionally used measurements. The fingertip measurement was chosen. According to Espina's research earflap measurement is less prone to motion artefacts and hydrostatic variation and more patients comfortable in long time measurements *(Espina et al. 2006).* We concluded that earflap measurement was incompatible for our needs. PTT measurement was wanted to be accurate. The measurement time on health chair would be measured in minutes. Earflap measurement would possibly require removal of earring. Earflap measurement is as well more prone to loose signal when patients suffer low blood pressure, which must be taken in consideration when measuring elderly people. Also, earflap measurement was estimated to lower patient comfort. Moyle (2002) tells that changes in pulse pressure during induction, maintenance and recovery from anaesthesia are greater when recorded from finger than from ear. He as well recommends monitoring PPG from finger whenever it is possible to gain the greatest amount of clinically useful information. (Moyle 2002, p. 56It should be noted when determining patient systolic blood pressure with pulse transit time method that the bigger the distance between PTT measurement point and the heart is, the less impact mistaken measurement values in time domain has on the PTT determination. *(Hey et al. 2009)* For this reason the pulse wave was detected from fingertip. Instrumentation of photoplethysmography and pulse oximeter was made on ChipOx miniaturized pulse oximeter module and to its development kit *(Corscience ChipOx, 2010).*

An open-source hardware module OpenEBI designed in Aalto University by Blomqvist was chosen to analyse electrical bioimpedance. The availability of commercial EBI analysers was limited. This module was easily available and knowledge and experience from it was well known. As well, setting up and validating commercial EBI measurements were estimated to be time consuming. The module uses four-electrode multifrequency measurement. MF-BIA measurement was obligatory that total body water and fat free mass could be measured. Four-electrode measurement was necessary to avoid the influence of the voltage generated by the electrode impedance. (*Blomqvist et al. 2012*) Testing of the openEBI module was executed and Cole-Cole plot, presented in figure 14, was drawn. At this stage, further investigation was not made.

Weight measurement was made with sensors taken from commercial weight scale. The possible inaccuracy with weight-scale-sensor measurement was well known, but as explained previously the aim of first pilot design was not to make as accurate measurement as possible. The sensors were placed on the bottom of the legs of the chair. Output current changes were observed with multi meter when weight was added. At this stage, further investigation was not made.

4.4 Software of the first pilot

Software interface between electronic modules and computer was implemented with LabVIEW (short for Laboratory Virtual Instrument Engineering Workbench). It is a design platform and development environment designed by National Instruments. LABVIEW is a graphical programming platform commonly used for data acquisition, instrument control and industrial automation. LabVIEW creates development systems and user interface, which are called front panels in the program. LabVIEW programs are called virtual instruments (VI's). Each VI consists from user interface and block diagram. Every user interface works in parallel with block diagram, which includes terminals, functions, constants, structures etc. Each virtual instrument can include various other virtual instruments when they are called sub virtual instruments (subVI's). *(National Instruments 2013)*

The communication protocol of ECG module EMB1 used point-to-point protocol (PPP). To filter out reserved bytes such as start flag, end flag and escape flag from data steam extra escape flags are used. This is also called octet stuffing. The octet stuffing in the transmitter occurs after the checksum calculation. For the checksum formation in the transmitter the start and end flag was not included. In the receiver, inverse octet stuffing was applied first, before the data stream is saved or further processed. In the receiver, the checksum algorithm is run over an entire packet, and then result must be zero. *(Corscience EMB1 2010, p. 16)*

Table 1 presents EMB1 packet structure and descriptions of individual fields *(Corscience EMB1 2010, p. 16)*

Start flag	Packet number	Command	Payload	Checksum	End Flag
0xFC	1 Byte	2 Bytes	x Bytes	2 Bytes	0xFD

EMB1 packet structure and individual fields are described in the table 1 above. Three special characters may not appear by accident in the packet:

- Start flag 0xFC
- End flag 0xFD
- Escape flag 0xFE

If one of these characters appeared in the data stream an escape flag is send first and then the original byte is linked with 0x20.

Table 2 describes data packet octet stuffing *(Corscience EMB1 2010, p.17)*

Characters within the packet	Are changed to the following when sent
0xFC	0xFE 0xDC
0xFD	0xFE 0xDD
0xFE	0xFE 0xDE

The packet number has a length of one byte and therefore sweeps through number 0 to 255, once 255 is reached the next packet start again with 0. The packet numbers are numbered so that missing packets can be detected, received packets can be confirmed,

undesired packets can be rejected and defective packets can be resent. The Command field is two bytes long and contains the command least significant bit (LSB) first. Payload includes the actual data to be transmitted. Checksum has a length of two bytes. The parameters of checksum are:

- CRC16 (CCIITT)
- Polynomial 0x1021
- Start value
- 0xFFFF LSB first

The checksum is calculated in the transmitter over the entire packet with the exception of the start flag, end flag and checksum. The checksum must be calculated in the transmitter before octet stuffing. In the receiver, the checksum is calculated over the entire packet with the exception of the start flag and the end flag. For valid packet the result must be zero. The checksum test must be carried out after octet stuffing. *(Corscience EMB1 2010, p. 17)*

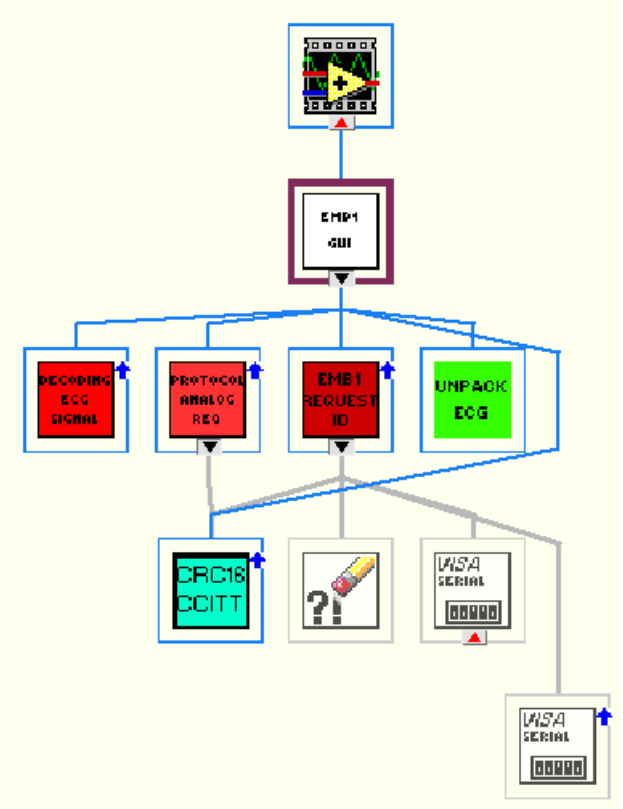

Figure 17 presents EMB1 LabVIEW VI hierarchy.

Implemented program is described in block diagram in figure 15 and explained with help of block diagrams in appendix 1. EMB1 module interface was designed so that the module would be found despite of various other devices and automatically with no need for the user to participate in finding the module. Finding EMB1 serial port was done in EMB1 request ID subVI, in figure 17. In this subVI it was necessary to send Identification Inquiry command to check that program has identified right device.

The subVI called CRC16 CCIITT to calculate the correct checksum over entire packet with the exception of the start flag, end flag and checksum. The checksum was necessary to calculate when commands were send from computer program to EMB1 module. Algorithm can be expressed in following way *(National Instruments 2010)*:

```
int x;
x = ((crc>>8)^data) & 0xff;
x^=x>>4;
crc=(crc << 8)^(x<<12)^(x<<5)^x;
crc &= 0xffff;
```

Main task of Protocol Analog Request subVI was to send Protocol Version Inquiry Configure Analog Request command, which was necessary to ECG module. Protocol Version Inquiry commands inquired the protocol version of the EMB1 module. This was done to assure that correct device was found among other devices. Configure Analog Request command configured the wanted sampling rate to 1 kHz, active ECG channels to one and used mains frequency of 50 Hz. The configuration of main frequency set the filter for internal QRS-wave detection algorithm. It was not used to filter the mains frequency out from ECG data stream. *(Corscience EMB1 2010, p.31)*

The reading of serial ports and data sent from EMB1 to computer was made on EMB1 VI. Start ECG Transmission and Stop ECG Transmission commands were send in this virtual instrument. R peak detection was made in this VI from where RR time interval was calculated. Both heart rate in beat per minute and ECG signal was served for user from this VI.

The ECG data send from EMB1 to program and finding of packet structures, presented intable 1, unpacking the octet stuffing and serving of QRS wave detection index to EMB1 VI were made on Decoding ECG Signal VI. This VI searched one packet structure with help of start and end flag. It unpacked octet stuffing in inverse way than presented in table 2.

Unpack ECG VI unpacked the ECG payload from ECG data packet structure. ECG payloads were packed so that if only 7 bits within a data value was used EMB1 packed the 15 bit value to 7 bits value which was necessary to convert pack to 15 bits value in to draw ECG signal for user monitor. Distinguishing between one and two byte values was made with mask bit. *(Corscience EMB1 2010, p. 29)* Unpacking these values is described more precisely in appendix 2.

ChipOx pulse oxymetry module LabVIEW program was designed in a way that it could find the module despite of multiple devices. In figure 17 VI hierarchy of ChipOx program is presented. ChipOX GUI VI describes of ChipOx user interface. ChipOx GUI VI, described in appendix 2, made data handling and draw the wanted signals for user. VISA (Virtual Instrument Software Architecture) serial box describes serial port communication between device and computer.

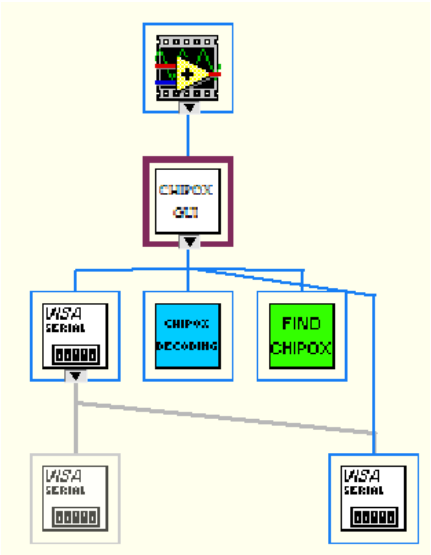

Figure 18 presents VI hierarchy of ChipOx LabVIEW user interface.

ChipOx program's block diagram is presented in appendix 2.Module was found automatically in Find ChipOx VI by identifying from the data stream hexadecimal characters A8 and 7F, which are 168 and 127 in decimals. Module started to measure PPG directly when switched on. ChipOx packet structure is presented in table 3. *(Corscience CipOx 2010, p.23)*

Table 3 presents data packet structure of ChipOx module and clarifies meaning of it parts. *(Corscience ChipOx 2010, p.23)*

Start Flag	Data	Checksum	Flag

Identifier:	Description:	Size:
Start Flag:	Beginning of packet 0xa8	1byte
Data:	Data packets	Variable
Checksum:	Checksum from all Data field	2 bytes
End Flag:	End of the packet 0xa8	1 byte

Module sent data packet consisting from data, checksum, start and end flag using byte-stuffing algorithm. According to manual the purpose of the stuffing is to detect packets securely without losing the synchronization due to extraneous traffic. Reserved values was in hexadecimals 0xa8 (in decimals 168) used in start and end flag and secondly 0xa9 (in decimals 169) use as control byte. If in the block of data or checksum a character appears, which was 0xa8 or 0xa9, it was coded with following two bytes:

0xa8 is coded as 0xa9, 0x88 (in decimals 169, 136)
0xa9 is coded as 0xa9, 0x89 (in decimals 169, 137)

The decoding of the communication protocol was done in the Decode ChipOx VI presented in appendix 2. The serial UART protocol of ChipOx is divided into communication layer and transfer layer. The communication layer is one layer above the transfer layer. It is completely contained in the Data-block of the transfer layer. *(Corscience ChipOx 2010, p.22-23)*

Table 4 presents communication layer is completely contained in Data-block in transfer layer. *(Corscience ChipOx 2010, p.24)*

Transfer layer:	Flag	Data		Checksum	Flag
or:	Flag	Data Channel-ID	User Data	Checksum	Flag

Decoded data channel-ID was 0x7F (127 in decimals) searched in Decode ChipOx- VI. Photoplethymography, blood oxygen saturation and pulse acquisition was made from real-time data channel marked with identifier 0x51 (in decimals 81). It was found from User Data- block right after data channel-ID. Character 0xa9 and 0x88 were decoded to 0xa8, as well 0xa9 and 0x89 was decoded to 0xa9. After decoding PPG signal was drawn and pulse and blood oxygen saturation was presented. *(Corscience ChipOx 2010, p.24)*

4.5 Discussion on the first pilot

It was well known and noted that the stainless steel dry-electrodes used in the test ECG measurement would give noise. Malmivuo and Plonsey *(1995)* noted that distortion adding factors in ECG measurement are muscular activity, respiration and electrode artefacts due to perspiration and electrode movement. One source of distortion was noted to come from skin-electrode contact. Chi *(et al. 2010)* wrote in his paper that relative motion of electrodes with respect to body give rise to artefacts in the received signals that are one of the main impediments against the acceptance of dry-electrodes. These artefacts arise in low-resistance wet-contact electrodes as well. They can be reduced, but not eliminated, by careful mechanical design. *(Chi et al. 2010)* In addition, one noise source could be that the measurement points where at the wrists and palms. To keep the speed and easiness of ECG measurement, points were not changed. Large motion artifacts on dry electrode surface resulted in loss of the signal. Chair handles provoked to squeeze the sensor parts. Squeezing added more base distortion to signal because of electromyography. ECG distortion removal was important for the next pilot designs. In case of monitoring ECG, the distortion factor was tried to be minimize. Due to poor ECG signal, estimating of blood pressure with pulse transit time method was dropped out from next pilot design. ECG signal removal was seen to demand more time than available before next pilot design would have to be in test stage. Other measurements were seen to be compatible for next pilot design.

5 Second pilot

5.1 Aim of the second pilot

Second pilot was designed for patient monitoring use to test the concept of health chair. Concept testing was necessary to see would health chair replace single traditional measurement devices, for instance blood pressure. Also, feedback from concept of combining measurements devices to one health chair was welcome. Aim of second pilot design was to make health chair, which would measure patients:

- Blood pressure
- Weight
- Bioelectrical impedance
- Blood oxygen saturation
- Heart rate
- Photoplethysmography

Each measurement device would be merged to the chair. Nurses could execute tests in nursing home. For this reason measurements were chosen to be traditional and familiar to nurses. This was one the reasons why pulse transit time measurement and ECG were dropped out for this pilot stage. Traditional measurements are familiar to nurses. By uniting the measurement to one single chair it would test if the chair would replace traditional measurement devices and in general be in nursing use. Design of the health chair was aimed to be patient comfortable. Aim was to combine measurement module to typical couched armchair.

5.2 Outlines of the second pilot

To test the health chair concept in nursing home, the measurement devices were limited to traditional type of measurements. To see the acceptance of healthcare personnel was important, which limited the chosen measurements. Blood pressure measurement with cuff, PPG, blood oxygen saturation, weight and pulse rate were considered to be traditional and well-known measurements. Bioelectrical impedance was not considered as well known or traditional. It was added to see acceptance of healthcare personnel and to consider if it would be fasted to next stage pilot.

5.3 Realization of the second pilot

Chosen blood oximeter device in second pilot was pulse oximeter board EG00352 and its test kit made by Medlab were chosen, because of it were able to operate with 3,3 V when needed power was easy to provide. It also operated with clear serial transmission protocol *(Medlab EG00352 2012).* Also, there was in-house experience from module made by Medlab. This pulse oximeter measured wanted photoplethymography, heart rate and blood oxygen saturation. Data was transmitted with Universal Serial Bus (USB). Supply voltage was provided from 3,3 V supply voltage pin from Arduino Uno. Data was conducted to USB hub with USB–to-serial converter.

Blood pressure was measured with NIBScan, a noninvasive blood pressure measurement device made by Medlab, and its test kit. The NIBScan module uses oscillometric method for measuring blood pressure. It calculates pulse rate, and mean, systolic and diastolic blood pressures. Supply voltage of 15 V was provided with external medical grade power supply and regulator coupling. Data was translated to USB hub with USB–to-serial converter. *(Medlab NIBSCAN 2012)*

The weight was measured with sensors taken from commercial weight scale. Sensors were attached to four points between chair legs and frame holding the wheels. Sensor data was conducted to amplifier coupling made from INA122P instrumentation amplifier *(Texas Instruments 2000)*. Measured analog signal was conducted through low pass RC-filter to Arduino Uno board *(Arduino 2011)*. Here the analog signal send by the sensors was converted to digital signal. Small program was produced to send necessary weight data from Arduino to personal computer. USB was used to conduct data from Arduino to PC. Small tests were conducted to discover that weight measurement system correlated linearly with the added weights.

Bioelectrical impedance module was added to chair and operation voltage was provided from USB bus, which was used to conduct data as well. EBI was measured with sensors made from stainless steel. These sensors were attached to armrests of chair. Four measurement points were from left and right palm and wrist. The connected sensor module inputs were:

- Left palm to I+ input
- Right palm to I- input
- Left wrist to V+ input
- Right wrist to V- input

Realized health chair pilot is presented in figure 19 where blood pressure cuff and photoplethysmography finger clip can be seen hanging on the right armrest. Four stainless steel sensors are clearly detectable on hand rests. User monitor is clearly detectable on the chair. Block diagram of connected modules, kits, connections and other devices is presented in appendix 3.

Figure 19 presents second stage pilot design. Blood pressure cuff and photoplethysmography finger clip can be seen hanging on the left armrest. Stainless steel sensors and user monitor are clearly detectable.

5.4 Software of the second pilot

Pulse oximeter board EG00352 provided two separate serial transmission protocol from which serial transmission protocol version two was used. The second protocol implemented the same functionality as the first one without the large redundant data overhead of the first variant. Plethysmographic waveform data was send with 50 Hz transmission rate. According to producer, this transmission rate was used because higher frequencies did not produce smoother waves, and lower frequencies would lead to incorrect impression of the waveform. *(Medlab EG00352 2012, p. 10)*

In this transmission protocol a block with new saturation value, pulse rate and perfusion index info is transmitted on each detected pulse. The pulse wave sample points were transmitted continuously 50 samples per second. Their values were located between 0 and 247 (0xF7 in hexadecimals). Byte values larger than 0xF7 were used for marking the next byte in the stream as a new value. Definitions of marker bytes are presented in table 5. *(Medlab EG00352 2012, p.10)*

Table 5 presents definitions of the marker bytes in EG00352 *(Medlab EG00352 2012, p. 10)*

Marker byte:	*Meaning of the following:*
0xF8	Wave sample points follow.
0xF9	SpO_2 value follows.
0xFA	Pulse value follows.
0xFB	Info byte follows.
0xFC	Quality and Perfusion index follows.

Programs for EG00352 plethysmograhic module were implemented with LabVIEW programming environment. Two virtual instruments EG00352 virtual instrument and Find POX virtual instrument were implemented. Their block diagrams are presented in appendix 4. EG00352 VI was implemented so that Find POX- virtual instrument would automatically search and connected EG00352 device to computers serial port. Find POX would provide the serial port to EG00352 VI. VI hierarchy can be seen in figure 20.

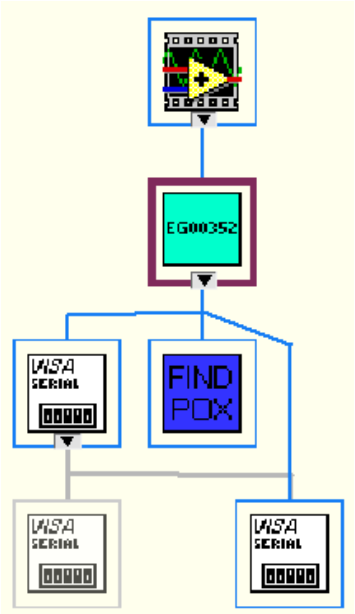

Figure 20 presents VI hierarchy of EG00352. Figure clarifies functioning of EG00352 and Find POX VIs

In EG00352 virtual instrument, communication protocol used by PPG module was un-packed. Appendix 4 introduces central part of EG00352 virtual instrument. This VI drew all the photoplethysmographic values, following byte 0xF8 (248 in decimals), to graphical user interface. This part also showed for the user SpO_2 value following byte 0xF9 and pulse value after 0xFA. Byte after 0xFC described quality and the perfusion index. This part also evaluated the situation in PPG finger probe, from bytes after the info byte 0xFB. The following bytes in order described:

- 0x00: OK
- 0x01: Sensor disconnected
- 0x02: No finger in probe
- 0x03: Low perfusion
- 0x2d: Self-test error

Blood pressure was measured with chosen non-invasive blood pressure NIBPScan module. Host controlled the measuring unit via command frames according to its transmission protocol. All data and commands were verified by checksum. Start and end flags were used to separate data strings. ASCII (The American Standard Code for Information Interchange) character 02 presents start flag and ASCII character 03 presented end flag. Software interface commands consisted of an eight ASCII character frame presented in table 6.*(Medlab NIBSCAN 2012, p. 6)*

Table 6 presents NIBP's eight ASCII frames *(Medlab NIBSCAN 2012, p.6)*

Char 1	Char 2	Char 3	Char 4	Char 5	Char 6	Char 7	Char 8
STX	c0	c1	;	;	x0	x1	ETX
Start	Command code	Command code	Semicolon	Semicolon	Checksum	Checksum	End

In each command existed codes: start of text, end of text, two semicolons and checksum. The checksum is presented with two ASCII characters and it was generated from by modulo 256 addition of all characters in the corresponding frame, without start and end flag. *(Medlab NIBSCAN 2012, p.6)*

In figure 20 virtual instrument block diagram is presented. To clarify function of NIBP VI and Find NIBP VI block diagram is presented in appendix 5. NIBP VI got serial port from Find NIBP VI. The latter VI was designed to find NIBP module from serial port despite of various other devices.

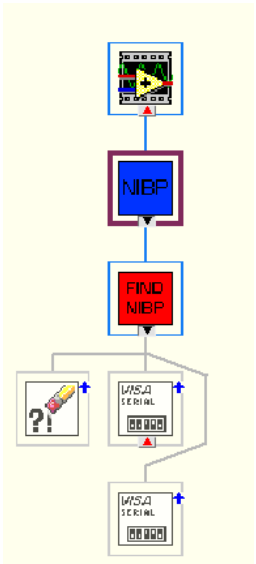

Figure 21 presents NIBP VI block diagram.

NIBP VI received resource, in this case serial port, from Find NIBP VI. Program waited till user pushed Start Measuring-button, when it automatically selected adult measuring mode and send Start Measuring-command. While measuring, temporal cuff pressure was measured and possible errors were analysed. End of measuring was detected if no bytes were detected in 300 ms. Cuff pressure was sent 5 times per second *(Medlab NIBSCAN 2012 p. 9)*. After the measurement end, cuff pressure transmission was read. Then Read Status from Slave command was send when module send previously measured heart rate and diastolic and systolic blood pressure could be read.

Bioelectrical impedance was measured with openEBI measurement module *(Blomqvist 2012)*. Appendix 6 describes functioning of virtual instruments Z and Find Z. Function of Find Z VI was to find module from various other devices connected to measurement computer. Find Z VI sent to opened serial port 's' command, which worked as start measurement command for openEBI. After sending the command serial port was read and regular expression for openEBI was recognized and serial port was send forward. Figure 22 describes the functioning of virtual instruments. When serial port of openEBI was found, 's'-command was send again. Serial port was read and received string was ensured to belong to openEBI by recognizing character '$', which was last element of string. From this string "abbc-(b+)=ac" VI changed each '\.' to ',' to clarify the decimal values. Each impedance value was complex number from which absolute values were calculated. Values were drawn to XY graph and mean value was calculated to present one impedance value for user.

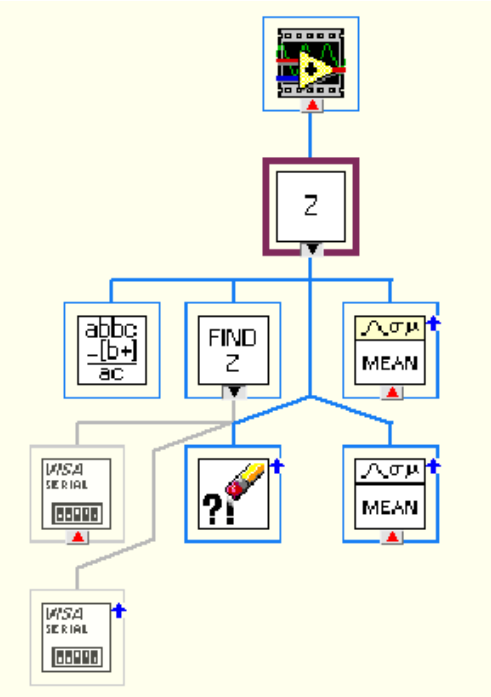

Figure 22 represents VI hierarchy of electrical bioimpedance measurement.

Weight measurement was executed with Arduino Uno board, weight measurement sensors and amplifier coupling. A LabVIEW program was executed with tree virtual instruments: Find Weight VI, Weight VI and A/B xtrac VI. To clarify functioning of virtual instruments block diagram is presented in appendix 7. Figure 23 presents VI hierarchy diagram of weight measurement program. Purpose of Find Weight VI was to find Arduino Uno board, which was connected between weight measurement sensors, amplifier coupling and computer. Appendix 3 clarifies connections made. Arduino was identified with regular expression: "-Arduino-". A small Arduino sketch was realised with Arduino Development Environment *(Arduino 2013)*. The board was programmed to send the regular expression to help to identify the board among other devices. Find Weight VI send the serial port found to Weight VI. Weight VI read the serial port and sent found port too A/B xtrac VI. This VI found expression 'W' from received string. If expression 'S' was found weight was simulated. This part was done to present the func-

tioning of whole graphical user interface for user during development of weight measurement. It was not used after weight measurement was carried out with sensor data. When expression ‘W’ was found weight data was send to Weight VI. Weight VI showed raw body weight data to user. Raw body weight data presented amplified signal. It was translated to kilograms with help of constant and body weight coefficient. The body weight of the patient was determined by calculating mean value from 25 different values from calculated body weight.

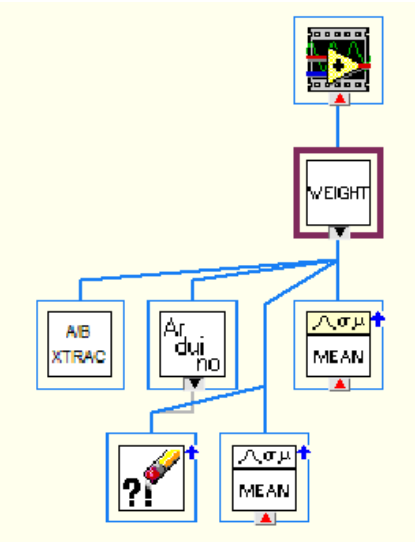

Figure 23 presents VI hierarchy of weight measurement program.

After implementing previously mentioned module interfaces, building of coherent system was started. The system included the module interfaces of NIBP, EG00352, Arduino Uno and EBI modules. When the program was started Arduino Uno module was found first after that in order EBI, POX and NIBP modules were found. If some of these modules were not found user of the program was asked, that some measurement modules have not been found. Possibly a new research was conducted if user chose so. Figure 24 clarifies initializing of measurements. If some module was not found the possibility was to choose to insert 0 to measurement or to simulate it. The procedure was done by providing possibility to execute measurements despite modules were missing. Simulations of measurement were used when user interface was tested. The possibility to simulate measurements was left to this pilot stage to introduce the function of graphical user interface during development and maintenance of modules.

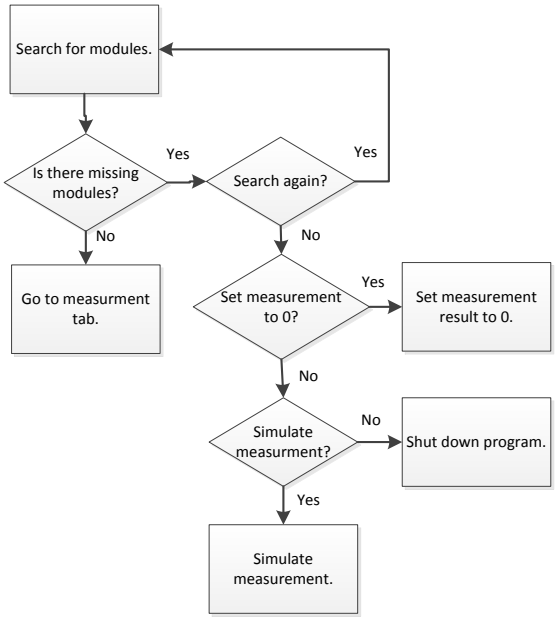

Figure 24 presents block diagram, which clarifies initializing of measurements.

When measurement procedure was started the program wanted to confirm that nurse had done obligatory tasks in order:

1. Client is seated
2. Blood pressure cuff is placed
3. Blood oxygen saturation sensor is placed
4. Palms are placed on the sensors
5. Legs are raised to footrest

After confirming these procedures the measurements could be started. The sitting of the client was confirmed when adjustable weight sensor threshold value was exceeded. Taking a test measurement ensured that blood pressure cuff was placed. The procedure took two to three minutes and took most of the time of the whole verification. For this reason during cuff measurement other measurements were ensured. This verification was run in parallel with others. Placement of blood oxygen saturation finger clip senor was ensured with help info byte from the module. EBI measurement was confimed by placing the palms placed on the impedance measurement sensors. The verification was done measuring increasing impedance, while measurement frequency was increased. This threshold was placed when absolute value of third measurement frequency was larger than thirtieth. Electrical bioimpedance was measured with 49 different frequencies *(Blomqvist 2013)*. Confirming that legs were raised on the footrest was left on responsibility of nurse. This measurement was not assured in anyway. The purpose of the question was to remind the nurse from it. When measurements were started they were processed in same order as in test stage.

There were different operators installed to health chair system. Installed prime operators in program were guest, admin and master. The guest was only able to make measurements, which were not recorded for later use. The admin was able to make measure-

ments and to add and remove users. These users were able to add clients and make measurement, which were saved for later monitoring use. Measurements, which were done under admin user, were recorded for later use. The master user was able to add and remove users and admins. He was also able to make measurements, which were recorded. Table 7 clarifies what each profile could do. Password was required from each user, despite guest. The password was set when first login into the profile was done.

Table 7 presents requirements and possibilities of each profile

	Guest:	User:	Admin:	Master:
Make measurement:	Yes	Yes	Yes	Yes
Add/remove user:	No	No	Yes	Yes
Add/remove client:	No	Yes	No	Yes
Add/remove admin:	No	No	No	Yes
Password required:	No	Yes	Yes	Yes

Priorities of second stage pilot design graphical user interface were ease of use and clearness of monitored measurements. Figure 25 clarifies the start page in the program where measured parameters can be seen. In each tab, for instance body weight (BW), history of each measurement could be monitored. Exception tabs were SpO_2 tab were the current photoplethysmography signal could be seen and Settings tab were user could change for instance weight measurement threshold.

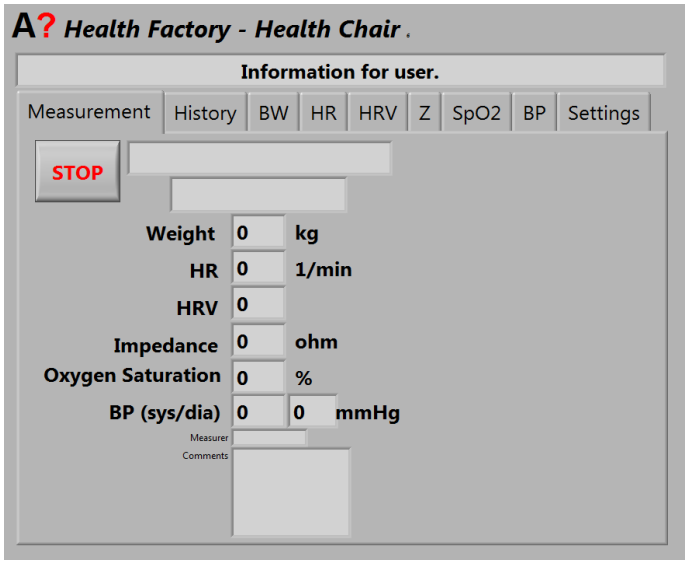

Figure 25 presents main page shown for user. Measurement tabs can be seen under text where information for user is shown.

5.5 Discussion on the second pilot

The pilot was implemented to discover that all the integrated measurement could be conducted in one health chair. The pilot showed this to be achievable as expected. Some issues should be improved, for instance occasionally tale was formed after drawn Cole-Cole plot. As explained previously, tale could be formed from unwanted capacitance. This can rise from increased sensing electrode polarization impedance between sensing electrodes and from improper adjustment of EBI module. The module was designed to

measure from abdominal with wet-gel electrodes, not with dry electrodes. As Ruiz (2011) explained these capacitive leakages are small at low frequencies but can cause a tail or hook at high frequencies to Cole-Cole plot. Other notable improvement should be done to weight measurement system. With proper adjustment of the linearity factors correct weight was measured but measurement were not been able to conduct from day to day without proper adjustment. During the thesis the second pilot design was tested in nursing home. The health chair was used and concept was seen useful.

6 Third pilot

6.1 Aim of the third pilot

Health chair's third pilot design was one step forward to dry-electrode measuring. The aim was to test the measurements designed and conduct them to their final state. The aim of the third pilot was to verify the applicability of dry-electrode ECG signal measurement and also RR and QT intervals measure from it. The aim was also to verify the applicability of the blood pressure estimated from pulse arrival time to blood pressure estimation. This thesis introduces testing of RR and QT interval estimation and blood pressure estimation from PTT in later chapters. The aim of the pilot was also to continue testing of these measurements and health chair concept after the thesis. The third pilot was not finished during this master's thesis. The third pilot design was aimed to measure patients:

- Electrocardiography
- Weight
- Bioelectrical impedance
- Blood oxygen saturation
- Hear rate
- Photoplethysmography
- Pulse transit time and estimate systolic blood pressure from it

Each measurement device would be merged under the chair and so they would be not clearly detectable. In this stage ECG measurement with RR and QT interval analysing was included. Also, patient blood pressure would be possible to estimate with pulse transit time method. Design of the health chair aimed to be patient comfortable.

6.2 Outlines of the third pilot

Limiting factors on third pilot design were that amount sensors attached to the skin surface of patient should be minimized. Design would be made in patient comfortable manner. The health chair would be built to typical couched armchair. ECG would be measure with the dry-electrodes instead of skin attachable wet electrodes to maximise fast and easy measurement. The measuring OEM modules were limited to modules already chosen to previous pilot designs. Blood pressure would be estimated with pulse transit time method in which ECG and pulse oximeter modules would be used. PPG wave would be measured from the fingertip of the patient. With fingertip measurement PTT is less prone to errors, because distance between heart and measurement point is longer, than in earlobe or nose clip measurements.

6.3 Realization of the third pilot measurements

Deployment of EMB1 ECG module started in first pilot with attaching skin electrodes and implementing small LabVIEW program. First test were conducted with skin electrodes. In this stage some distortion was noted in ECG signal. After this stage on third pilot stage digital filters were added to program. A fourth order bandstop Bessel filter was added to frequency range of 49-51 Hz to bloc distortion from mains frequency. A

second order lowpass inverse Chebysev filter with 30 dB attenuation was added to limit the frequency range to 150 Hz. According to Webster (*2011, p. 253*), ECG's upper cut-off frequency can be set to 150 Hz. EMB1 module included software baseline filter. This baseline filter used 0,3 Hz filtering 2,65 seconds after starting ECG transmission to ensure fast recovery time of the baseline. After this time baseline filter of 0,05 Hz was used to ensure not disturbing ST segment. *(Corscience EMB1 2010, p. 10)*

Secondly stainless steel sensors were added to test chair and ECG measured with them. After this, distortion increased in whole frequency range of 0,05 – 150 Hz. Lots of high frequency transients, presented in figure 26, with high amplitude was noted. This caused the amplifier to saturate and finite period of time was required to bring the ECG back. In addition, small amplitude base line noise, which reminded electromyography (EMG) noise, was noted.

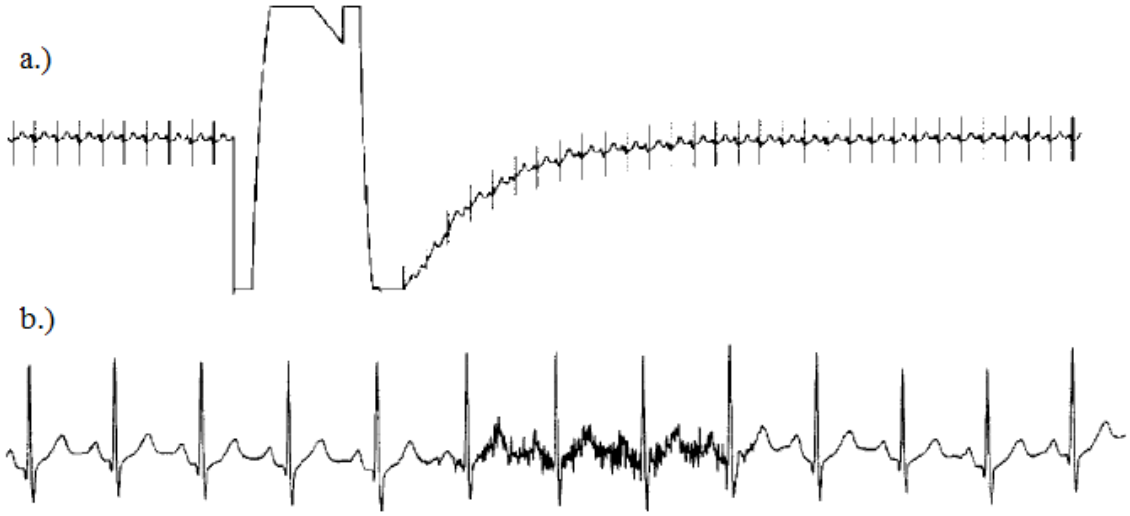

Figure 26 (a.) presents effect of a voltage transient on an ECG. *(Webster 2010, p. 256, picture modified)* and (b.) presents EMG interference on the ECG. *(Webster 2010, p. 256, picture modified)*

Most of the noise was suspected to rise from skin-electrode contact, EMG and movement on skin-electrode contact and so from changing input impedance. To better the signal active electrodes made from OPA277 operational amplifier *(Teaxas Instruments OPA277)* were added after sensors. Active electrodes reduce noise by impedance matching. Figure 27 presents schema from OPA277 type of active electrode. Active electrodes were placed after stainless steel sensors.

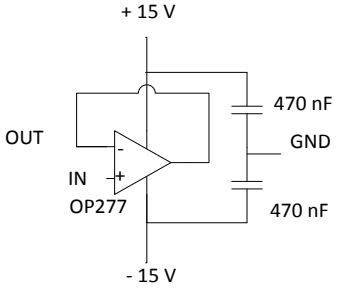

Figure 27 presents amplifier circuit made to OPA277.

After placing active electrodes some distortion was still included into the measured ECG signal. According to Lee and Kruse *(2008)* input bias current on front-end amplifiers can polarize the electrode if there is poor skin electrode contact. Non-polarized electrodes are also better than polarized electrodes in terms of their rejection of motion artefacts. Minimizing bias current was seen necessary. Active electrodes were changed to AD8627, which provided maximum 1 pA bias current *(Analog Devices 2013)*. Compared to OPA277's 0,5 nA bias current. Also AD8627 had wide operating voltage (±2,5 V to ± 13 V), which was close to OPA 277's (± 2V to ± 18 V), when health chair power supply design did not have to be changed. Analogue low pass filter was added to active electrode design to filter out high-frequency components. Also after transients' digital filters required time to bring back to baseline. Low pass filter was expected to avoid this.

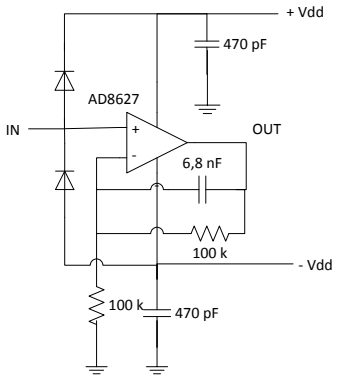

Figure 28 presents schema from designed active electrode AD8627 amplifier circuit with low pass filter.

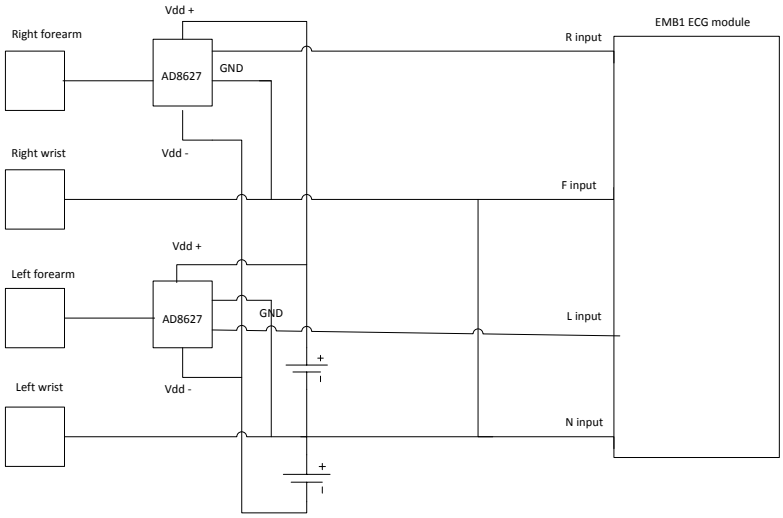

Figure 29 presents designed measurement circuit with AD8627 active electrodes and EMB1 ECG module.

Geddes and Baker *(1968, p.241-246)* conducted square wave, with known voltage and current, through different electrode materials and measured the surface area and amplifier input impedance for materials. They noted the same small amplitude noise on baseline as we, when using stainless steel electrode material. Geddes and Baker *(1968, p.245)* explained that silver-silver chloride, silver, and copper are less noisy materials than stainless steel. Silver-silver chloride was the least noisy. There was more baseline noise in silver, but copper had more baseline drift. Stainless steel produced the poorest result. They conclude that loading caused distortion, because when the electrode polari-

zation impedance becomes dominant part of the input circuit and the voltage across the input terminals of the recorder is reduced. Secondly, the amount of phase shift is different for various frequency components. With loading, the electrode current density is increased and the resistive and reactive components of the electrode polarization impedance become nonlinear, resulting in the magnitude of the electrode polarization impedance becoming a function of the amplitude of the event. Thus small and large amplitude signals will encounter different impedances *(Geddes & Baker 1968, p. 240-245)* Based on this, the measurement electrodes were changed to silver electrodes. It is assumed that human skin and especially human sweat includes lot of chloride ions, which in contact with silver electrode make more conductive surface.

6.4 Software of the third pilot

RR and QT interval calculations were made in EMB1 VI presented in appendix 1. R wave was detected after Decoding ECG signal VI. EMB1 module sent 0x0772-command immediately after detecting R wave. This packet command was recommended to host R wave triggering. *(Corscience EMB1 2010, p. 32)* Third and fourth bytes in data packet structure presented in table 1were named command bytes. Command bytes were waited after Decoding ECG Signal VI. When program received the commands it gave each R wave a millisecond timer value, which was used in pulse transit time calculation. This time was also put into shift register. This R wave time was used to calculate RR time intervals. Each RR time interval was result of subtraction between R wave and previous R wave taken from shift register. This command was also used to chop RR intervals in QT interval detection.

QT interval detection was made in following way. After Unpack ECG VI, the band stop Bessel filter was used to frequency range of 49-51 Hz and also a low-pass inverse Chebysev filter was used to limit the frequency range to 150 Hz. After this data array was put into shift register. Program read ECG data from shift register. Amount of data read to shift register was limited by R wave, so that the data between two consecutive R waves was read to shift register. Modules own hardware R wave detection was used to chop data into shift registers (*Corscience EMB1 2010, p.32*). When data was read, VI found T peak after R wave. Threshold value was set to avoid detecting too small peaks. After T peak detection next valley was found, this was the end of T wave. Now program took time from previous wave's R peak to Q valley from shift register and calculated QT interval. After finding end of T wave, P peak was searched. Threshold value was set to find values large enough. After finding P wave next valley was searched which was supposed to be Q valley. This Q valley time, from R peak to Q valley, was put into shift register and used in next QT interval detection. This next QT interval detection used this Q time of previous RR interval data. After it searched end of T wave from its data and calculated the QT interval time again. Figure 30 clarifies chopping of RR interval data and QT interval calculations from two consecutive RR intervals.

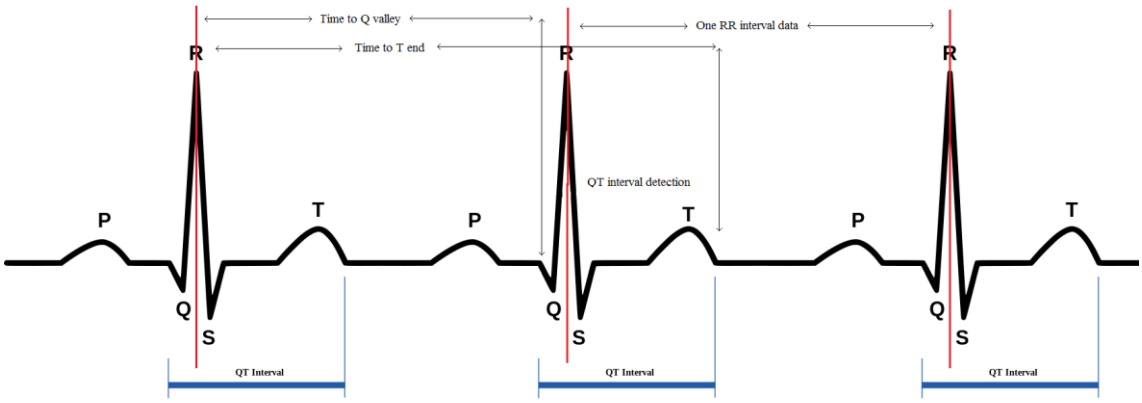

Figure 30 clarify how QT interval was detected from two consecutive RR intervals.

PTT values were calculated from peak of R wave to peak of PPG wave. McCarthy *(et al. 2011)* and Zakaria *(et al. 2010)* used this method. Pulse transit time calculation was conducted in parallel with EMB1 VI presented in appendix 1 and EG00352 VI presented in appendix 4. In addition one while loop was made to update local variables "R wave time" and "PPG peak time". R wave was detected in EMB1 VI with help of specific command bytes 0x0772. When R wave was detected millisecond timer value was updated to local variable called "R wave time". EG00352 VI detected PPG peak from data following 0xF8 marked byte. Wave samples were transmitted 50 samples per second, which limited pulse transit time accuracy to 20 ms *(Medlab EG00325 2012, p.10)*. Previous chapters and appendix 4 describes more detail functioning of EG00352 VI. Peak of PPG wave was detected with Peak Detector VI. Threshold value was set to 100. When peak detector triggered a millisecond timer value was updated to local variable "PPG peak time". From this time 20 ms were subtracted because peak detection triggered always too late. This systematic error was noted when PPG signal was drawn with Matlab and peak detection times were compared to peak times seen from Matlab. After PPG peak detection next peak would be ignore if it would appear inside 300 ms. This was done to avoid detecting dictoric notch as a PPG peak. PTT times were calculated in another while loop with help of R wave time and PPG peak time local variables. To secure that one local variable time was not read two times, PTT calculating loop used "PTT val" flag. This loop checked "PTT val" to false after a read and EG00352 loop checked "PTT val" to true when PPG peak was detected, so PTT value was only update after PPG peak detection. To verify that R wave was detected only once "R found" flag was set to true when R wave was detected and set to false when PPG peak was detected. PTT was only calculated when "PTT val" was set to true. PPG peak detection was ignored if R wave was not found before it. PTT calculation loop also calculated ΔPTT, which was difference between consecutive pulse transit times. This was done inserting previous PTT value to shift register. Another while loop was set to calibrate and calculate blood pressure estimations from pulse transit times. Systolic blood pressure was estimated with two different methods:

1. With method presented by Chen *(et al. 2000)* described previously
2. With taking two different reference point from systolic blood pressures and pulse transit times and estimating blood pressure with help of these points

Method presented by Chen *(et al. 2000)* used equation 13 to estimate systolic blood pressure. In equation systolic blood pressure was estimated with known base blood pressure *(P_b)* and corresponding PTT value *(T_b)*. Chen also used constant *γ*, which described elastic modulus of the vessels. Systolic blood pressure was estimated with calculated changes in pulse arrival times *(ΔT)*.

Our idea was to take two reference points with typical systolic blood pressure and corresponding PTT value and also higher systolic blood pressure and its corresponding PTT value. Typical values were measured in relaxed state. Second values were measured after and during physical activity. It was noted during the tests and before the tests that physical activity raises blood pressure for certain amount of time. As mentioned when arterial pressure increases the pulse wave travels more quickly and lowers pulse transit time and conversely when blood pressure decreases PTT lengthens *(Zakaria et al. 2010; Larkin 2005, p. 35)*. The idea was to get two reference points and estimate systolic blood pressure from pulse transit times with help of straight. With help of two known point straight can be drawn between and factors *m* and *b* can be solved.

$$y_1 = mx_1 + b \quad (21)$$

$$y_2 = mx_2 + b \quad (22)$$

Factor *b* can solved from equation 21.

$$b = y_1 - mx_1 \quad (23)$$

Inserting equation 23 in equation 22 solves factor m.

$$m = \frac{y_2 - y_1}{x_2 - x_1} \quad (24)$$

Placing equation 24 to equation 23 solves factor b.

$$b = y_1 - \left(\frac{y_2 - y_1}{x_2 - x_1}\right) * x_1 \quad (25)$$

Calibration of systolic blood pressure estimation and the estimation process was made in one separate while loop. First PTT values were measured during one minute, while this minute blood pressure should be measured with blood pressure cuff. Measured systolic blood pressure value was added to program. Mean value was calculated from recorded PTT values. The mean value worked as x_2 value for straight blood pressure estimation method and base blood pressure (P_b) presented by Chen *(et al. 2000)*. Measured blood pressure value was set to y_2, which was also corresponding PTT value (T_b) for Chen's method. Elastic modulus *(γ)* coefficient of the vessels was set to 0.018.

After first calibration second calibration was made. During tests grip strength meter was squeezed during one minute to raise blood pressure level. After second calibration loop was started. During this loop PTT values were recorded during one minute. From these PTT values mean value was calculated. Systolic blood pressure was again measured during one minute's calibration. The mean value worked as x_1 and systolic blood pressure value as y_1 for straight blood pressure estimation method. Second calibration values were not used in Chen's method. After calibration, loop solved *m* and *b* values presented in equation 24 and 25 for straight blood pressure estimation method. Then loop also set "Calibrated" flag to true, when program started to show PTT values and estimate BP values. Program estimated BP values from each PTT values. These values were recorded in 30 seconds intervals from which mean value was calculated. This mean value was recorded in test.

6.5 Discussion on the third pilot

As mentioned earlier third pilot design was not finished during this master's thesis. Some development ideas could be mentioned about the subjects the thesis discussed. In QT valley detection QT was detected to Q valley, but according to Malmivuo & Plonsey *(1995)* it should have been detected from the beginning of Q wave. It can be supposed that this can affect a few to tens of milliseconds too low QT values. Threshold values in detection of QT interval were problematic. As mentioned, detection of P and T peaks was used in detection of Q valley and T peak. Noisy signal affected that some or many of these valleys of peak were detected to wrong location. According to tests, amplitude of theses valleys and peaks is individual in most persons. Setting threshold values too high would affect that some or none of peaks would be undetected. On the other hand setting it too low, would affected that peaks were triggered in wrong locations. PTT values were calculated from peak of R wave to peak of PPG wave. This was done in matter of simplicity. One idea was to calculate PTT values by indexing each sample taken by EMB1 ECG module and EG00352 module. Problematic was that EMB1 module send samples to computer in arrays in 50 ms to 100 ms intervals. EG00352 PPG module sends samples in bytes in 20 ms intervals. This clearly lowers the accuracy of PPG peak detection. PTT values were confirmed by drawing PPG and ECG signals with Matlab. PTT values drawn with Matlab and calculated by LabVIEW matched. Unfortunately, in long term recordings there was noted that distance between R wave and PPG signal increased during time. The failure was noted in Matlab when signals where plotted using sampling frequencies producer promised. EMB1 had sampling frequency of 1 kHz *(Corscience EMB1 2010, p. 10)* and EG00352 50 Hz *(Medlab EG00352 2012, p.10)* Probably sampling interval of EMB1 or EG00352 is different than promised by producer. Even 0,001 ms fail would cost 0,001x5x60x1000 = 300ms error after five minutes recording with sampling rate of 1 kHz. If accuracy of calculating PTT would be main focus of a research, same internal clock would be required for both OEM modules. This would eliminate errors, which can appear from two different internal clocks. Due to this problem PTT values were calculated using tick counter times, not indexes.

7 Tests and results

7.1 Aim of the tests

We conducted two separate tests series: firstly to verify that measurements can be done with second pilot design and secondly to test the functionality of RR and QR interval calculation and estimation of systolic blood pressure with pulse arrival time for health chair third pilot design. First test series was supposed to verify that following measurements can be done with second pilot design:

- Blood pressure
- Weight
- Bioelectrical impedance
- Blood oxygen saturation
- Heart rate
- Photoplethysmography

The aim of the second test was to test and verify the functionality and accuracy of ECG signal's RR and QT intervals measure from it. The aim was also to verify the functionality of blood pressure estimated from pulse arrival time.

7.2 Tests and results

Measurements were made to five test persons from different age categories and with basic health. Firstly, measurements were made with health chair second pilot. The results were analysed. Secondly, test persons ECG was measured with EMB1 ECG module and RR and QT intervals were measured with made LabVIEW program. Thirdly, test persons ECG and PPG were measured and pulse transit time was measured. Blood pressures were estimated using PAT and blood pressure were also measured using cuff blood pressure measurement.

Measurements were conducted for five persons from different age categories. All of the test persons were healthy and without known cardiovascular diseases. Before tests, persons were questioned about age and gender. Test persons weight, height and maximum grip strength were measured. Weight was measured with commercial personal scale for which producers give an accuracy of 100 grams. Height was measured with centimetre measure. Maximum grip strength was measured with Electronic Hand Dynamometer EH101 produced by Gloway Invent. Produces gives it an accuracy of (± 0,5 kg/ 1 lb). *(Golway Invent 2012)* Table 8 presents measured parameters from five test persons.

Table 8 presents firstly measured parameters from test persons

Test Person	**A**	**B**	**C**	**D**	**E**
Age:	59	31	29	61	54
Gender:	M	M	M	M	F
Weight (kg):	93,1	101,8	76,4	83,3	66,4
Height (m):	1,78	7,76	1,73	1,73	1,62
Max grip (kg):	32,7	54,7	45,7	44,2	21,6

After measuring properties presents in table 8, measurements were conducted with health chair's second pilot design. Test procedure started when test person sat on the chair. After, blood pressure measuring cuff and PPG finger clip was attached. Test person was asked to place hand on stainless steel sensor on the health chair's armrests. After this, measurement was conducted with health chair's measurement procedure. Table 9 presents measured parameter from each test person.

Table 9 presents measured parameters from second pilot design

Test Person	**A**	**B**	**C**	**D**	**E**
Weight (kg):	74	113	78	93	70
HR (1/min.):	81	60	53	71	69
Impedance (Ω):	178	144	152	158	206
Ox. Sat (%).:	98	96	98	95	96
BP sys. (mmHg):	163	125	117	142	110
BP dia. (mmHg):	100	79	71	87	73

Aim of the test was to verify that measurements could be done with second pilot. Weight of test persons was measured before the test to have a reference. Second pilot design measured weight of test person A too low. Measured weight was 93,1 kg but the result of the test was 74 kg. Difference was 19,1 kg Measurements for test person B, C, D and E were conducted on different day. For these measurements results were too high. Differences were 11,2 kg, 2,9 kg, 9,7 kg and 3,6 kg in order from test person B to E. These results, compared to reference weights, refer that weight was measured but accuracy was low. Low accuracy could have been a result from coupling of all four leads of weight measurements sensors to one analogue input of Arduino board. Higher accuracy could have been reached with coupling each lead wire to one analogue input of Arduino. This way each signal could be filtered and measured separately. Also, filtering of weight measurement signal could be redesigned. According to Webster *(2010, p. 153)* typical human heart rate is about 70 beats per minute. Measured heart rates of all test persons gave typical hear rate values. Mean value was calculated from measured impedance values, which were measured from 10 kHz to 100 kHz. Measurement system also used stainless steel electrode sensors. Blomqvist *(et al 2012)* conducted impedance measurements with different wet-electrodes from abdominal fat. He got impedance values varying 20 Ω to 120 Ω. All of the test persons had higher impedance than this. Probably affecting factors to measurements are used stainless steel sensor and senor-skin contact, which is known to be less conductive on dry-electrode interface than wet-electrode interface. Test person C and E were females. Females have typically higher fat percentage than males, when impedance is higher. This can be seen as positive sign when considering reliability of measurement. To give a statement about reliability of measurement it would require deeper investigation, but considering statements above we consider that we were measuring at least partially human impedance. Healthy individuals blood oxygen saturation values should be over 95 % *(Moyle 2002, p. 82)*. Test persons A, B and E had over this value and C and D this value. Patients' blood oxygen saturations were close to this value. According to Larkin (2005, p. 19) normal systolic blood pressure is under 130 mmHg and diastolic under 85. Test persons B, C and E ful-

filled normal blood pressure limits. Person A and D had higher blood pressure but these persons were also older, which can affect to blood pressure values.

After second pilot design tests, tests to measure ECG's RR and QT intervals were conducted. Aim of the test was to compare the results made with automated LabVIEW measurements and manually calculated result with Matlab. Ag/Ag-Cl wet electrodes (Ambu Blue Sensor L) were attached to test person. Arm electrodes were attached on right and left side few centimetres below collateral bones. Leg electrodes were attached above of highest point of ilium. This attachment is described in manual of EMB1 *(Corscience EMB1 2010, p. 46).* During measurement test persons were sitting on office environment. Tests persons' ECG was measured and recorded during one minute during which QT and RR intervals were calculated by LabVIEW program. ECG signal was measured with EMB1 ECG module. RR and QT intervals were measured with programs introduced. Appendices 8, 11, 13, 16 and 19 introduces results from measured and calculated RR and QT intervals from test persons A, B, C, D and E. In appendices "Measured RR" and "Measured QT" describes RR interval measured with LabVIEW program. In appendices "Calculated RR" and "Calculated QT" describes manually calculated QT and RR intervals. These intervals were calculated manually from recorded ECG signal, which was drawn with Matlab program. Following Matlab sketch was made to draw ECG signal:

```
%% ECG data was read before this from .txt file to dataecg
%% ECG drawing
Fs1 = 1000;
N1=length(dataecg);
n = 0:1:(N1-1);
time1 = n./Fs1;
figure(1);
plot(time1,dataecg);
title('Person A ECG');
xlabel('time');
```

Figure 31 present that RR intervals were calculated from peak of R wave to next R peak. QT interval was calculated from the beginning of Q wave to the end of T wave.

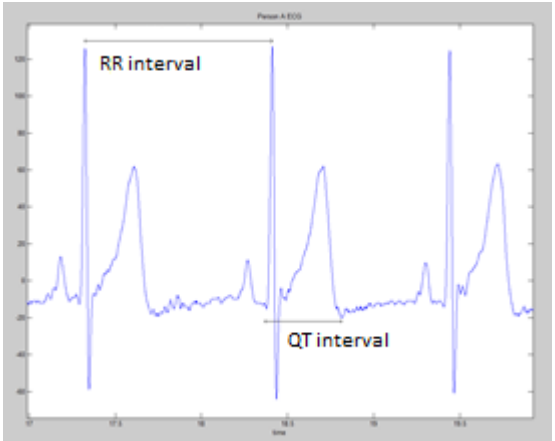

Figure 31 presents ECG signal drawn with Matlab. RR interval was calculated from peak of R wave to the peak of next wave and QT interval was calculated from the beginning of Q valley to the end of T wave.

Table 10 presents median values from measured and calculated RR and QT intervals, their median differences and their standard deviations (σ). Appendix 8, appendix 11, appendix 13, appendix 16 and appendix 19 present the test results from measured and calculated RR and QT values.

Table 10 presents median values and standard deviations from measured and calculated RR and QT intervals.

Test person	A	B	C	D	E
Measured RR median:	1170	907	1320	1322,5	1094
Calculated RR median:	1180	938	1333	1350,5	1108
Median difference:	-11	-28	3	-38	-18
Measured RR σ:	46,33	44,01	51,95	37,89	29,64
Calculated RR σ:	81,67	125,83	82,00	83,09	84,32
Measured QT median:	387	364	411	375	387
Calculated QT median:	426	421	453	481	460
Median difference:	-50	-57	-44	-109	-83
Measured QT σ:	347,89	143,99	21,99	230,13	280,00
Calculated QT σ:	27,77	39,47	22,79	24,73	30,66

Table 10 reveals that median differences of RR interval detection stays under 1 % , despite of person B who has 3 %, compared against "Measured RR median". "Measured RR median" was time measured with LabVIEW. Measured RR standard deviation (σ) tells that RR intervals stay under 55 ms close to their average. Median differences of QT intervals compared against values measured with LabVIEW are 12,9 %; 15,6 %; 10,7 %; 30 % and 21,4 % in order from A to E. Automatically measured QT standard deviations are large on test persons A, B, D and E. Test person C has smallest standard deviation and QT intervals have been narrowly spread. RR intervals have larger standard deviation from manual calculation than with automated LabVIEW calculation. This speaks that automated measurements are more precise than manual calculations. In case of QT intervals situation is opposite. Manually calculated results ("Calculated QT σ") have smaller standard deviation than with results measured with LabVIEW ("Measured QT σ").

Appendices 9, 12, 14, 17 and 20 present drawn Bland-Altman plots where mean values and differences between two methods are presented. Bland-Altman plots are supposed to describe precision of measured values. As can be seen from theses appendices precision of RR interval detection is spread to small area. Few larger differences between measurements can be detected on each test person. The phenomena imply that algorithm cannot detect every R peak, because it is detected with manual examination. Precision of all point RR interval points is satisfying. I suspect that small fluctuation between RR intervals is natural. Precision of QT interval detection is widely spread on test persons A, B, D, and E. QT intervals of test person C have been spread on small area, in appendix 14. In appendix 12, test person B has few erroneous measurements but majority of QT intervals are on narrow area. On tests persons A, D and E (in appendices 9, 17 and 20) QT intervals have been spread. These persons have clearly detectable groups of QT

intervals on smaller area and these groups are more widely spread. I assume that these refer to systematic error. This systematic error can rise from peak or valley detection method used. Probably on these cases T peak, P peak, Q valley or the end of T wave cannot clearly be detected by algorithm. Also, PQRST- complex is individual and can vary depending on person. Noise on the signal could have been caused error to QT intervals. Figure 32 presents two QRST-complexes from each test person.

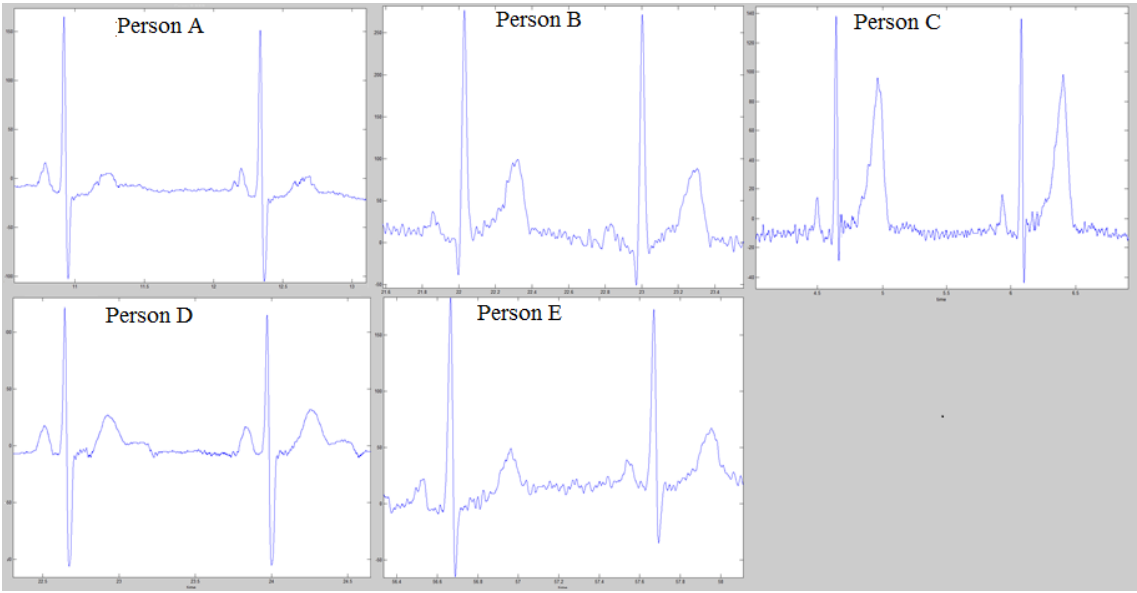

Figure 32 present two PQRST complexes from each test person.

After testing test persons RR and QT detection, blood pressure was estimated with pulse transit time from each test person. Test persons were seated in office environment during the test. ECG signal of test persons was measured with EMB1 ECG module. Same electrodes and electrode attachments were used as described in previous chapter. PPG signal was measured with EG00352 pulse oxymeter board *(Medlab EG00352 2012).* Pulse oximeter finger clip was attached to left little finger. Blood pressures were measured from right arm of the patient with Omron M6 Comfort Blood Pressure meter (model HEM-7000-E). Producer promises accuracy of ± 3 mmHg to it *(Omron 2013).* Patient also squeezed grip strength meter with his right hand.

Tests were firstly calibrated to estimate blood pressure from pulse transit times. First calibration was done after starting PPG and ECG signal measurements. It was done without physical activity. In the calibration stage, test person was relaxed and PTTs were measured during one minute. Mean value for pulse arrival times was calculated, which gave reference value to higher PTT. During calibration systolic blood pressure was measured with blood pressure cuff attached to right arm of the patient. This value gave reference to lower blood pressure value. After first calibration, test person was asked to squeeze grip strength meter for one minute with half from maximum grip strength. After one minute of squeeze it was continued and second calibration was started. Again one minute of PTT values were recorded and mean value was calculated from it. This gave reference value to lower PTT. This time measurement was done during physical activity. During squeeze and PTT calculation systolic blood pressure was

measured. This gave reference to higher blood pressure value. After the calibrations, test persons PTTs were recorded. These PTT values were compared against lower and higher PTT values with known systolic blood pressure values. With this comparison blood pressure values were estimated from measured PTT values. Blood pressures were estimated and recorded during four minutes. Before one-minute blood pressure estimation was done without physical activity. After one-minute to the end of measurement, which lasted four minutes, was recorded squeezing with half force from maximum grip strength. During this measurement systolic blood pressure values were estimated using PTT's. Following list clarifies measurement procedure:

- 1st calibration
  - No physical activity
  - Systolic blood pressure measured
  - PTTs measured and mean value calculate from them
- 2nd calibration
  - Physical activity
  - Systolic blood pressure measured
  - PTTs measured and mean value calculate from them
- 0th minute measurement
  - No physical activity
  - PTTs measured and systolic BP estimated
- 1st minute measurement
  - Systolic blood pressure measured in time 1:00
  - Physical activity added after measurement
  - PTTs measured and systolic BP estimated
- 2nd minute measurement
  - Physical activity
  - Systolic blood pressure measured in time 2:30
  - PTTs measured and systolic BP estimated
- 3rd minute measurement
  - Physical activity
  - Systolic blood pressure measured in time 3:30
  - PTTs measured and systolic BP estimated

Hey *(et al. 2009)* estimated length of pulse arrival time to be 0,11- 0,475 seconds measured from R peak to P base point of PPG wave. Our measurements introduce that pulse transit times varies around 300 -550 ms measured from R peak to peak of PPG. Calculated medians were 509 ms from person A and B, 422 ms from person C, 469 ms from person D and E. Comparing this to numbers introduced by Hey measured PTTs are large, which is obvious because of later PPG measurement point . Measured PTTs can be considered reliable. The results from measured PTTs during 4 minutes measurements are presented in appendices 10, 12, 15, 18 and 21.

Figure 33 has been drawn from table 11. It presents estimated blood pressures measured from test person A. Column "Estimated BP dPTT" presents estimated systolic blood pressures with method introduced by Chen *(et al. 2000).* Column "Estimated BP straight" introduces systolic blood pressure values estimated with help of two reference

points. Column “Sys BP” presents systolic blood pressure values measured with cuff blood pressure measurement device Omron M6 Comfort. “Difference dPTT” is the difference between “Estimated BP dPTT” and “Sys BP”. “Difference straight” is the difference between “Estimated BP straight” and “Sys BP”.

Table 11 present estimated and measured blood pressures from person A

min	Estimated BP dPTT	Estimated BP straight	Sys BP	Difference dPTT	Difference straight
0,5	141	139			
1	177	168	154	-23	-14
1,5	141	138			
2	141	139			
2,5	204	187	168	-36	-19
3	141	140			
3,5	141	139	181	40	42
4	141	141			

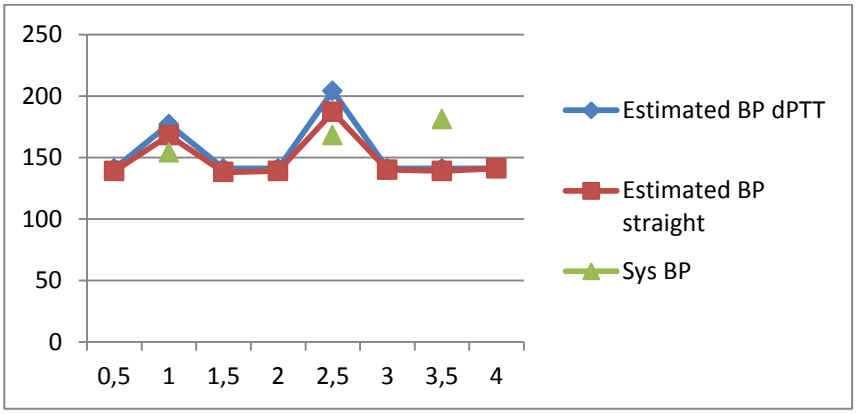

Figure 33 presents systolic blood pressure estimations and measured systolic blood pressures from test person A.

In figure 33 measured blood pressure raises almost linearly. From figure 33 we can see that “Estimated BP dPTT” and “Estimated BP straight” behaves almost same way. Increase in systolic BP can be seen in times of one and two and half minutes in both estimation methods. Both estimation methods give low blood pressure values at the beginning when person was note doing physical activity, which yields to lower values. “Estimated BP dPTT” estimates BP a bit higher than “Estimated BP straight”. Measured systolic blood pressure has been measured with in certain point of time. Estimated blood pressure has been estimated continuously. Figure 33 reveals that both blood pressure estimation methods follow “Sys BP” in two first points. Following of the third point cannot be noted in this chart, but could happen later because the “Sys BP” measurement was made from right hand of the patient. Same hand gripped the strength meter, which can raise blood pressure in right hand faster than in whole body. PTT estimation method estimated whole body blood pressure.

Table 12 present estimated and measured blood pressures from person B

min	Estimated BP dPTT	Estimated BP straight	Sys. BP	Difference dPTT	Difference straight
0,5	123	122			
1	124	121	117	-7	-4
1,5	117	122			
2	117	122			
2,5	117	122	123	-117	-122
3	117	122			
3,5	117	123	131	-117	-123
4	126	121			

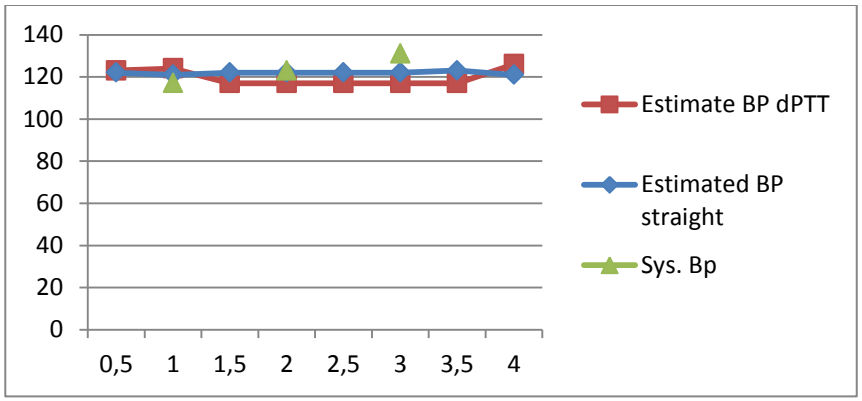

Figure 34 presents systolic blood pressure estimations and measured systolic blood pressures from test person B.

Table 12 presents measured and estimated systolic blood pressure values from test person B. Figure 34 has been drawn from table 12. Figure 34 reveals that measured "Sys BP" increases almost linearly during measurement. "Estimated BP straight " and "Estimated BP dPTT" behaves almost linearly. "Estimated BP dPTT" seems under estimate systolic blood pressure a bit more than "Estimated BP straight". Both methods seem to be quite precise in time of one minute and one and half minute. In time of three minute both estimation methods get less precise.

Table 13 present estimated and measured blood pressures from person C

min.	Estimated BP dPTT	Estimated BP straight	Sys. BP	Difference dPTT	Difference straight
0,5	113	113			
1	113	113	115	2	2
1,5	112	113			
2	167	120			
2,5	113	113	125	12	12
3	113	113			
3,5	113	112	139	26	27
4	114	113			

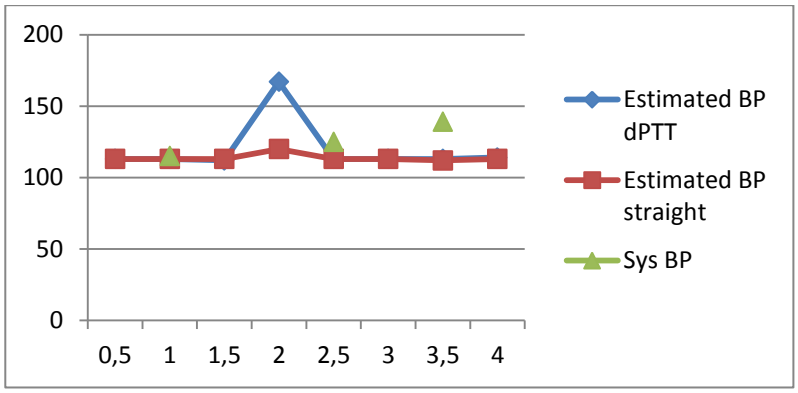

Figure 35 presents systolic blood pressure estimations and measured systolic blood pressures from test person C.

Tests done for test person C reveals with help of table 13 and 35 that differences "Estimated BP dPTT" and "Estimated BP straight" measurement points are the same, but Chen's method has a large increase in time of two minutes. "Estimated BP straight" has a small increase in estimated systolic blood pressure but does not yield to significant increase. As in all previous tests, here as well "Sys BP" increases almost linearly. Here neither estimation methods does follow the systolic blood pressure, but could follow it if the measurement would be longer. I assume that whole body's blood pressure does not increase that fast as local blood pressure in right arm. Table 13 reveals that both estimation method have exactly same difference with systolic BP values in times of one minute and two and half minute.

Table 14 present estimated and measured blood pressures from person D

min	Estimated BP dPTT	Estimated BP straight	Sys. BP	Difference dPTT	Difference straight
0,5	141	130			
1	133	131	118	-15	-13
1,5	117	147			
2	137	127			
2,5	117	148	136	19	-12
3	143	121			
3,5	166	107	147	-19	40
4	142	122			

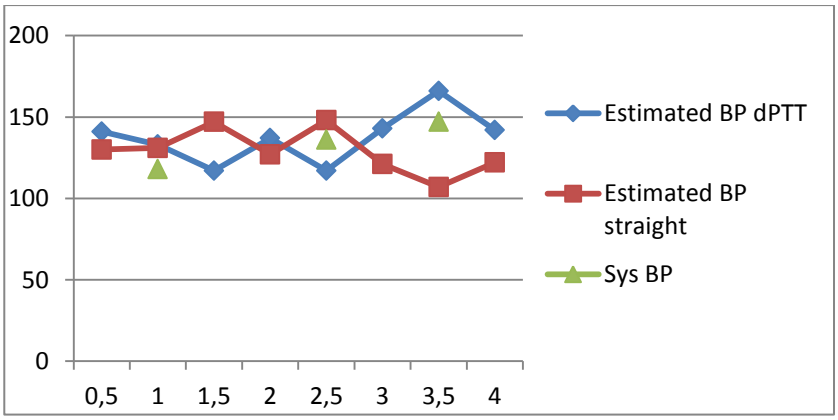

Figure 36 presents systolic blood pressure estimations and measured systolic blood pressures from test person D.

From table 14 and from figure 36 we can see that “Sys BP” increases almost linearly. “Estimated BP dPTT” and “Estimated BP straight” behaves inversely. Interestingly in one minutes time, which has been measured when test person has been relaxed, is almost the same. In two minutes and half time when physical activity has been included “Estimated BP dPTT” under estimated and “Estimated BP straight” over estimated the value. At the point of tree and half minute the estimations change to opposite. “Estimated BP dPTT” have smaller median difference which speaks about it could be more accurate on test person D.

Table 15 present estimated and measured blood pressures from person E

min.	Estimated BP dPTT	Estimated BP straight	Sys. BP	Difference dPTT	Difference straight
0,5	106	167			
1	132	108	111	-21	3
1,5	106	161			
2	105	159			
2,5	106	162	127	21	-35
3	106	162			
3,5	106	162	152	46	-10
4	153	92			

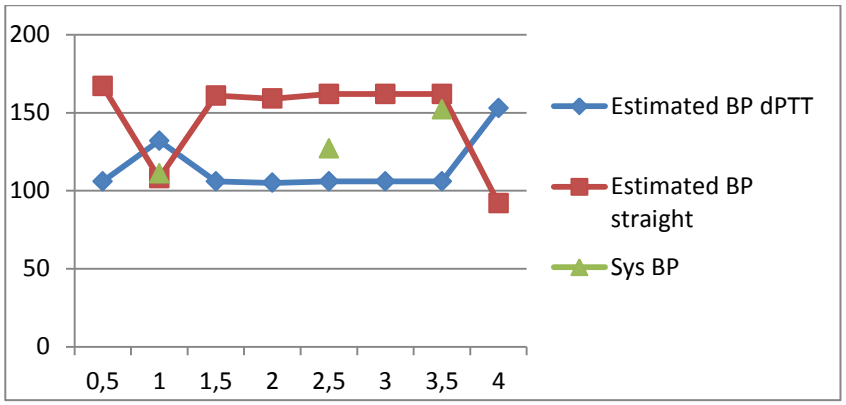

Figure 37 presents systolic blood pressure estimations and measured blood pressures measured from person E.

Figure 37 revels that “Estimated BP dPTT” estimates systolic blood pressure lower compared to again almost linearly increasing systolic blood pressure. “Estimated BP straight” shows estimated blood pressure almost correctly in point of one-minute time. After, it estimates blood pressure too high and drops down in after tree and half minutes point. “Estimated BP dPTT” show a bit more accurate median difference in table 15 than “Estimated BP straight”.

To summarize the tests, estimated systolic blood pressure was compared against systolic blood pressure values measured with intermittent cuff method. With cuff measurement a single determination of blood pressure was obtained. Cuff estimated systolic blood pressure had linear growth, which was aimed and achieved. Two systolic blood pressure estimation methods were compared and systolic blood pressure was estimated with them. In two from five tests inverse behaviour between estimation methods was noted. In three from five tests both estimation method had same behaviour. This can be algorithm depended. Both estimation methods had different estimation algorithms. Differ-

ence in behaviours can be explained that other method (“Estimated BP straight”) used two calibration points instead of one. The median differences between estimation methods varied widely. Larger scale test would be needed to separate the estimation methods precision. More tests would also be needed to decide which of the methods is more convenient to clinical use. Main difficulty in this method is that the elasticity of the vessels walls is not constant. The elasticity of the arterial wall differs from individual to individual and is affected by neuro-humoral factors. Some authors recommended re-calibration between PTT and measured systolic BP at 5 minutes intervals to the method. Considering these results calibration is essential and re-calibration would be recommended. Considering these results the method is neither compatible for determine absolute blood pressure or detecting small changes of blood pressure but could be compatible for monitoring blood pressure in long periods.

7.3 Conclusion

In the thesis ECG was measured with dry-electrodes with satisfying quality, the blood pressure was estimated with pulse transit time and RR and QT intervals were measured. ECG was measured with Ag-electrodes with using active electrodes and ECG module presented. PTT estimation method was used for continuous non-invasive systolic blood pressure estimation with using re-calibration in short-term intervals. According to results systolic blood pressure can be estimated using calibration and measuring PTT values. In measurement arrangement more continuous BP values would have been archived with invasive measurement. I suspect that errors in cuff placement can yield to some errors in BP values. With invasive method this could be avoided, but the method would complicated the test process with necessary medical permissions and presence of medical personnel. Increase of BP was done with squeezing grip strength meter. Increase could have been done with medication or other kind of physical activity. Medication would have needed authorizations. All kind of physical activity needs muscle movement, which can add error to BP measurement. Grip strength meter was seen proper way. In measurement arrangement test person was sitting on the chair. Other option could be that test person would be lying on the bed. I suspect that lying position is not recommendable position to cuff BP measurement, if so this method would possible require invasive BP measurement method. More accurate measurements would have been received from PPG peak detection if sampling frequency of module had been larger. In used module, sampling frequency was 50 Hz. Measurement system was done with two separate OEM modules and with one LabVIEW program. The information processing speed of the program stayed unknown. One solution to measurement arrangement would be designing a system, which measures both ECG and PPG using one internal clock. One internal clock would possible that the program could assume that the intervals between received samples are the same. In this way PTT could be calculated from sample intervals. Sampling frequency of the system should be set to high. Then time intervals would stay constant between samples and error between two different clocks would not sum during time. This way using counter clocks inside the program would be avoided. It would simplify the measurement and avoid the possible errors rising from them.

Considering the results, BP estimation method is compatible for systolic blood pressure estimation when re-calibration is used. QT interval measurement had good precision on one of the test persons. With RR interval measurements satisfying accuracy was reached with all of the test persons. To assure their compatibility to real human diagnostics QT interval detection should be designed differently. It should achieve satisfying precision on all of the test persons. Considering all of the method introduced more larger scale test would be needed before these designed methods could be used in clinical use. If the elasticity of the vessel could be known the systolic blood pressure estimation using PTT would enable new method for blood pressure estimation. It would have large impact commercially and in clinical use.

Considering health chair's RR and QT interval economic value, it is large as they form necessary part from its ECG diagnostic it enables. The economic value of health chair

can be large. It decreases the time used to measurement by fastening the measurement procedure. With appropriate operating system it could send the measurement to external server where health care personnel could analyse the data. This would ease analysing health data and would allow automated alarm setting when unhealthy signs are detected. Also, this would enable long-term patient monitoring and disease diagnostic from home or from health care facility. Also, health chair could cut down health device cost by integrating all necessary measurements to one concept. This would enable manufacturing on large scale and it would cut down device costs.

8 Summary

This master's thesis was part of larger development process, which aimed to realize a health chair for monitoring patient state of health. It was a research of Aalto University's Health Factory. It was participated also by the Institute of Healthcare Engineering, Management and Architecture (HEMA). Aim of this master's thesis was to participate in to technical development of the health chair by realizing wanted measurements to health chair pilot designs from selected modules. This includes doing all the necessary coupling and programming to implement wanted measurements. In addition, aim was to design automated calculations of RR and QT intervals from ECG module and test their compatibility in use. Aim was also to design, execute and test estimating of patient blood pressure with pulse transit time method. Two different estimating methods was implemented and tested. The thesis introduced a design of dry-electrode contact electrocardiography measurement from chosen ECG module. It also collects information related to realize pilot designs measurements.

The thesis introduces health chair's first pilot design, which worked as test platform to test the chosen measurement modules and verify their compatibility to use. Realization of measurements was made with EMB1 electrocardiography module, ChipOx photoplethysmography module, openEBI electrical bioimpedance module and weight sensors. Necessary LabVIEW programs were made to monitor the measurements. Secondly the master's thesis introduces second health chair pilot design. The design was more developed and it included blood pressure, weight, photoplethysmography, electrical bioimpedance, blood oxygen saturation and heart rate measurements. All these measurement were executed on this health chair. The thesis also introduces made LabVIEW programs to monitor measurement modules and understand its operating system made. The third pilot design was not realized to the end during this master's thesis, although work done and introduced in this master's thesis play essential role in its measurements. The third pilot design was designed to include electrocardiography, weight, bioelectrical impedance, blood oxygen saturation, hear rate and photoplethysmography measurements and systolic blood pressure estimation from pulse transit time. The thesis introduces realized dry-electrode ECG measurement and two realized systolic blood pressure estimation methods. RR and QT interval calculations and BP estimation methods were made with LabVIEW. The designs of these programs are presented.

This master's thesis present tests made to five persons from different age categories. Firstly, functioning of second pilot design measurements were tested. Aim of the test was to verify that measurements could be done with second pilot design. Results are present in the thesis and refer that all the tests were done. Secondly, compatibility of RR and QT intervals calculations were tested. Aim of the test was to compare the results made with automated LabVIEW measurements and manually calculated result with Matlab. The results are presented. RR interval calculations had small standard deviation and median error than QT interval calculations. RR interval calculations were considered precise. Lastly, systolic blood pressure was estimated with measured pulse transit times from these five test persons. Two different estimation methods were used. Con-

sidering the results the method is neither compatible for determine absolute blood pressure or detecting small changes of blood pressure but could be compatible for monitoring blood pressure in long periods.

Bibliography

ANALOG DEVICES, 2013-last update, AD 8627, AD8625/AD8626/AD8627 Data Sheet [Homepage of Analog Devices], [Online]. Available: http://www.analog.com/static/imported-files/data_sheets/AD8625_8626_8627.pdf [09/09, 2013].

ARDUINO, 27/5/2013, 2013-last update, Arduino Uno [Homepage of Arduino], [Online]. Available: http://arduino.cc/en/Main/ArduinoBoardUno [26/6, 2013].

BAURA, G.D., cop. 2002. *System theory and practical applications of biomedical signals.* [Piscataway, N.J.]: IEEE Press.

BAURA, G.D., 2008. *A biosystems approach to industrial patient monitoring and diagnostic devices.* San Rafael, Calif: Morgan & Claypool Publishers.

BLOMQVIST, K.H., 05/2013, 2013-last update, OpenEBI for Electrical Bioimpedance [Homepage of GitHub, Inc], [Online]. Available: https://github.com/openebi [07/10, 2013].

BLOMQVIST, K.H., SEPPONEN, R.E., LUNDBOM, N. and LUNDBOM, J., 2012. An open-source hardware for electrical bioimpedance measurement, *Electronics Conference (BEC), 2012 13th Biennial Baltic* 2012, pp. 199-202.

CHEN, W., KOBAYASHI, T., ICHIKAWA, S., TAKEUCHI, Y. and TOGAWA, T., 2000. Continuous estimation of systolic blood pressure using the pulse arrival time and intermittent calibration. *Medical and Biological Engineering and Computing*, 38(5), pp. 569-574.

CHI, Y.M., TZYY-PING JUNG and CAUWENBERGHS, G., 2010. Dry-Contact and Noncontact Biopotential Electrodes: Methodological Review. *Biomedical Engineering, IEEE Reviews in*, 3, pp. 106-119.

CORSCIENCE GMBH & CO. KG, 2010. *ChipOx, User manual, Technical Integration Instructions, Digital Pulse Oximeter Module ChipOx.* Erlangen, Germany: Corscience GmbH & Co. KG.

CORSCINCE GMBH & CO. KG, ed, 2010. *EMB1, User manual, Techincal Integration Instructions, EMB1, EMB3/6.* Erlangen, Germany: Corscince GmbH & Co. KG.

ESPINA, J., FALCK, T., MUEHLSTEFF, J. and AUBERT, X., 2006. Wireless Body Sensor Network for Continuous Cuff-less Blood Pressure Monitoring, *Medical Devices and Biosensors, 2006. 3rd IEEE/EMBS International Summer School on* 2006, pp. 11-15.

FAHEY, T., MURPHY, D. and HART, J.T., 2004. *High blood pressure : the 'at your fingertips' guide.* 3rd ed. edn. London: Class Publishing.

GEDDES, L.A. and BAKER, L.E., 1968. *Principles of applied biomedical instrumentation.* Wiley.

GLASZIOU, P., ARONSON, J.K. and IRWIG, L., 2008. *Evidence-based medical monitoring : from principles to practice.* Malden, Mass: Blackwell Pub./BMJI Books.

GLOWAY INVENET, , Puristusvoimamittari. Available: http://www.gloway.fi/index.php/tuotteet/digitaalinen-kasivoimamittari/ [9/11, 2013].

GRUETZMANN, A., HANSEN, S. and MÜLLER, J., 2007. Novel dry electrodes for ECG monitoring. *Physiological Measurement,* 28(11), pp. 1375.

HAARNOJA, P., 2012. *Verenpaineen kajoamaton mittaus pulssin kulkuajan avulla. Master's thesis.*, Aalto University.

HEMA INSTITUTE, 03/04/2013, 2013-last update, Home Page of HEMA Institute [Homepage of Aalto University], [Online]. Available: http://hema.aalto.fi/en/ [07/16, 2014].

HEY, S., GHARBI, A., VON HAAREN, B., WALTER, K., KONIG, N. and LOFFLER, S., 2009. Continuous Noninvasive Pulse Transit Time Measurement for Psycho-physiological Stress Monitoring, *eHealth, Telemedicine, and Social Medicine, 2009. eTELEMED'09. International Conference on* 2009, IEEE, pp. 113-116.

KHANDPUR, R.S., cop. 2005. *Biomedical instrumentation : technology and applications.* New York: McGraw-Hill.

KYLE, U.G., BOSAEUS, I., DE LORENZO, A.D., DEURENBERG, P., ELIA, M., GÓMEZ, J.M., HEITMANN, B.L., KENT-SMITH, L., MELCHIOR, J., PIRLICH, M., SCHARFETTER, H., SCHOLS, A.M.W.J. and PICHARD, C., 2004. Bioelectrical impedance analysis—part I: review of principles and methods. *Clinical Nutrition,* 23(5), pp. 1226-1243.

LARKIN, K.T., 2005. *Stress and hypertension : examining the relation between psychological stress and high blood pressure.* New Haven: Yale University Press.

LEE, S. and KRUSE, J., 2008. *Biopotential Electrode Sensors in ECG/EEG/EMG Systems.* Analog Devices.

LEE, C., SIK SHIN, H. and LEE, M., 2011. Relations between ac-dc components and optical path length in photoplethysmography. *J Biomed Opt,* 16(7),.

MA, T. and ZHANG, Y.T., 2005. A Correlation Study on the Variabilities in Pulse Transit Time, Blood Pressure, and Heart Rate Recorded Simultaneously from Healthy Subjects, *Engineering in Medicine and Biology Society, 2005. IEEE-EMBS 2005. 27th Annual International Conference of the* 2005, pp. 996-999.

MALMIVUO, J. and PLONSEY, R., 1995. *Bioelectromagnetism : principles and applications of bioelectric and biomagnetic fields.* http://www.bem.fi/book/index.htm edn. New York: Oxford U.P.

MARTINEZ, F.S., 2007. *Electrical Bioimpedance Cerebral Monitoring: Fundamental Steps towards Clinical Application*, Chalmers University of Technology.

MCCARTHY,B.M. AND O'FLYNN B. AND MATHEWSON A., 2011. An Investigation of Pulse Transit Time as a Non-Invasive Blood Pressure Measurement Method. *Journal of Physics: Conference Series,* 307(1), pp. 012060.

MEDLAB, MEDLAB MEDIZINISCHE DIAGNOSEGERÄTE GMBH, 2012. *EG00352, Pulse Oximeter OEM Board EG00352, Technical Manual.* http://www.medlab-gmbh.de/english/downloads/eg00352_30.pdf edn. Karlsruhe, Germany: Medlab medizinische Diagnosegeräte GmbH.

MEDLAB, MEDLAB MEDIZINISCHE DIAGNOSEGERÄTE GMBH, 2012. *NIBScan, Hospital Grade Miniature Non-Invasive Blood Pressure OEM Module for Professional Applications.* http://www.medlab-gmbh.de/english/downloads/nibpscan-14.pdf edn. Karlsruhe, Germany: Medlab medizinische Diagnosegeräte GmbH.

MOYLE J.T.B., ed, 2002. *Pulse Oximetry.* 2 edn. London: BMJ Books.

MUOBARAK, J.T., 2012. Bioelectrical Impedance as a Diagnostic Factor in the Clinical Practice and Prognostic Factor for Survival in Cancer Patients: Prediction, Accuracy and Reliability. *Journal of Biosensors & Bioelectronics,* .

NATIONAL INSTRUMENTS, 2013-last update, LabVIEW System Design Software [Homepage of National Instruments], [Online]. Available: http://sine.ni.com/np/app/main/p/docid/nav-104/lang/fi/ [05/24, 2013].

NATIONAL INSTRUMENTS, 03/02/2011, 2011-last update, CRC-16-CCITT of serial packets [Homepage of National Instruments], [Online]. Available: http://forums.ni.com/t5/LabVIEW/CRC-16-CCITT-of-serial-packets/td-p/1471386 [17/06, 2013].

NEWLIN, D.B., 1981. Relationships ol Pulse Transmission Times to Pre-ejection Period and Blood Pressure. *Psychophysiology,* 18(3), pp. 316-321.

NIH, NATIONAL HEART, LUNG AND BLOOD INSTITUTE, August, 02 2013, 2013-last update, NIH, National Heart, Lung and Blood Institute [Homepage of NIH, National Heart, Lung and Blood Institute], [Online]. Available: http://www.nhlbi.nih.gov/index.htm [08/05, 2013].

OMRON, , Omron M6 automaattinen verenpainemittari [Homepage of Omron], [Online]. Available: http://www.omaomron.fi/tuotteet?ryhma=Poistuneet+mallit+verenpainemittarit&tuote=M6&r=10.50&t=18392558 [09/16, 2013].

PARATI, G., 1989. Comparison of finger and intra-arterial blood pressure monitoring at rest and during laboratory testing. *Hypertension, 1989, Vol.13(6 Pt 1), pp.647-55,* 13(6), pp. 647-55.

REIJULA, J., 2007. *Älykäs potilasvuode tehohoitopotilaan seurannassa*, Helsinki University of Technology.

RUIZ, J.C.M., 2011. *On the Feasibility of Using Textile Electrodes for Electrical Bioimpedance Measurements,* Royal Institute of Technology.

SANS, S., KESTELOOT, H. and KROMHOUT, D., 1997. The burden of cardiovascular diseases mortality in Europe Task Force of the European Society of Cardiology on Cardiovascular Mortality and Morbidity Statistics in Europe. *European heart journal,* 18(8), pp. 1231-1248.

TEXAS INSTRUMENTS, 04/2005, 2005-last update, OPA 277, OPA 2277, OPA 4277 [Homepage of Texas Instruments], [Online]. Available: http://www.ti.com/lit/ds/symlink/opa277.pdf [09/09, 2013].

TEXAS INSTRUMENTS, 09/27/2000, 2000-last update, INA 122 [Homepage of Texas Instruments], [Online]. Available: http://www.ti.com/lit/ds/symlink/ina122.pdf [06/26, 2013].

TOIVONEN, T., 2009. *Ballistografisen mittaustuolin anturivahvistimen kehitys ja toteutus.*, Helsinki University of Technology.

TORTORA, G.J. and DERRICKSON, B., 2007. *Principles of anatomy and physiology.* 11. ed. edn. New York: Wiley.

URPALAINEN, K., 2011. *Development of a fractional multi-wavelength pulse oximetry algorithm,* Aalto University School of Electrical Engineering.

WEBSTER, J.G. and CLARK, J.W., cop. 2010. *Medical instrumentation : application and design.* 4. ed. edn. Hoboken, NJ: John Wiley & Sons.

YONG GYU LIM, KO KEUN KIM and SUK PARK, 2006. ECG measurement on a chair without conductive contact. *Biomedical Engineering, IEEE Transactions on,* 53(5), pp. 956-959.

ZAKARIA, N.A., SHARIFMUDDIN, N.B., RIDZWAN, W.M.F.W. and MAHMOOD, N.H., 2010. Pulse Wave Transit Time and Its Relationship with Systolic Blood Pressure. In: C.T. LIM and J.C.H. GOH, eds, Springer Berlin Heidelberg, pp. 1354-1357.

List of appendices

Appendix 21. Presents RR and QT interval Bland-Altman plots measured from test person E. 1 page.

Appendix 22. Present pulse transit times measured from test person E. 1 page.

Appendix 1. Presents EMB1 VI where its parts EMB1 Request ID VI, CRC 16 CCIITT VI, Protocol Analog Req VI, Decoding ECG signal VI and Unpack ECG block diagrams.
1 page.

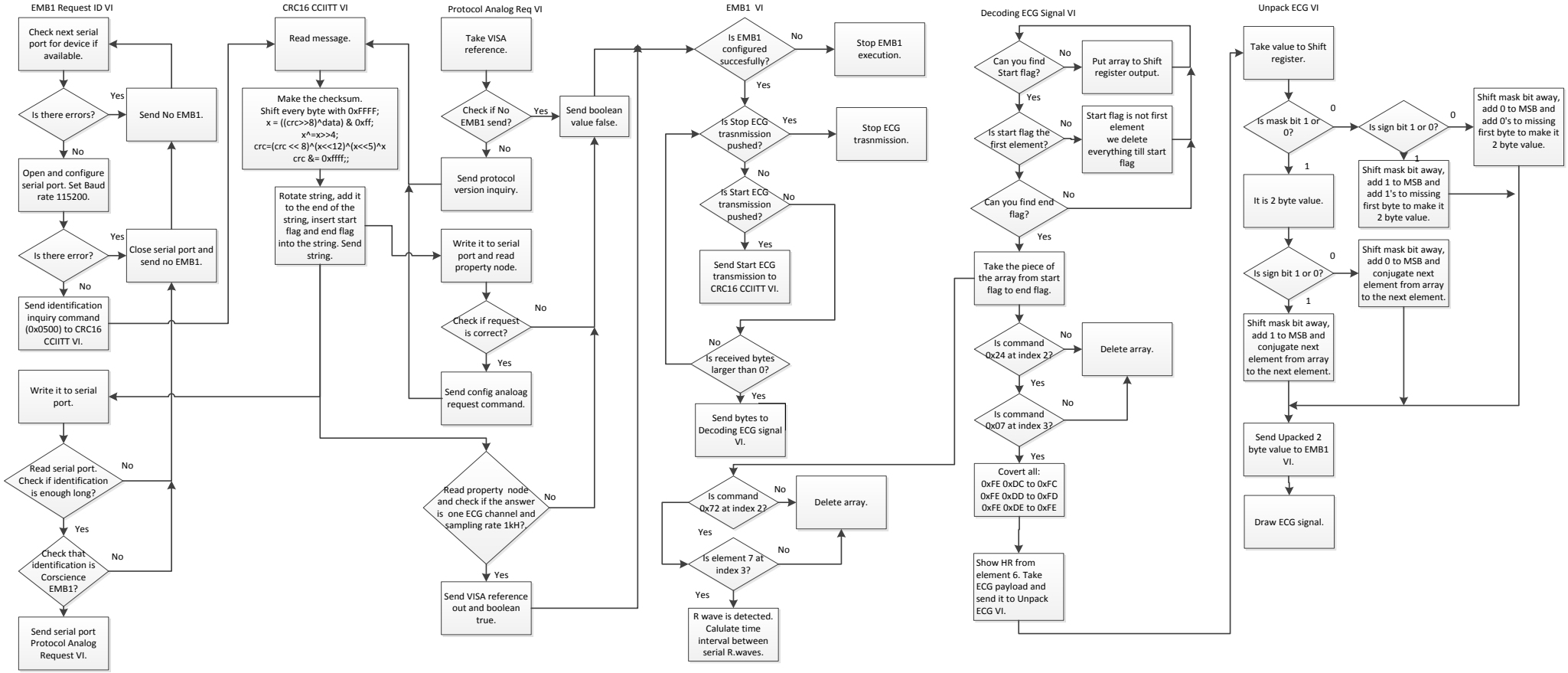

Appendix 2. Presents block diagrams of ChipOx user interface, Find ChipOx and ChipOx decodingVIs. 1 page.

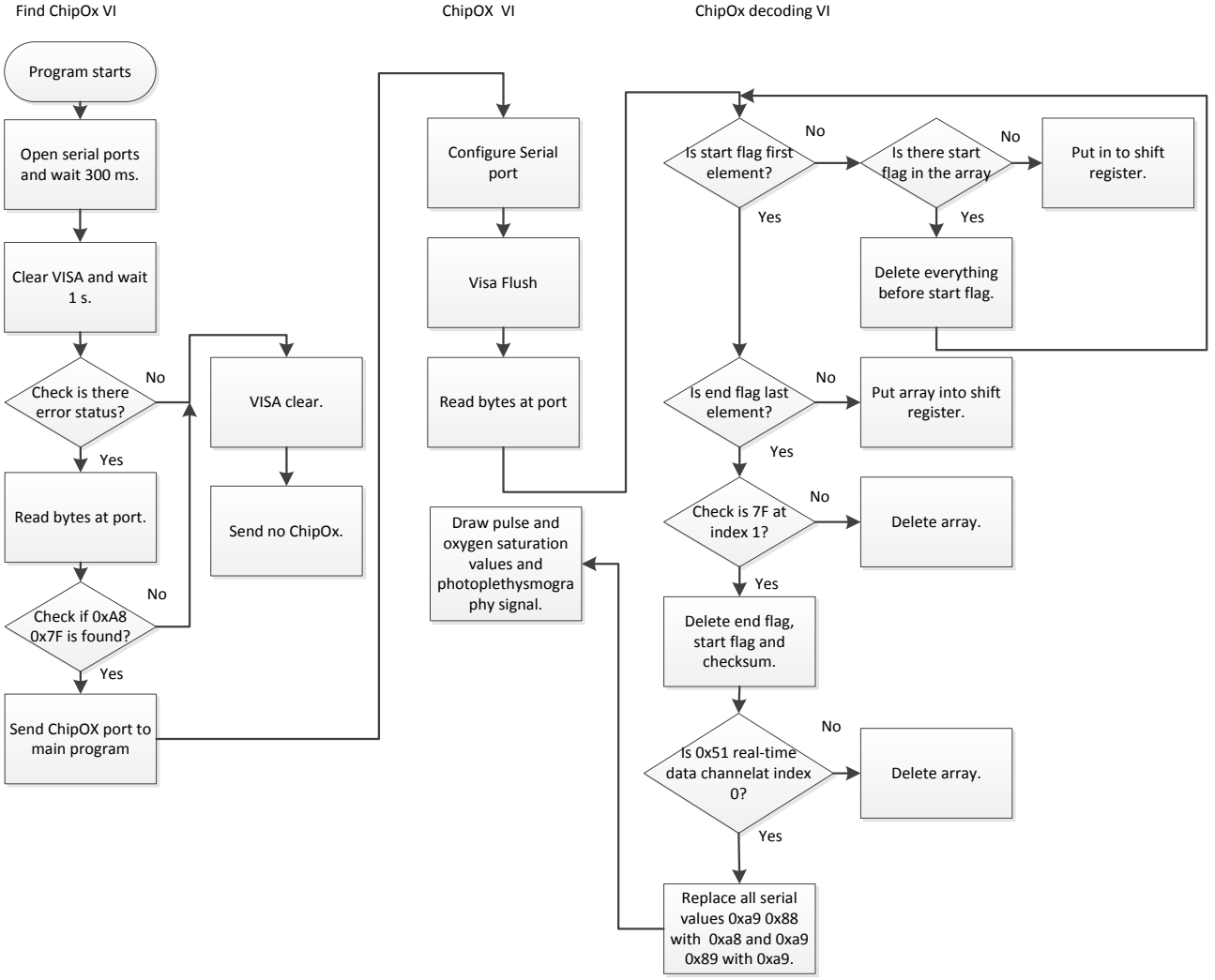

Appendix 3. A broad-minded block diagram arrangements of connection, modules and other devices in pilot two. 1 page.

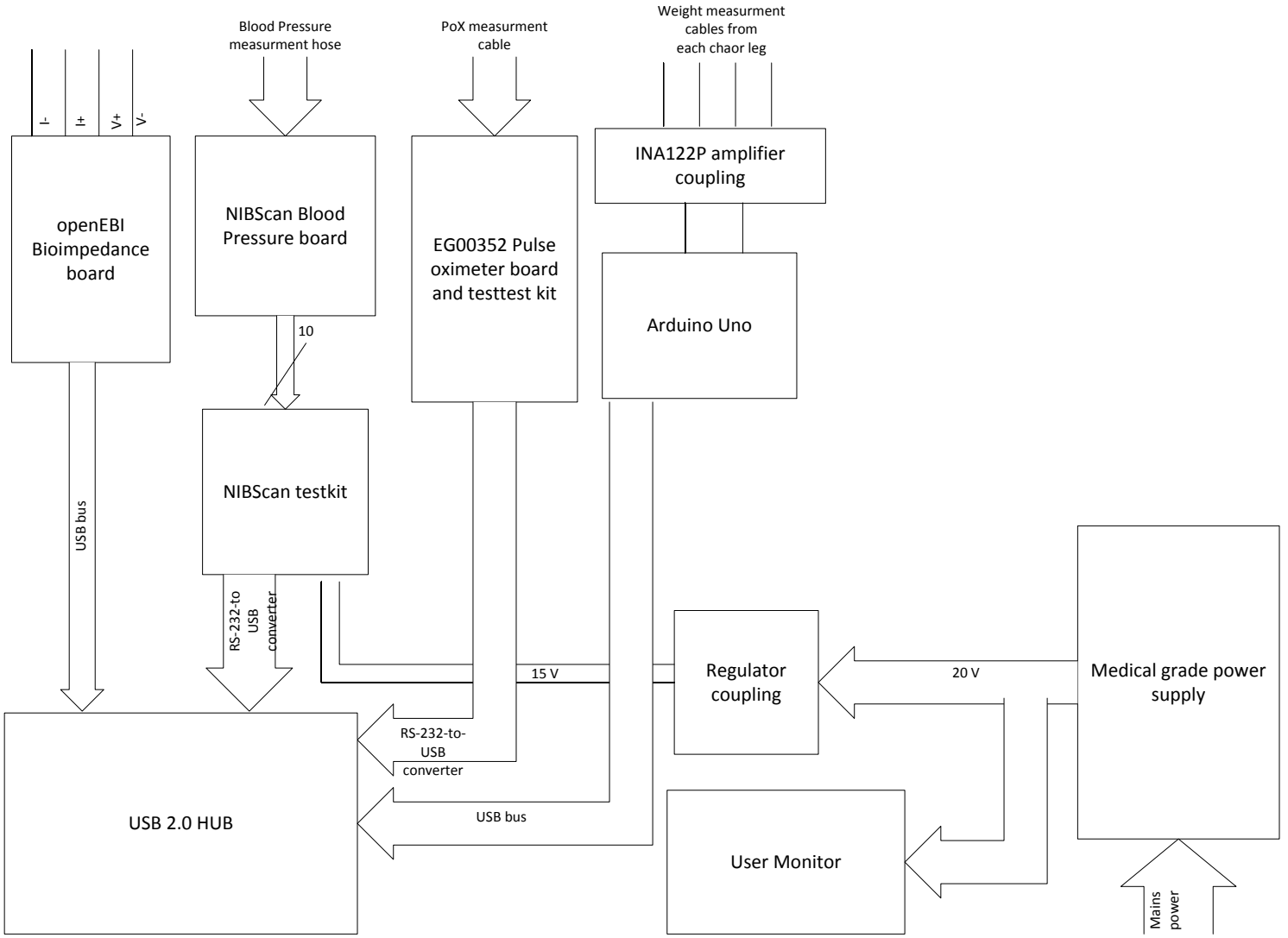

Appendix 4. Block diagram of EG00352 VI and Find POX VI. 1 page.

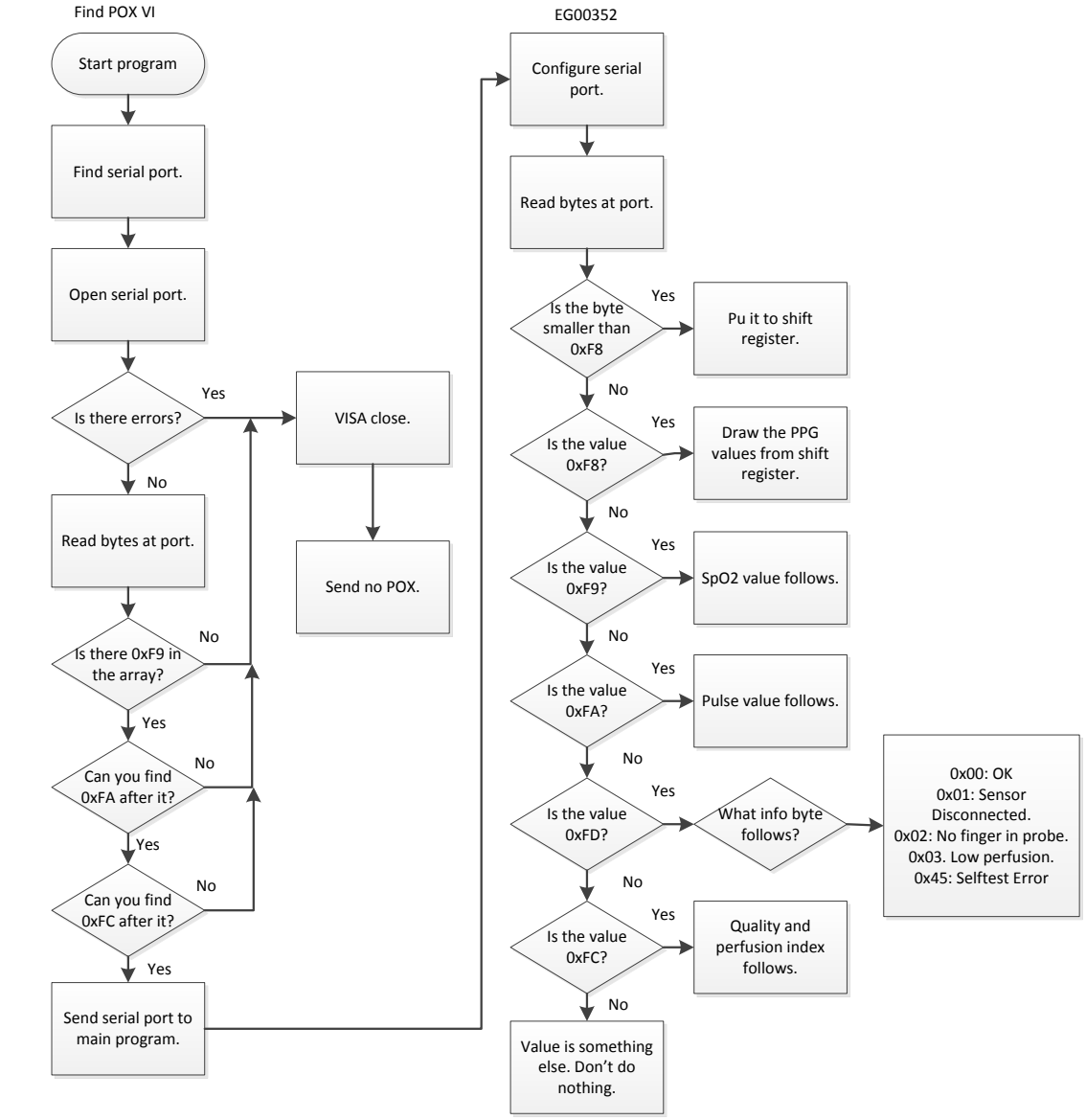

Appendix 5. Block diagram of Find NIBP VI and NIBP VI. 1 page.

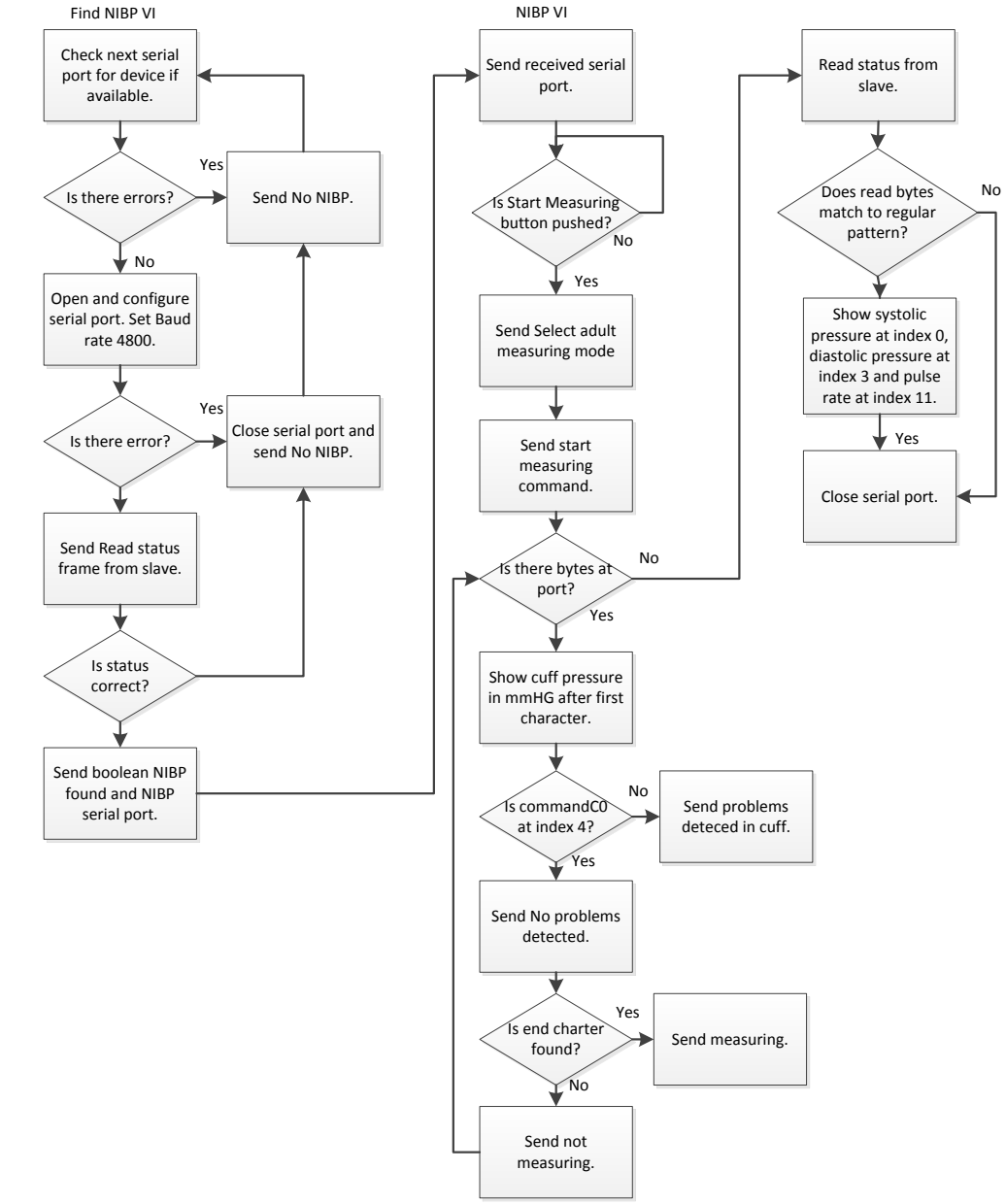

Appendix 6. Block diagram of Z VI and Find Z VI. 1 page.

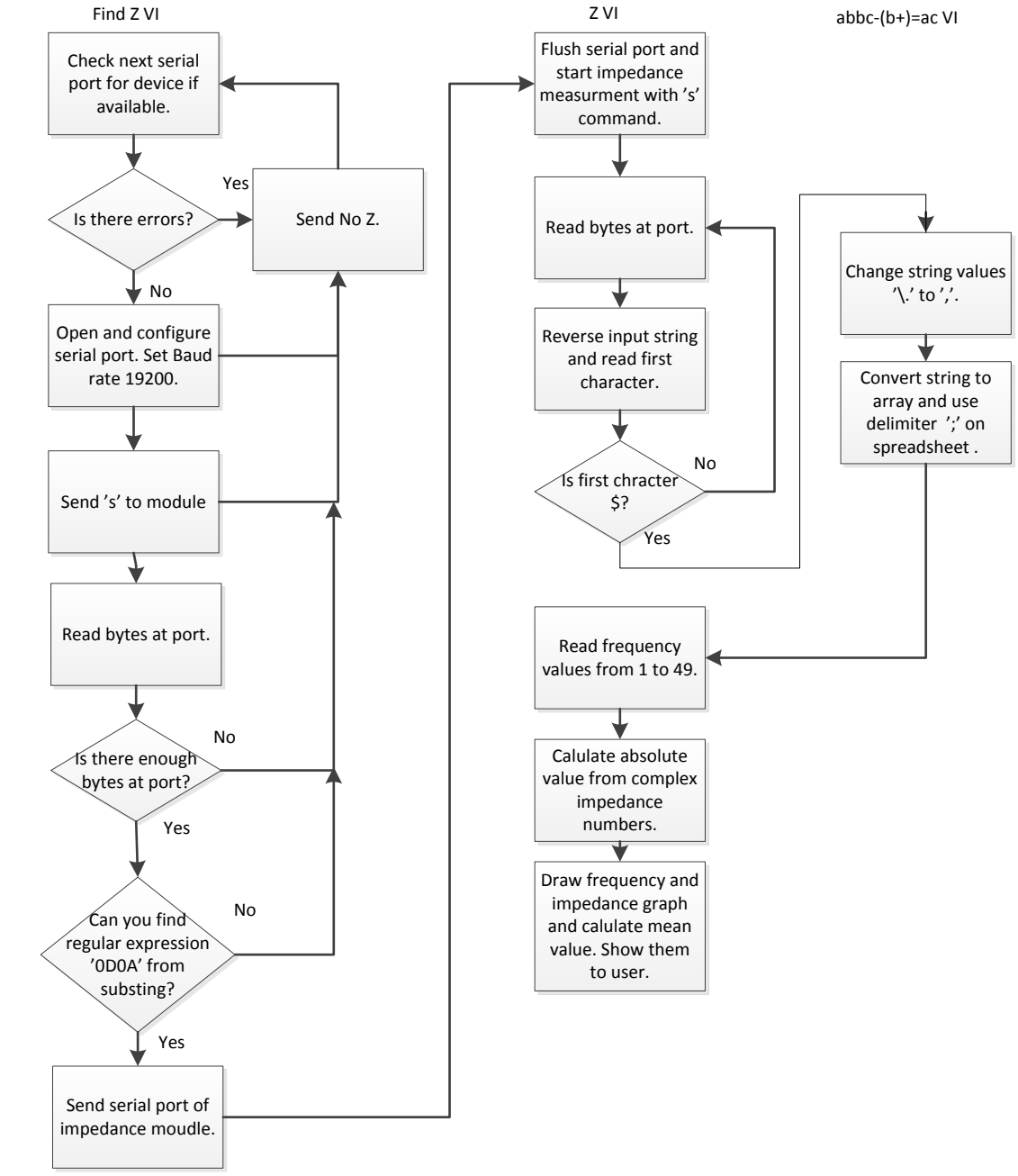

Appendix 7. Block diagram clarifies function of Weight VI, A/B xtrac VO and Find Weight VI. 1 page.

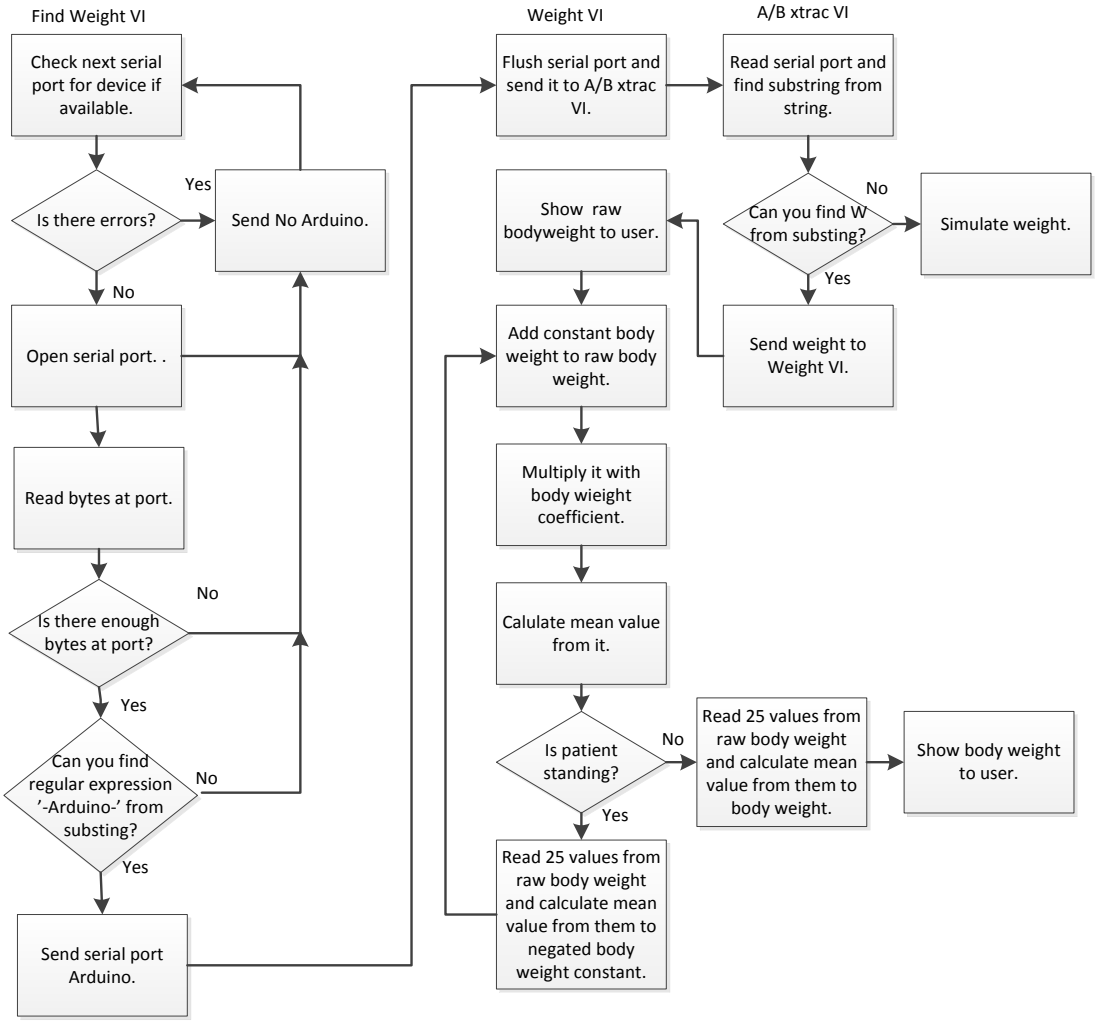

Appendix 8. Presents measured and calculated RR, QT intervals and their differences from test person A. 1 page.

Person A

Measured RR:	Calculated R:	Calculated RR::	Diff:	Measured QT:	Calculated QT:	Diff:	min.	Measured BP dPTT:	Measured BP straight:	Sys BP
	391									
1174	1597	1206	-32	352	473	-121	0,5	141	139	
1190	2814	1217	-27	392	462	-70	1	177	168	154
1215	4039	1225	-10	49	453	-404	1,5	141	138	
1233	5291	1252	-19	26	424	-398	2	141	139	
1213	6537	1246	-33	399	449	-50	2,5	204	187	168
1246	7813	1276	-30	48	451	-403	3	141	140	
1257	9077	1264	-7	405	449	-44	3,5	141	139	181
1234	10030	953	281	408	451	-43	4	141	141	
1242	11283	1253	-11	36	445	-409				
1237	12530	1247	-10	384	451	-67				
1247	13747	1217	30	391	422	-31				
1181	14894	1147	34	392	401	-9				
1146	16051	1157	-11	401	442	-41				
1154	17220	1169	-15	399	472	-73				
1182	18337	1117	65	27	416	-389				
1115	19451	1114	1	388	418	-30				
1091	20559	1108	-17	395	457	-62				
1116	21678	1119	-3	44	419	-375				
1130	22792	1114	16	1108	407	701				
1094	23948	1156	-62	1	438	-437				
1124	25062	1114	10	31	438	-407				
1080	26176	1114	-34	387	476	-89				
1125	27322	1146	-21	1115	448	667				
1118	28465	1143	-25	2	511	-509				
1124	29563	1098	26	43	447	-404				
1085	30676	1113	-28	410	425	-15				
1113	31823	1147	-34	44	469	-425				
1138	32959	1136	2	1132	461	671				
1088	34093	1134	-46	398	428	-30				
1143	34960	867	276	35	445	-410				
1157	36106	1146	11	22	367	-345				
1137	37256	1150	-13	394	412	-18				
1156	38460	1204	-48	382	410	-28				
1170	39640	1180	-10	11	422	-411				
1166	40787	1147	19	389	393	-4				
1151	42000	1213	-62	387	395	-8				
1213	43235	1235	-22	1244	426	818				
1206	44424	1189	17	33	400	-367				
1178	45614	1190	-12	421	423	-2				
1197	46863	1249	-52	49	408	-359				
1215	48065	1202	13	11	389	-378				
1189	49249	1184	5	426	438	-12				
1173	50481	1232	-59	375	386	-11				
1228	51677	1196	32	1224	468	756				
1174	52856	1179	-5	390	402	-12				
1158	54077	1221	-63	386	428	-42				
1232	55296	1219	13	25	421	-396				
1171	56452	1156	15	55	401	-346				
1148	57647	1195	-47	378	406	-28				
1182	58853	1206	-24	375	404	-29				
1207	59714	861	346	1212	T wave lost					
1159	60897	1183	-24	831	421	410				
1156	62114	1217	-61							
	Median diff:		**-11**		**Median diff:**	**-50**				

Appendix 9. Presents RR and QT interval Bland-Altman plots measured from test person A. 1 page.

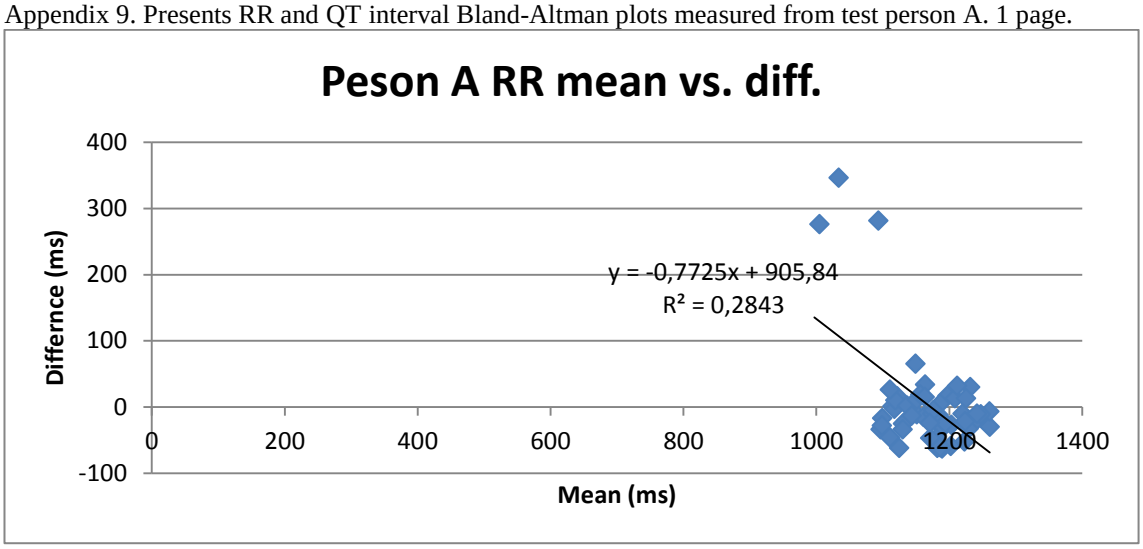

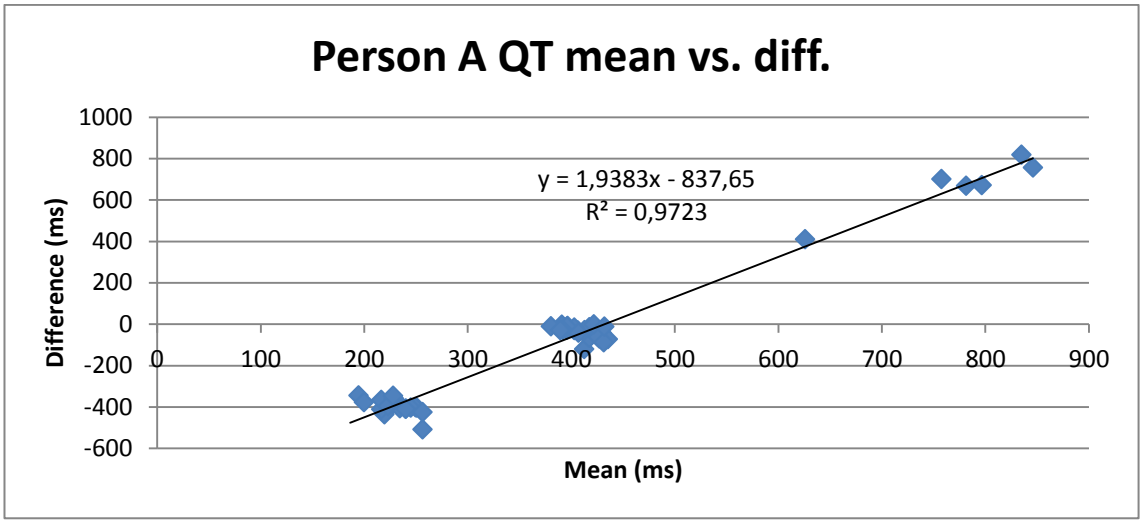

Appendix 10. Presents measured pulse transit times from test person A. 1 page.

Person A

Pulse transit times:

1	509	58	511	115	519	172	502
2	509	59	499	116	492	173	500
3	525	60	518	117	481	174	510
4	502	61	503	118	495	175	508
5	513	62	493	119	535	176	515
6	501	63	478	120	504	177	530
7	503	64	496	121	1581	178	528
8	482	65	498	122	2648	179	486
9	502	66	501	123	3716	180	516
10	510	67	487	124	513	181	504
11	478	68	528	125	534	182	505
12	511	69	518	126	533	183	487
13	513	70	479	127	529	184	505
14	519	71	529	128	532	185	505
15	488	72	463	129	518	186	511
16	509	73	522	130	520	187	536
17	503	74	505	131	517	188	522
18	482	75	514	132	518	189	541
19	506	76	519	133	520	190	530
20	499	77	517	134	494	191	522
21	505	78	510	135	495	192	519
22	505	79	493	136	493	193	522
23	473	80	475	137	529	194	499
24	513	81	489	138	508	195	517
25	502	82	503	139	500	196	507
26	506	83	485	140	501	197	514
27	516	84	514	141	537	198	511
28	513	85	502	142	514	199	529
29	503	86	504	143	520	200	530
30	482	87	523	144	529	201	523
31	507	88	512	145	521	202	514
32	499	89	497	146	497	203	507
33	497	90	511	147	512	204	499
34	522	91	526	148	498	205	524
35	500	92	506	149	499	206	514
36	507	93	511	150	524	207	510
37	483	94	509	151	525	208	519
38	533	95	511	152	492	209	522
39	475	96	506	153	521	210	519
40	538	97	504	154	525	211	537
41	510	98	507	155	494	212	503
42	1668	99	516	156	512	213	513
43	2845	100	516	157	511		
44	497	101	505	158	516		
45	484	102	507	159	504		
46	491	103	515	160	526		
47	492	104	502	161	502		
48	484	105	503	162	501		
49	489	106	500	163	512		
50	514	107	527	164	495		
51	514	108	523	165	485		
52	484	109	517	166	524		
53	489	110	517	167	504		
54	494	111	513	168	504		
55	507	112	1620	169	499		
56	494	113	2718	170	507		
57	523	114	498	171	459		

Appendix 11. Presents measured and calculated RR, QT intervals and their differences from test person B. 2 pages.

Person B :

Measured RR:	Calculated R:	Calculated RR::	Diff:	Measured QT:	Calculated QT:	Diff:			Estimated BP dPTT:	Estimated BP straight:	Sys. BP
	687							min			
1015	1646	959	56	355	431	-76		0,5	123	122	
952	2657	1011	-59	382	454	-72		1	124	121	117
977	3672	1015	-38	337	514	-177		1,5	117	122	
1000	4696	1024	-24	1010	415	595		2	117	122	123
963	5729	1033	-70	331	452	-121		2,5	117	122	
3892	6744	1015	2877	57	556	-499		3	117	122	131
	7765	1021						3,5	117	123	
	8760	995						4	126	121	
	9772	1012									
971	10771	999	-28	362	437	-75					
972	11741	970	2	363	410	-47					
918	12713	972	-54	354	400	-46					
937	13682	969	-32	377	432	-55					
919	14632	950	-31	338	480	-142					
919	15583	951	-32	367	420	-53					
957	16532	949	8	383	411	-28					
918	16542	10	908	347	420	-73					
957	17483	941	16	945	432	513					
931	18434	951	-20	324	421	-97					
962	19158	724	238	127	393	-266					
969	20108	950	19	369	410	-41					
973	21087	979	-6	361	188	173					
944	22029	942	2	386	435	-49					
967	23002	973	-6	361	404	-43					
974	24001	999	-25	375	442	-67					
919	24936	935	-16	349	414	-65					
955	25918	982	-27	381	423	-42					
946	26906	988	-42	393	424	-31					
931	27864	958	-27	376	414	-38					
889	28789	925	-36	360	419	-59					
895	29718	929	-34	353	408	-55					
872	30614	896	-24	367	430	-63					
880	31501	887	-7	366	406	-40					
861	32409	908	-47	352	430	-78					
841	33278	869	-28	375	429	-54					
859	34163	885	-26	364	413	-49					
853	35054	891	-38	385	406	-21					
832	35883	829	3	363	429	-66					
861	36728	845	16	343	419	-76					
834	37582	854	-20	348	397	-49					
932	38512	930	2	951	394	557					
925	39481	969	-44	327	424	-97					
923	40449	968	-45	341	408	-67					
918	41410	961	-43	358	413	-55					
890	42093	683	207	34	484	-450					
893	43026	933	-40	358	420	-62					
847	43907	881	-34	350	T wave lost	0					
856	44775	868	-12	398	415	-17					
851	45636	861	-10	351	447	-96					
849	46513	877	-28	400	445	-45					
860	47400	887	-27	347	405	-58					
860	48321	921	-61	378	445	-67					
864	49220	899	-35	335	418	-83					
870	50125	905	-35	389	425	-36					
875	51063	938	-63	405	400	5					
907	52023	960	-53	369	426	-57					
892	52960	937	-45	374	448	-74					
901	53887	927	-26	357	425	-68					
906	54802	915	-9	344	429	-85					
883	55757	955	-72	424	418	6					

872	56648	891	-19	376	404	-28
885	57546	898	-13	369	447	-78
869	58470	924	-55	332	433	-101
884	59384	914	-30	365	428	-63
900	60314	930	-30	383	412	-29
905	61254	940	-35	385	407	-22
922	62216	962	-40	370	427	-57
907	63133	917	-10	382	439	-57
904	64099	966	-62	363	420	-57
	Median diff:		**-27,5**	**Median diff:**		**-57**

Appendix 12. Presents RR and QT interval Bland-Altman plots measured from test person B. 1 page.

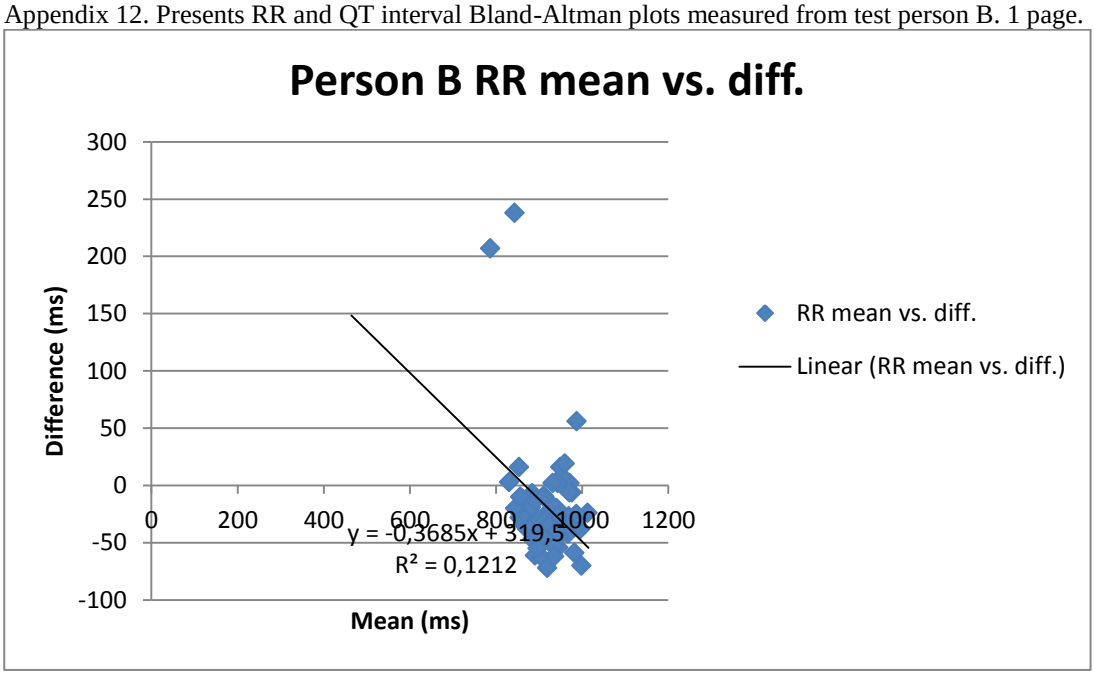

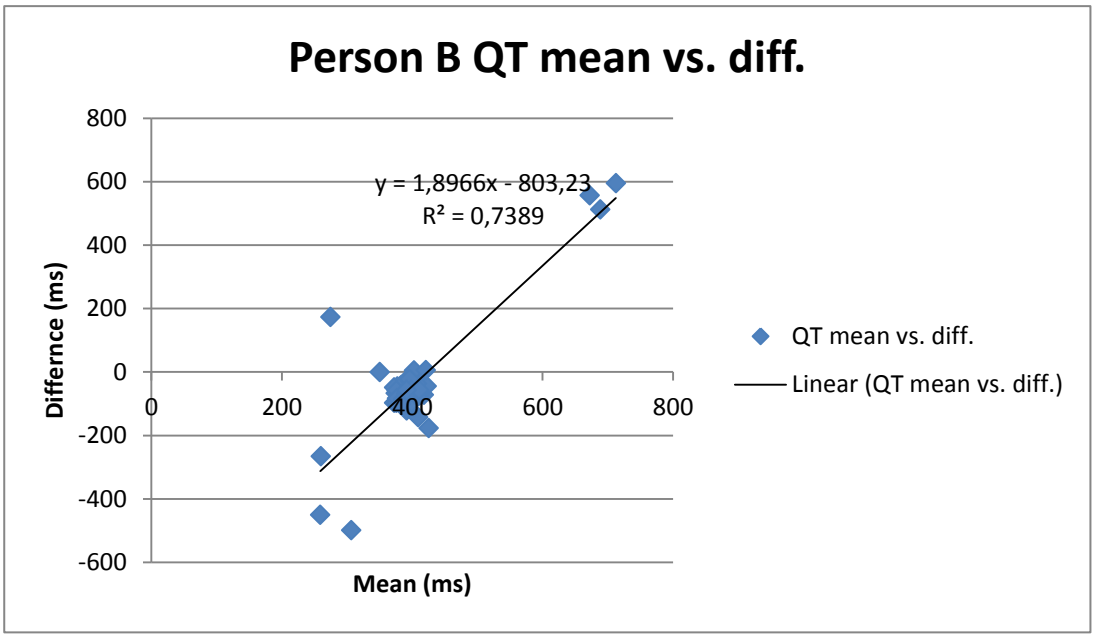

Appendix 13. Present pulse transit times measured from test person B. 1 page.

Person B Pulse transit times:

1	509	58	511	115	519	172	502
2	509	59	499	116	492	173	500
3	525	60	518	117	481	174	510
4	502	61	503	118	495	175	508
5	513	62	493	119	535	176	515
6	501	63	478	120	504	177	530
7	503	64	496	121	1581	178	528
8	482	65	498	122	2648	179	486
9	502	66	501	123	3716	180	516
10	510	67	487	124	513	181	504
11	478	68	528	125	534	182	505
12	511	69	518	126	533	183	487
13	513	70	479	127	529	184	505
14	519	71	529	128	532	185	505
15	488	72	463	129	518	186	511
16	509	73	522	130	520	187	536
17	503	74	505	131	517	188	522
18	482	75	514	132	518	189	541
19	506	76	519	133	520	190	530
20	499	77	517	134	494	191	522
21	505	78	510	135	495	192	519
22	505	79	493	136	493	193	522
23	473	80	475	137	529	194	499
24	513	81	489	138	508	195	517
25	502	82	503	139	500	196	507
26	506	83	485	140	501	197	514
27	516	84	514	141	537	198	511
28	513	85	502	142	514	199	529
29	503	86	504	143	520	200	530
30	482	87	523	144	529	201	523
31	507	88	512	145	521	202	514
32	499	89	497	146	497	203	507
33	497	90	511	147	512	204	499
34	522	91	526	148	498	205	524
35	500	92	506	149	499	206	514
36	507	93	511	150	524	207	510
37	483	94	509	151	525	208	519
38	533	95	511	152	492	209	522
39	475	96	506	153	521	210	519
40	538	97	504	154	525	211	537
41	510	98	507	155	494	212	503
42	1668	99	516	156	512	213	513
43	2845	100	516	157	511		
44	497	101	505	158	516		
45	484	102	507	159	504		
46	491	103	515	160	526		
47	492	104	502	161	502		
48	484	105	503	162	501		
49	489	106	500	163	512		
50	514	107	527	164	495		
51	514	108	523	165	485		
52	484	109	517	166	524		
53	489	110	517	167	504		
54	494	111	513	168	504		
55	507	112	1620	169	499		
56	494	113	2718	170	507		
57	523	114	498	171	459		

Appendix 14. Presents measured and calculated RR, QT intervals and their differences from test person C. 1 page.

Person C :

Measured RR:	Calculated R:	Calculated RR:	Diff:	Measured QT:	Calculated QT:	Diff:	min.	Estimated BP dPTT:	Estimated BP straight:	Sys. BP
	457									
1314	1865	1408	-94	393	477	-84	0,5	113	113	
1376	3198	1333	43	400	467	-67	1	113	113	115
1306	4646	1448	-142	454	453	1	1,5	112	113	
1453	6084	1438	15	445	462	-17	2	167	120	
1409	7449	1365	44	390	460	-70	2,5	113	113	125
1335	8876	1427	-92	394	516	-122	3	113	113	
1409	9979	1103	306	440	510	-70	3,5	113	112	139
1398	11353	1374	24	410	482	-72	4	114	113	
1364	12676	1323	41	386	453	-67				
1291	14053	1377	-86	434	462	-28				
1369	15430	1377	-8	457	475	-18				
1359	16735	1305	54	413	480	-67				
1287	18120	1385	-98	454	516	-62				
1373	19438	1318	55	434	473	-39				
1307	20824	1386	-79	421	465	-44				
1373	22121	1297	76	411	437	-26				
1297	23407	1286	11	436	474	-38				
1287	24745	1338	-51	429	426	3				
1318	26098	1353	-35	379	440	-61				
1366	27512	1414	-48	398	442	-44				
1406	28837	1325	81	420	463	-43				
1319	30175	1338	-19	430	446	-16				
1350	31461	1286	64	406	444	-38				
1286	32827	1366	-80	433	432	1				
1353	33819	992	361	394	454	-60				
1266	35143	1324	-58	430	477	-47				
1320	36415	1272	48	387	443	-56				
1232	37814	1399	-167	410	435	-25				
1394	39147	1333	61	406	458	-52				
1315	40483	1336	-21	412	448	-36				
1310	41775	1292	18	395	440	-45				
1295	43029	1254	41	397	449	-52				
1256	44344	1315	-59	462	432	30				
1325	R lost			410	441	-31				
1245	R lost			387	444	-57				
1330	48143			396	469	-73				
1202	49429	1286	-84	397	442	-45				
1288	50711	1282	6	440	416	24				
1304	52056	1345	-41	412	424	-12				
1329	53372	1316	13	398	462	-64				
1321	54694	1322	-1	432	440	-8				
		Median diff:	**2,5**		**Median diff:**	**-44**				

Appendix 15. Presents RR and QT interval Bland-Altman plots measured from test person C. 1 page

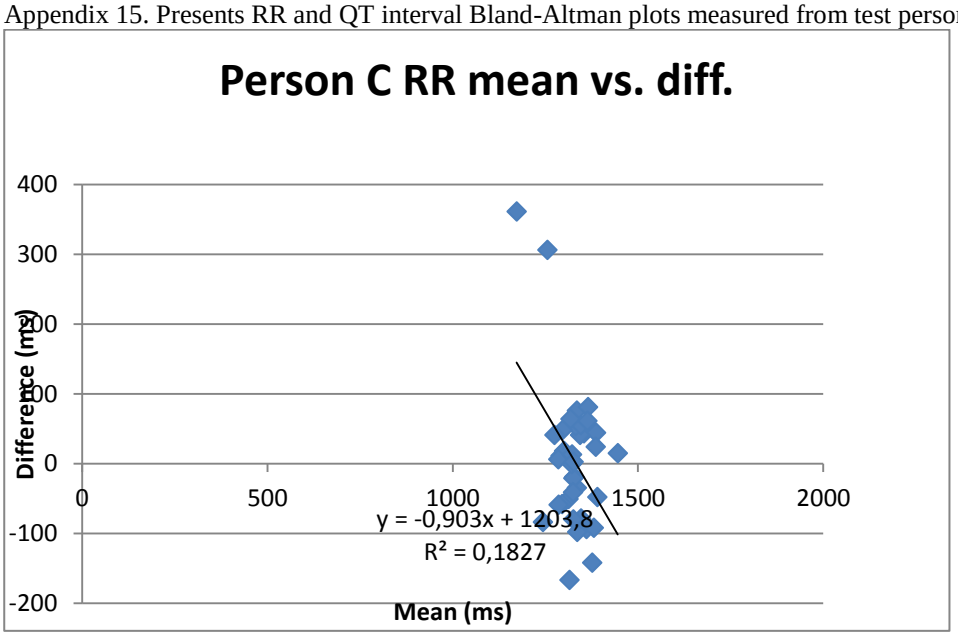

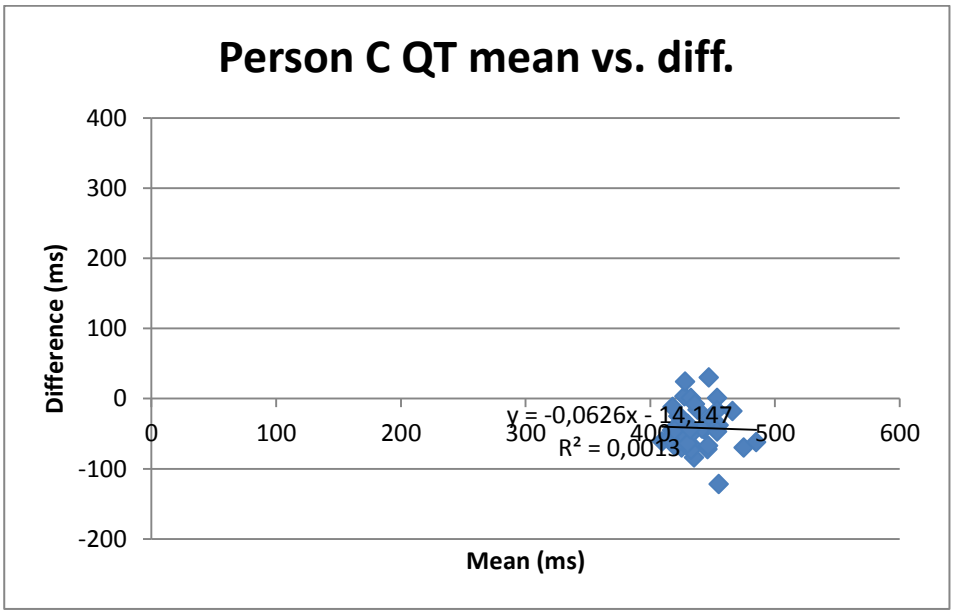

Appendix 16. Present pulse transit times measured from person C. 1 page.

Person C: Pulse transit times:

1	386	48	435	95	427	142	426	189	404	236	425
2	396	49	431	96	445	143	430	190	397	237	448
3	426	50	441	97	449	144	470	191	400	238	415
4	406	51	440	98	455	145	467	192	402	239	431
5	388	52	414	99	451	146	425	193	409	240	409
6	405	53	450	100	444	147	460	194	411	241	427
7	417	54	437	101	462	148	443	195	411	242	435
8	412	55	442	102	452	149	427	196	406	243	420
9	431	56	456	103	439	150	437	197	403		
10	433	57	447	104	435	151	420	198	419		
11	426	58	439	105	400	152	442	199	405		
12	415	59	417	106	436	153	417	200	422		
13	462	60	416	107	409	154	437	201	413		
14	463	61	411	108	407	155	402	202	414		
15	446	62	418	109	425	156	431	203	411		
16	433	63	417	110	435	157	432	204	399		
17	409	64	411	111	450	158	414	205	399		
18	414	65	416	112	427	159	435	206	389		
19	425	66	409	113	454	160	425	207	394		
20	433	67	401	114	464	161	425	208	400		
21	423	68	416	115	458	162	439	209	400		
22	426	69	396	116	448	163	454	210	421		
23	406	70	398	117	439	164	431	211	448		
24	416	71	406	118	453	165	429	212	430		
25	415	72	397	119	461	166	418	213	421		
26	411	73	411	120	465	167	420	214	419		
27	424	74	405	121	470	168	408	215	398		
28	416	75	437	122	449	169	395	216	396		
29	419	76	416	123	463	170	373	217	411		
30	408	77	429	124	465	171	402	218	416		
31	409	78	456	125	440	172	388	219	417		
32	389	79	434	126	446	173	412	220	391		
33	382	80	428	127	457	174	400	221	423		
34	418	81	443	128	441	175	406	222	431		
35	414	82	1570	129	440	176	405	223	401		
36	421	83	2588	130	435	177	392	224	386		
37	399	84	3705	131	434	178	404	225	401		
38	414	85	467	132	436	179	362	226	418		
39	413	86	448	133	452	180	392	227	400		
40	421	87	407	134	440	181	416	228	414		
41	424	88	419	135	455	182	408	229	398		
42	393	89	425	136	451	183	415	230	426		
43	395	90	447	137	472	184	401	231	409		
44	411	91	444	138	450	185	417	232	420		
45	424	92	423	139	460	186	397	233	405		
46	403	93	428	140	466	187	388	234	415		
47	443	94	425	141	460	188	407	235	429		

Appendix 17. Presents measured and calculated RR, QT intervals and their differences from test person D. 1 page.

Person D :

Measured RR:	Calculated R:	Calculated RR:	Diff:	Measured QT:	Calculated QT:	Diff:	min.	Estimated BP dPTT:	Estimated BP straight:	Sys. BP
	975									
1397	2362	1387	10	546	500	46	0,5	141	130	
1352	3790	1428	-76	387	495	-108	1	133	131	118
1320	5176	1386	-66	46	484	-438	1,5	117	147	
1340	6611	1435	-95	42	478	-436	2	137	127	
1357	8063	1452	-95	40	489	-449	2,5	117	148	136
1426	9468	1405	21	386	482	-96	3	143	121	
1359	10920	1452	-93	225	492	-267	3,5	166	107	147
1431	12337	1417	14	544	446	98	4	142	122	
1380	13705	1368	12	540	448	92				
1354	15033	1328	26	403	464	-61				
1345	16370	1337	8	589	478	111				
1334	17396	1026	308	590	407	183				
1317	18734	1338	-21	42	477	-435				
1346	20016	1282	64	41	481	-440				
1300	21337	1321	-21	546	471	75				
1342	22588	1251	91	53	470	-417				
1255	23893	1305	-50	536	465	71				
1288	25204	1311	-23	35	479	-444				
1335	26537	1333	2	608	505	103				
1293	27890	1353	-60	50	455	-405				
1358	29212	1322	36	53	462	-409				
1310	30552	1340	-30	535	450	85				
1352	31863	1311	41	407	471	-64				
1328	33171	1308	20	383	456	-73				
1277	34496	1325	-48	536	434	102				
1342	35789	1293	49	367	462	-95				
1277	37213	1424	-147	33	500	-467				
1345	38574	1361	-16	397	486	-89				
1298	39922	1348	-50	54	461	-407				
1347	41282	1360	-13	45	492	-447				
1322	42410	1128	194	631	530	101				
1325	43869	1459	-134	55	492	-437				
1286	45209	1340	-54	632	492	140				
1286	46562	1353	-67	42	534	-492				
1305	47921	1359	-54	387	489	-102				
1274	49250	1329	-55	486	449	37				
1296	50751	1501	-205	48	471	-423				
1323	52222	1471	-148	572	496	76				
1277	53599	1377	-100	40	465	-425				
1344	54859	1260	84	39	487	-448				
1271	56233	1374	-103	44	535	-491				
1319	57726	1493	-174	197	504	-307				
1302	59046	1320	-18	44	495	-451				
1292	60383	1337	-45	514	480	34				
1309	61753	1370	-61	40	483	-443				
1313	63166	1413	-100	408	517	-109				
	Median diff:		**-37,5**	**Median diff:**		**-109**				

Appendix 18. Presents RR and QT interval Bland-Altman plots measured from test person D. 1 page

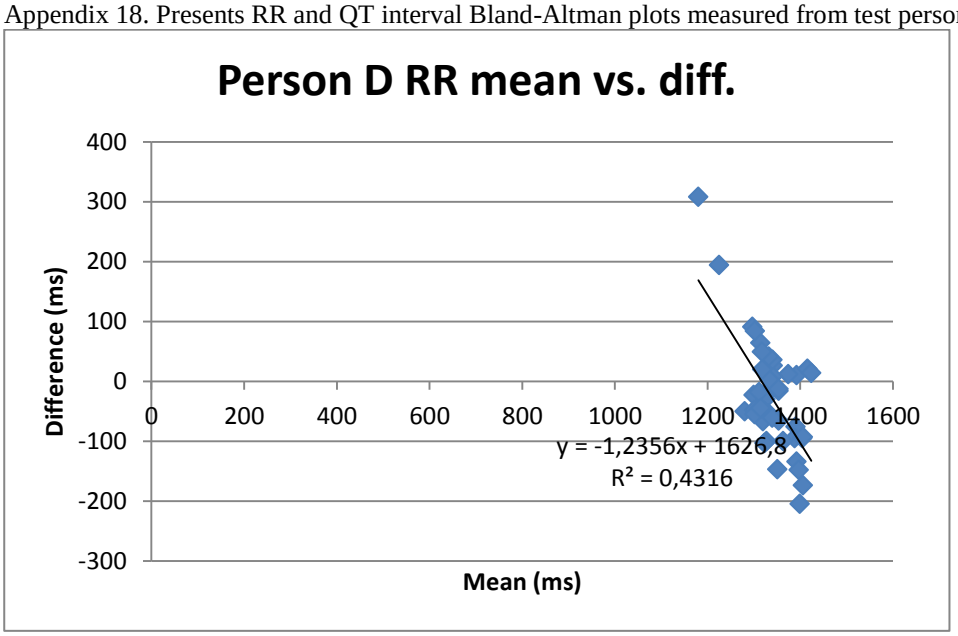

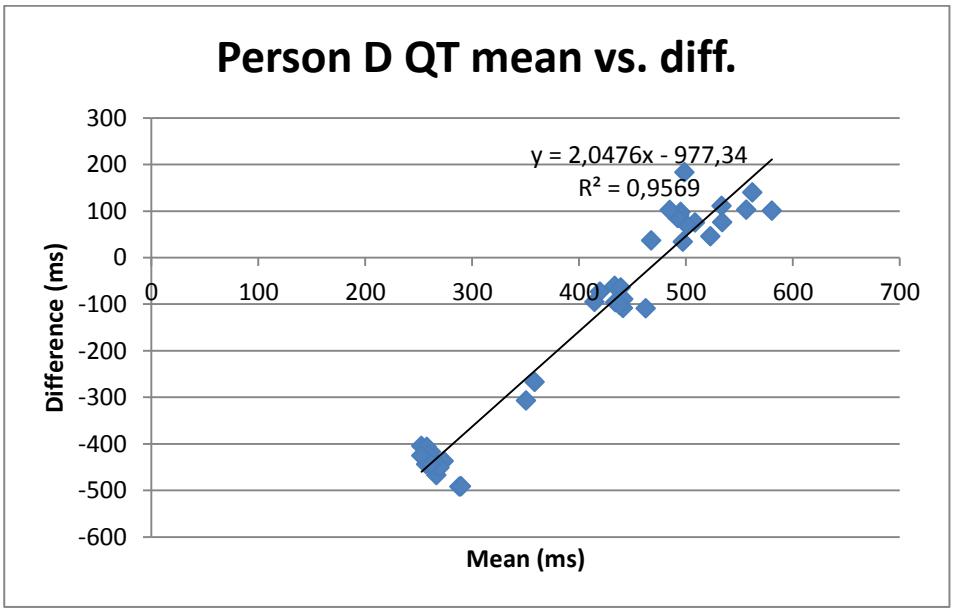

Appendix 19. Present pulse transit times measured from test person D. 1 page.

Person D Pulse transit times:

1	402	58	482	115	513	172	487
2	454	59	467	116	481	173	464
3	455	60	451	117	490	174	467
4	463	61	485	118	487	175	468
5	433	62	470	119	462	176	457
6	430	63	460	120	1745	177	455
7	445	64	470	121	3002	178	478
8	416	65	474	122	458	179	489
9	427	66	476	123	457	180	481
10	430	67	483	124	474	181	482
11	460	68	458	125	468	182	455
12	447	69	475	126	479	183	464
13	470	70	470	127	490	184	469
14	464	71	458	128	452		
15	466	72	474	129	483		
16	477	73	453	130	458		
17	465	74	463	131	462		
18	498	75	487	132	482		
19	461	76	484	133	464		
20	478	77	478	134	477		
21	1695	78	142	135	458		
22	2892	79	580	136	465		
23	463	80	460	137	477		
24	458	81	475	138	480		
25	492	82	461	139	463		
26	466	83	461	140	479		
27	475	84	1738	141	465		
28	475	85	2825	142	463		
29	475	86	491	143	475		
30	473	87	480	144	465		
31	476	88	475	145	464		
32	483	89	472	146	1681		
33	470	90	468	147	4065		
34	456	91	462	148	447		
35	498	92	460	149	498		
36	475	93	466	150	471		
37	475	94	474	151	466		
38	464	95	461	152	496		
39	453	96	461	153	472		
40	464	97	467	154	457		
41	463	98	470	155	477		
42	492	99	463	156	467		
43	462	100	455	157	468		
44	488	101	473	158	447		
45	485	102	465	159	462		
46	448	103	468	160	469		
47	465	104	447	161	468		
48	457	105	461	162	465		
49	471	106	463	163	1682		
50	487	107	465	164	2920		
51	471	108	472	165	478		
52	478	109	473	166	499		
53	470	110	454	167	482		
54	467	111	480	168	490		
55	465	112	443	169	479		
56	474	113	476	170	475		
57	482	114	462	171	469		

Appendix 20. Presents measured and calculated RR, QT intervals and their differences from test person E. 1 page.

Person E :

Measured RR:	Calculated R:	Calculated RR:	Diff:	Measured QT:	Calculated QT:	Diff:	min.	Estimated BP dPTT:	Estimated BP straight:	Sys. BP
	268									
965	1325	1057	-92	968	424	544	0,5	106	167	
1022	2419	1094	-72	352	489	-137	1	132	108	111
1055	3492	1073	-18	389	481	-92	1,5	106	161	
1061	4553	1061	0	1077	438	639	2	105	159	
1027	5674	1121	-94	347	483	-136	2,5	106	162	127
1059	6859	1185	-126	393	486	-93	3	106	162	
1101	7997	1138	-37	401	509	-108	3,5	106	162	152
1075	9155	1158	-83	419	514	-95	4	153	92	
1090	10301	1146	-56	416	479	-63				
1129	11625	1324	-195	63	520	-457				
1124	12757	1132	-8	449	470	-21				
1125	13958	1201	-76	65	460	-395				
1121	15091	1133	-12	378	440	-62				
1136	16208	1117	19	398	440	-42				
1114	17318	1110	4	391	440	-49				
1100	18492	1174	-74	374	450	-76				
1123	19281	789	334		T lost					
1089	20370	1089	0	14	460	-446				
1078	21478	1108	-30	381	430	-49				
1110	22681	1203	-93	381	460	-79				
1133	23786	1105	28	42	480	-438				
1093	24876	1090	3	401	480	-79				
1084	25993	1117	-33	396	470	-74				
1104	27129	1136	-32	978	510	468				
1096	28212	1083	13	40	440	-400				
1075	29295	1083	-8	420	460	-40				
1084	30415	1120	-36	382	430	-48				
1120	31521	1106	14	61	500	-439				
1076	32609	1088	-12	354	500	-146				
1075	33705	1096	-21	1075	470	605				
1096	34792	1087	9	387	430	-43				
1110	35856	1064	46	387	470	-83				
1072	36942	1086	-14	399	480	-81				
1085	38233	1291	-206	387	500	-113				
1103	39422	1189	-86	393	490	-97				
1074	40568	1146	-72	428	450	-22				
1077	41666	1098	-21	425	430	-5				
1118	42770	1104	14	60	460	-400				
1111	43865	1095	16		T lost					
1079	44677	812	267	37	410	-373				
1096	45864	1187	-91	42	500	-458				
1119	47071	1207	-88	61	460	-399				
1072	48183	1112	-40	1195	500	695				
1094	49342	1159	-65	373	460	-87				
1100	50435	1093	7	495	520	-25				
1086	51649	1214	-128	35	490	-455				
1128	52907	1258	-130	38	450	-412				
1099	54019	1112	-13	67	450	-383				
1085	55109	1090	-5	381	450	-69				
1104	56204	1095	9	387	450	-63				
1099	57279	1075	24	38	360	-322				
1084	58350	1071	13	64	460	-396				
1080	59440	1090	-10	412	480	-68				
1094	**30415**	**1108**	**-18**	**387**	**460**	**-83**				

Appendix 21. Presents RR and QT interval Bland-Altman plots measured from test person E. 1 page.

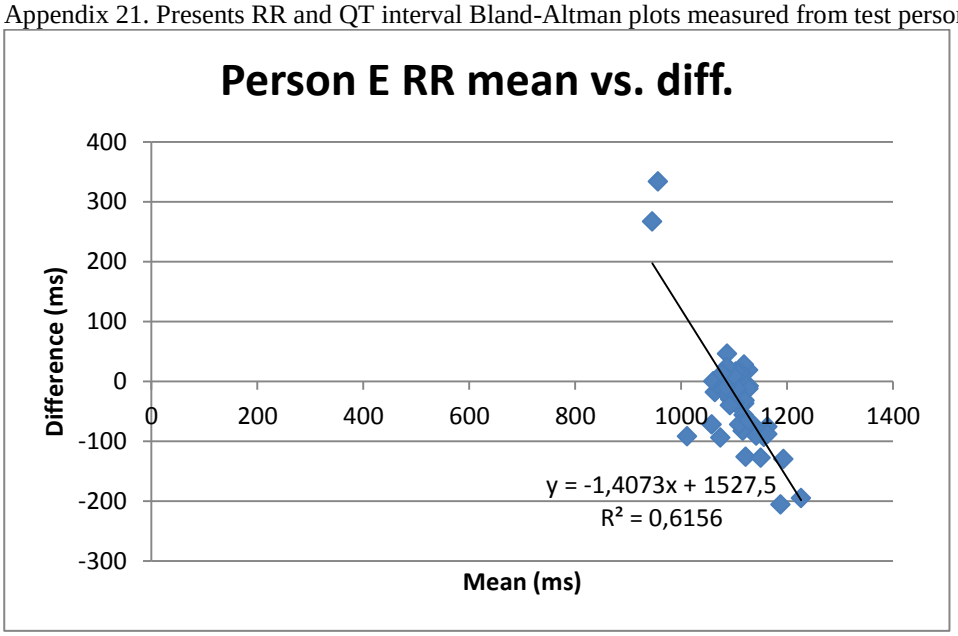

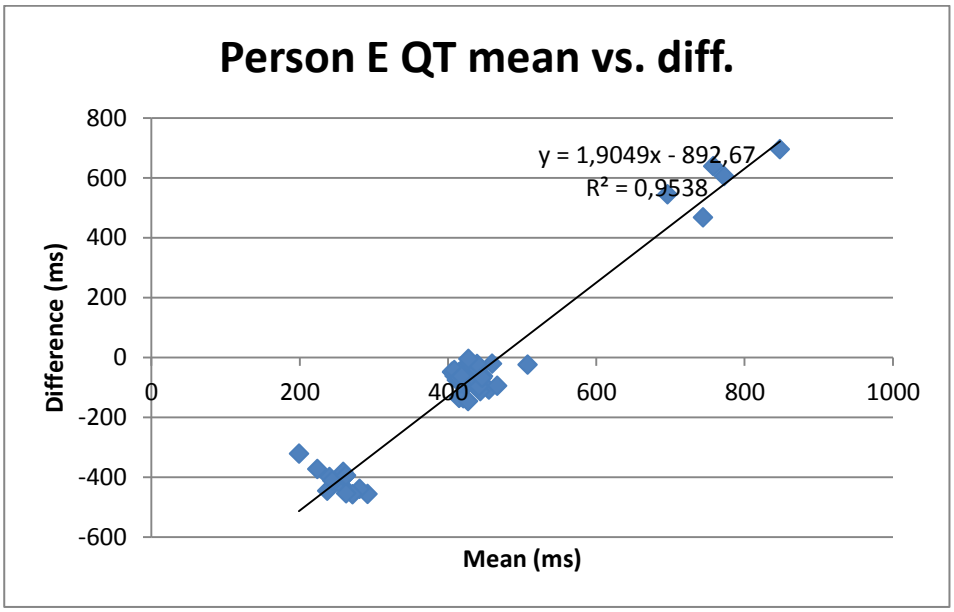

Appendix 22. Present pulse transit times measured from test person E. 1 page.

Person E Pulse transit times:

1	402	58	482	115	513	172	487
2	454	59	467	116	481	173	464
3	455	60	451	117	490	174	467
4	463	61	485	118	487	175	468
5	433	62	470	119	462	176	457
6	430	63	460	120	1745	177	455
7	445	64	470	121	3002	178	478
8	416	65	474	122	458	179	489
9	427	66	476	123	457	180	481
10	430	67	483	124	474	181	482
11	460	68	458	125	468	182	455
12	447	69	475	126	479	183	464
13	470	70	470	127	490	184	469
14	464	71	458	128	452		
15	466	72	474	129	483		
16	477	73	453	130	458		
17	465	74	463	131	462		
18	498	75	487	132	482		
19	461	76	484	133	464		
20	478	77	478	134	477		
21	1695	78	142	135	458		
22	2892	79	580	136	465		
23	463	80	460	137	477		
24	458	81	475	138	480		
25	492	82	461	139	463		
26	466	83	461	140	479		
27	475	84	1738	141	465		
28	475	85	2825	142	463		
29	475	86	491	143	475		
30	473	87	480	144	465		
31	476	88	475	145	464		
32	483	89	472	146	1681		
33	470	90	468	147	4065		
34	456	91	462	148	447		
35	498	92	460	149	498		
36	475	93	466	150	471		
37	475	94	474	151	466		
38	464	95	461	152	496		
39	453	96	461	153	472		
40	464	97	467	154	457		
41	463	98	470	155	477		
42	492	99	463	156	467		
43	462	100	455	157	468		
44	488	101	473	158	447		
45	485	102	465	159	462		
46	448	103	468	160	469		
47	465	104	447	161	468		
48	457	105	461	162	465		
49	471	106	463	163	1682		
50	487	107	465	164	2920		
51	471	108	472	165	478		
52	478	109	473	166	499		
53	470	110	454	167	482		
54	467	111	480	168	490		
55	465	112	443	169	479		
56	474	113	476	170	475		
57	482	114	462	171	469		